NASA CR-159453
Acurex Final Report 78-284

Acurex Project 6497

September 1978

PHASE-LOCKED TELEMETRY SYSTEM FOR ROTARY INSTRUMENTATION OF TURBOMACHINERY PHASE I

By Alan Adler and Bas Hoeks

Prepared Under Contract No. NAS3-20290 by
Acurex Corporation/Autodata Division
485 Clyde Avenue
Mountain View, California 94042

for

National Aeronautics and Space Administration

(NASA-CR-159453) PHASE-LOCKED TELEMETRY SYSTEM FOR ROTARY INSTRUMENTATION OF TURBOMACHINERY, PHASE 1 Final Report (Acurex Corp., Mountain View, Calif.) 192 p HC A09/MF A01 CSCL 09F G3/17

N80-14182

Unclas 44237

ABSTRACT

This report describes Phase I design of a telemetry system for use in making strain and temperature measurements on the rotating components of high speed turbomachines. The system described here represents a new systems approach, employing phase-locked transmitters, which offers greater measurement channel capacity and reliability than existing systems -- which all employ L-C carrier oscillators. A prototype transmitter module was tested at 175^{O}C combined with 40,000 g's acceleration.

SUMMARY

This report details Phase I design work performed by Acurex-Autodata under contract from NASA Lewis Research Center. The goal of this program is to develop an improved rotating telemetry system for strain and temperature measurements on the rotating components of operating gas turbine engines. Although such rotating telemetry systems have been in use for nearly 10 years, a recent study, sponsored by the Air Force Aero Propulsion Laboratory, identified propulsion industry requirements for several improvements in these systems. These desired improvements are listed (in approximate order of importance):

- An increase in the capacity for simultaneous dynamic strain measurements from the present 40 channels to 100 channels
- An increase in the maximum transmitter ambient temperature from +125°C (present) to +175°C
- Addition of capability for static strain measurements

Furthermore, it was desired to standardize the transmitter package design and take advantage of developments in microelectronic circuitry in order to improve performance and reliability.

Acurex had (previous to contract initiation) conceived of a system to meet these requirements and applied for a patent. This patent was subsequently granted (U.S. pat. no. 4,011,551). The system employs a number of independent transmitters, each phase-locked to a 200 kHz

inductively coupled clock signal which is also rectified and regulated to provide power for the transmitters and transducers.

The work performed under this, Phase I, program has included:

- Systems analysis of the "communications link" (channel carrier spacing, crosstalk, signal-to-noise ratio, etc.)
- Design and testing of typical antenna systems
- Circuit design and breadboard testing of:
  - -- Two alternate receivers
  - -- Three alternate static strain modulators
  - -- A phase-locked FM transmitter
- Transmitter package design including development of fabrication techniques and component selection for operation at up to $175^{o}C$ and 50,000 g's centrifugal force
- Fabrication of a prototype transmitter and testing at $175^{o}C$ combined with 40,000 g's

The prototype transmitter was tested incomplete because of outside delays in obtaining a monolythic integrated circuit frequency-synthesizer.

The overall results of the program were quite successful. All analyses and tests validated the basic phase-locked concept and demonstrated performance in excess of minimum requirements.

Phase II of the program is scheduled to result in completion of the detailed design and the fabrication and testing of a small prototype system.

TABLE OF CONTENTS

TABLE OF CONTENTS (Concluded)

LIST OF ILLUSTRATIONS

LIST OF TABLES

SECTION 1

INTRODUCTION

This report describes phase I of the rotary instrumentation system development.

The developments include:

- System design
- Transmitter circuit design
- Receiver circuit design
- Transmitter packaging design for high accelerations and temperature
- Construction and testing of a prototype transmitter module

Results from Air Force Contract F33615-75-C-2055 (which was a study of industry and government requirements, and of high temperature circuitry feasibility) have contributed to this design.

1.1 OBJECTIVE

The Air Force sponsored study contract F33615-75-C-2055 identified increased channel capacity for simultaneous dynamic strain data as a primary objective. Present systems are limited to a maximum of 40 channels. Government and industry requirements in the next decade are for up to 120 channels.

Other objectives included increased transmitter operating temperatures, the addition of static strain capability, improved reliability, and modularity of design. Finally, enhanced ease of operation was desirable so that existing test personnel would be able to cope with the tasks of monitoring the greatly increased number of measurement channels.

Performance goals for the system are given in Table 1-1. This table accounts for error sources such as internal wire, resolution, common mode rejection, zero drift, input impedance, excitation voltage stability, and channel crosstalk (including crosstalk during conditions of extreme transducer signals such as intermittance of strain gages). Additional error sources, also accounted for, include effects of ambient temperature, centrifugal force, vibration, and eccentricity in mounting.

1.2 SYSTEM CONCEPT

As with previous rotating instrumentation systems, this system consists of two subsystems (See Figure 1-1):

1. Rotating Subsystem

   Shaft-mounted electronics which interface with the transducers (strain gages, thermocouples or pressure transducers) and encode their signals onto carriers and/or subcarriers for transmission to a stationary subsystem.

2. Stationary Subsystem

   Receivers and demodulators which decode the signals from the rotating system and restore them to amplified analogs of the original transducer outputs

The stationary system also includes a 200 kHz power supply which couples power inductively (without physical contact) to the electronics of the rotating system.

The most important difference between this new system, and previous systems is that the inductively coupled power is also employed as a

TABLE 1-1. TABLE OF PERFORMANCE GOALS

Characteristic	Limit	Strain or Pressure		Temperature
		Dynamic	Static	
Accuracy	Minimum Design Goal	$\pm5\%$ $\pm2\%$	$\pm2\%$ $\pm1\%$	$\pm0.5\%$
Frequency Range	---	10 Hz - 30 kHz	0 - 500 Hz	0 - 25 Hz
Most Sensitive Full-Scale Range	---	500μ strain	500μ strain	20 mV
Phase Correlation (Channel-to-Channel)	Minimum Design Goal	$\pm10^{\circ}$ (to 30 kHz) $\pm5^{\circ}$ (to 30 kHz)	$\pm10^{\circ}$ (to 500 Hz) $\pm10^{\circ}$ (to 500 Hz)	---
Ambient Temperature Range	Minimum Design Goal	0°C - 150°C 0°C - 175°C		
Centrifugal Force Limit	Minimum Design Goal	40,000 g's 50,000 g's		

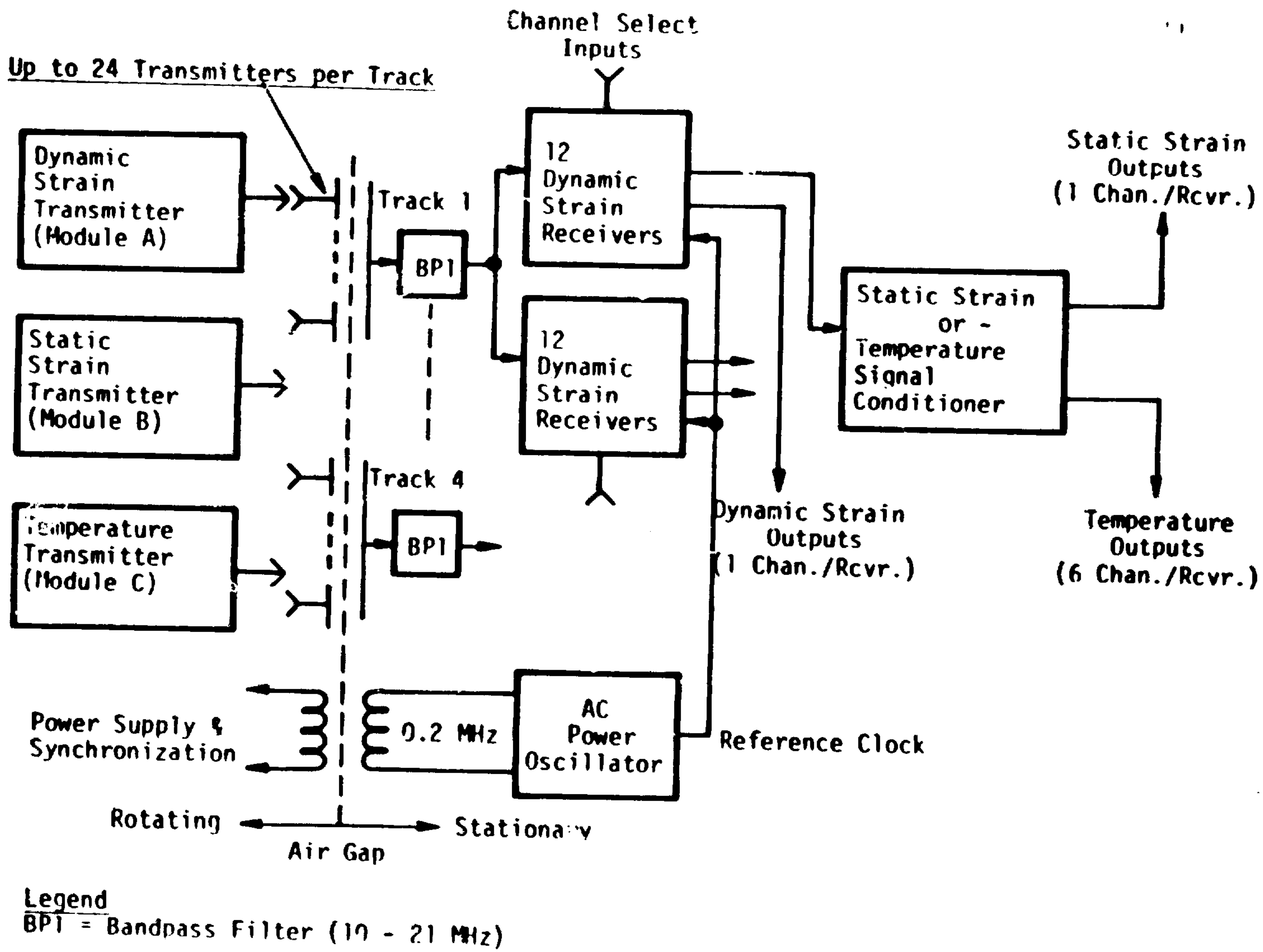

Figure 1-1. System block diagram.

reference clock to synchronize the carrier frequency of each transmitter. Furthermore this same 200 kHz signal is employed as a reference to the receivers of the stationary system.

This permits precise digital tuning by merely selecting the desired channel number on the receiver.

1.2.1 Rotating Electronics

The system includes three basic types of transmitter modules:

- Module A -- Dynamic strain transmitter
- Module B -- Static strain transmitter
- Module C -- Temperature transmitter containing six time-division multiplexed thermocouple channels

The physical locations of the modules in relation to the engine shaft and the capacitive antenna tracks is shown in Figure 1-2. In this example there are four layers of modules. Each layer may consist of up to 24 RF channels and is sensed a small distance away by a narrow conducting circular strip which acts as an antenna track. The four tracks are mounted on a stationary insulated disc with a grounded plane on its opposite side. In addition, grounded guard bands are placed between the tracks in order to reduce crosstalk. Further reduction of crosstalk between adjacent tracks is achieved by alternating the tracks with odd- and even-numbered channels. The channel frequency allocations are shown in Table 1-2.

Each channel carrier is frequency modulated with a nominal frequency deviation of ± 75 kHz. The modulating frequency band ranges from 20 Hz to 40 kHz.

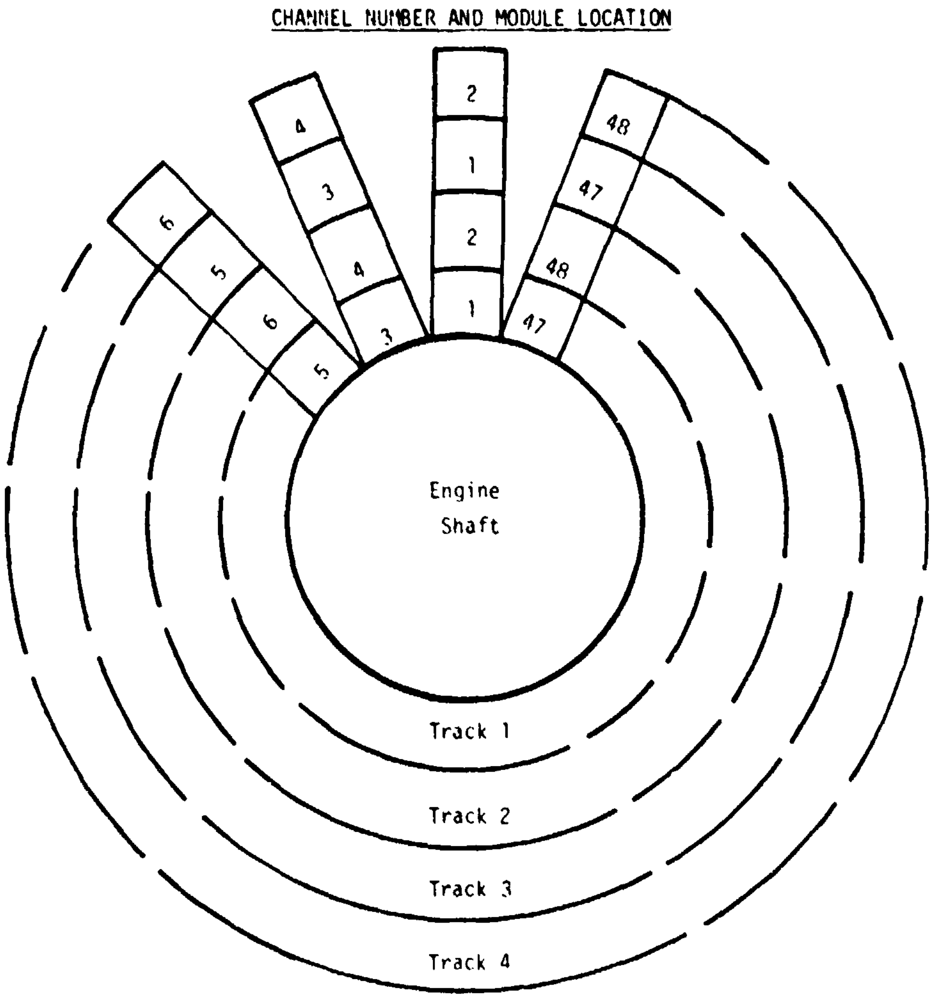

Figure 1-2. Module locations.

TABLE 1-2.

CHANNEL NUMBER	CARRIER FREQUENCY (MHz)
1	10.4
2	10.6
3	10.8
.	.
.	.
.	.
51	20.4
52	20.6

1.2.2 Stationary Electronics

Referring to Figure 1-1, note that each group of up to 24 dynamic strain receivers is preceded by a bandpass filter (BP1). Bandwidth and group delay characteristics should be such that the fundamental frequency components of all incoming frequency-modulated carriers are passed virtually distortion free.

Its purpose is twofold:

- Prevention of receiver input saturation due to crosstalk from the inductive power system
- Reduction of the receiver image frequency response due to transmitter carrier harmonics

Each receiver frequency is digitally programmable. Any of its outputs may be selected for either dynamic strain, static strain or temperature measurements.

For dynamic strain, which employs direct frequency modulation, the outputs of the receivers are ready-to-use analogs of the original strain gage signals.

For static strain or temperature the D.C. data is encoded onto a 6 kHz subcarrier and additional signal processing is performed by static strain or temperature demodulating cards which restore the signals to analogs of the original sensor signals. These demodulator cards are plugged-in (when required) to the receiver. The receiver chassis is 19 inches wide, rack-mountable, and accepts up to 12 plug-in cards which may be receivers, demodulators or mixes of each.

SECTION 2

ROTARY ELECTRONICS

2.1 INTRODUCTION

In this section the following modules will be discussed:

- Module A -- Dynamic strain transmitter
- Module B -- Static strain transmitter
- Module C -- Temperature transmitter

2.2 MODULE A -- DYNAMIC STRAIN TRANSMITTER

Referring to Figure 2-1 and 2-2, Module A contains:

- An isolated, regulated DC power supply, operating from the 200 kHz induced power. The isolation permits accurate measurements on grounded strain gages
- An AC coupled amplifier for amplifying low level dynamic strain signals

  The 3 db frequency response of each basic AC transmitter, when used alone is 10 Hz to 40 kHz
- A synchronized FM transmitter, responding to the AC amplifier, driving a capacitively coupled antenna
- A 40 kHz self-test signal injection circuit

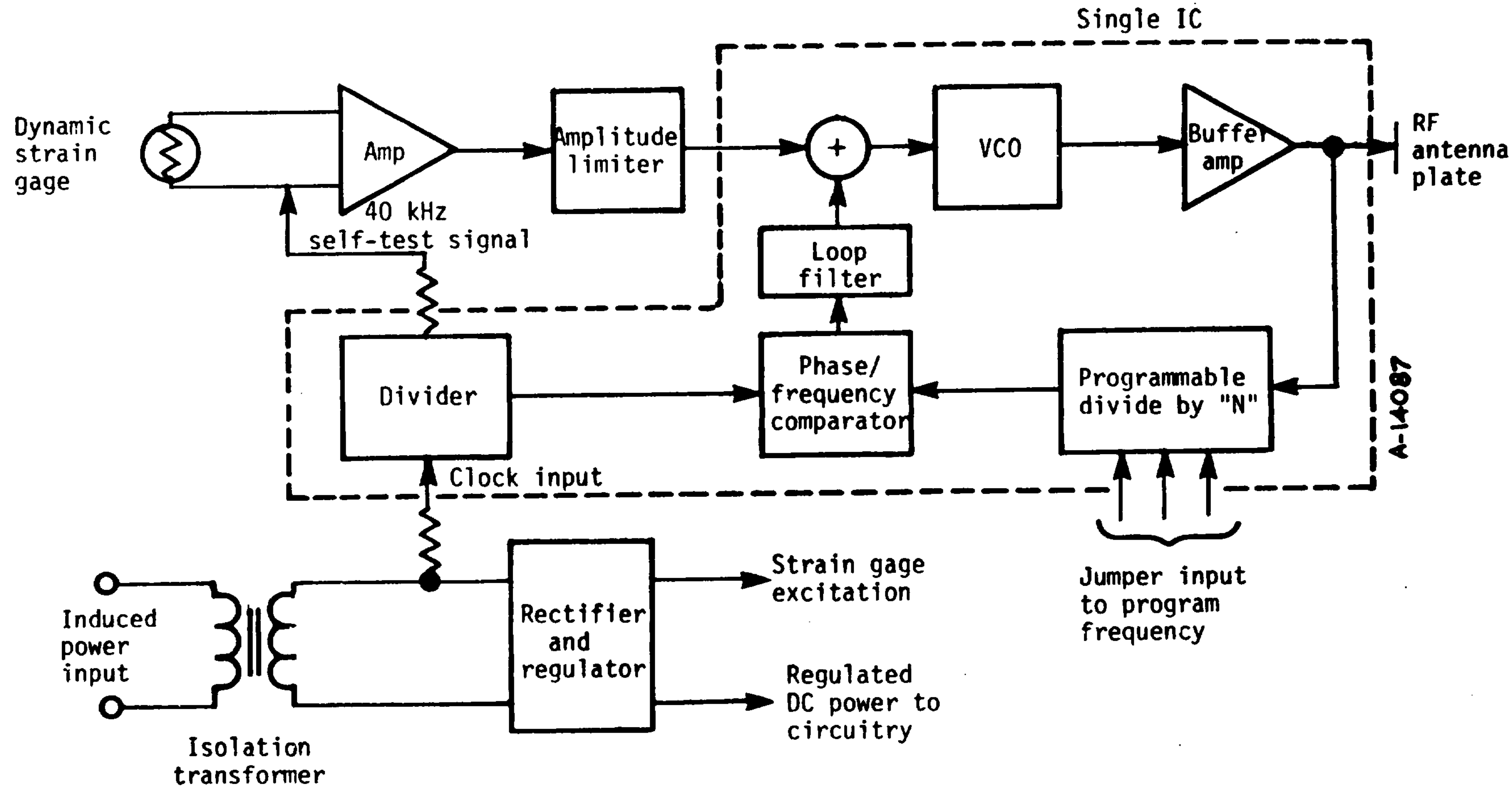

Figure 2-1. Block diagram of Module A (Dynamic strain transmitter).

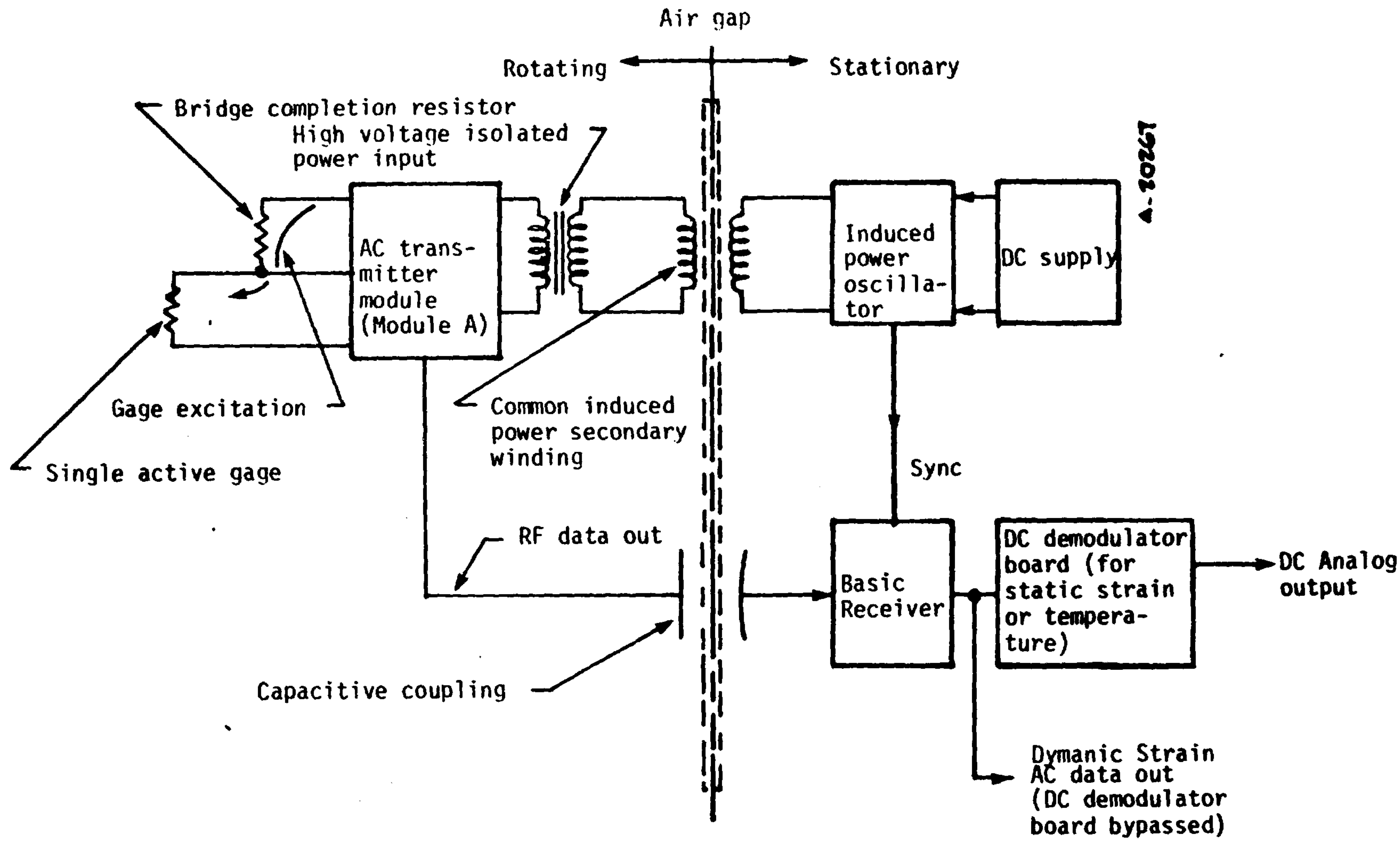

Figure 2-2. Basic data link (shown for dynamic strain using a single active gage).

- An open gage detection circuit. The strain amplifier is designed to bias itself into saturation if the strain gage circuit becomes open. This cuts off transmission of the 40 kHz self-test signal and permits positive differentiation between open and "quiet" gages.

The FM transmitter incorporates a phase-lock circuit which maintains its center frequency at a digitally preset multiple of the induced power frequency.

It was planned to employ a new RCA circular-CMOS integrated circuit frequency sysnthesizer to implement this phase-locked transmitter in the final product. However development delays at RCA combined with market changes eventually caused the cancellation of this I.C. development.

A new I.C., employing an RCA, Silicon-on-Saphire (SOS) universal gate array is currently on order and will be tested during Phase II of the telemetry program.

Schematic and test results of an initial breadboard design are shown in Figures 2-3(a) to 2-3(d). A schematic of the dynamic strain transmitter is included in Appendix K.

2.3 MODULE B -- STATIC STRAIN TRANSMITTER

Referring to Figure 2-4, the static strain transmitter operates as follows.

First, a differential chopper converts the static strain signal (DC-500Hz) to an amplitude modulated square wave of 3.125 kHz. Additionally, a 6.25 kHz calibration signal of amplitude equal to approximately 30 percent of the full-scale strain signal is superimposed. Next, these signals are transmitted by an AC FM transmitter which is identical to Module A.

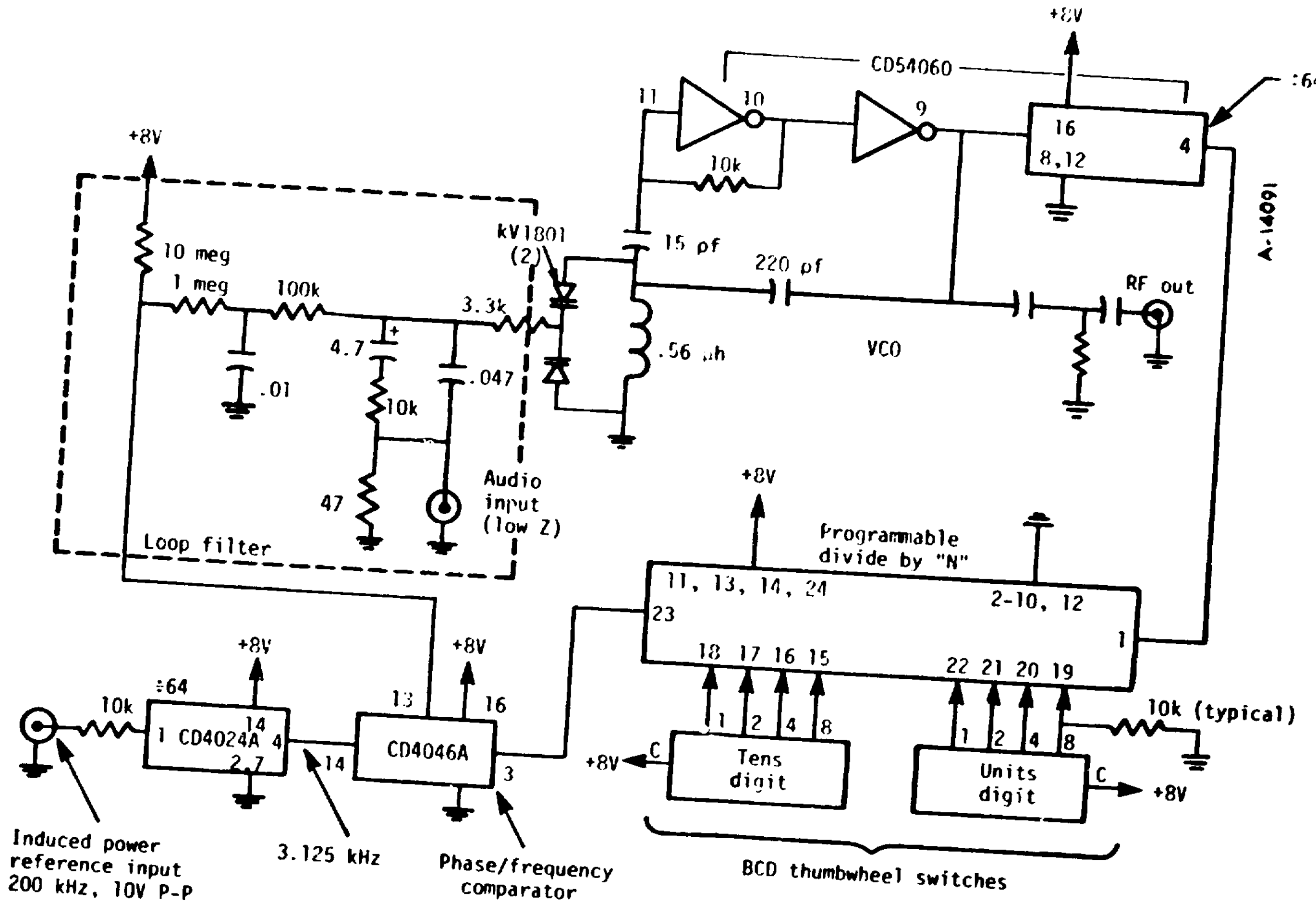

Figure 2-3(a). Schematic diagram breadboard phase-locked transmitter.

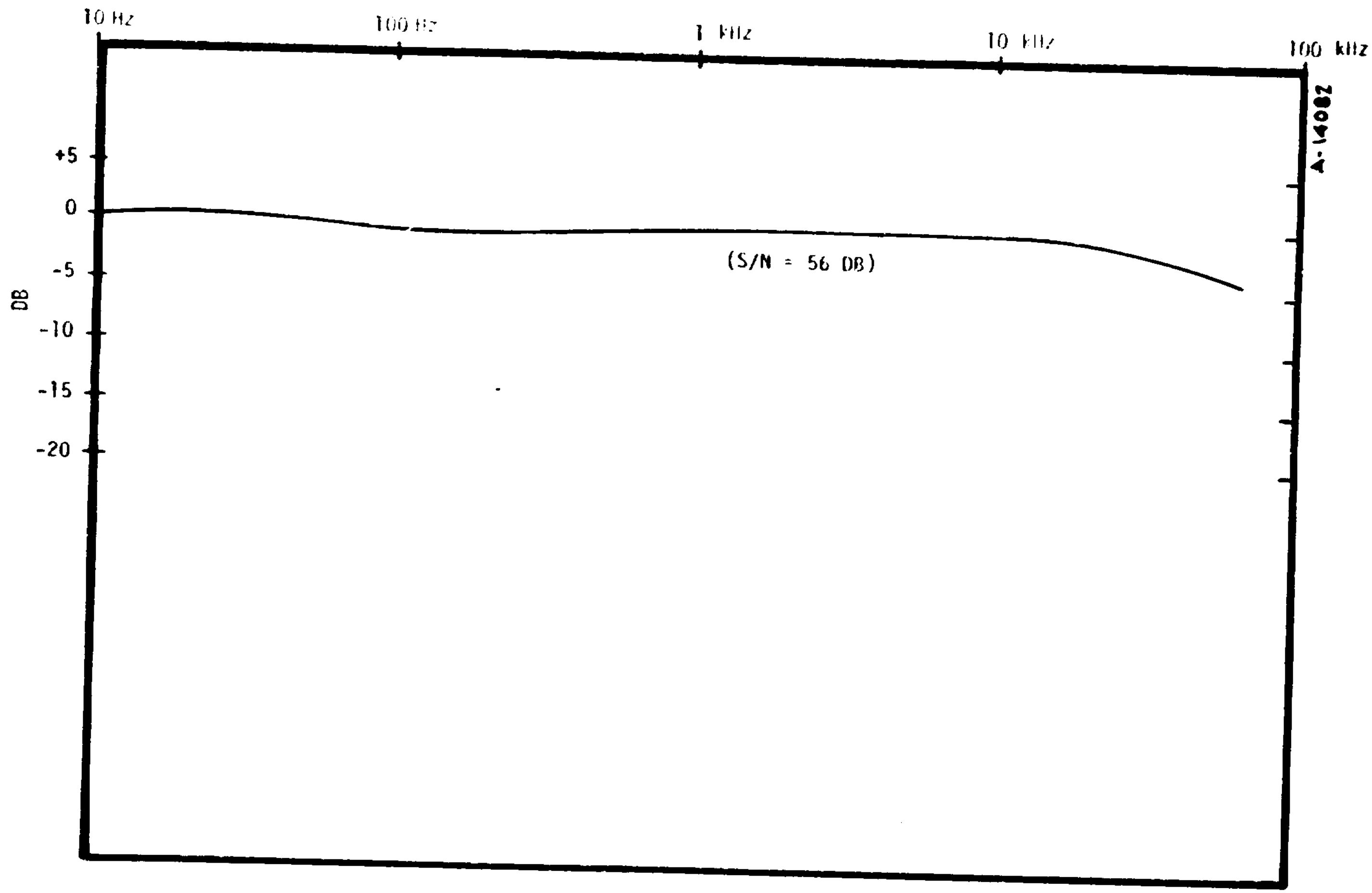

Figure 2-3(b). Frequency response of breadboard phase-locked transmitter-receiver link.

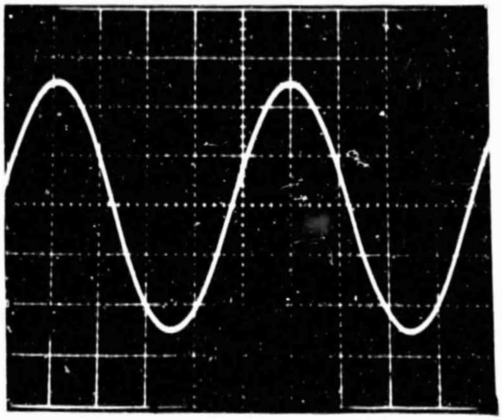

20 Hz - Sine Wave

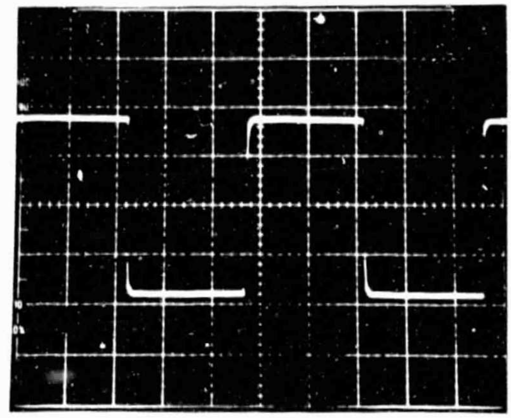

AD/S-081

2 KHz - Square Wave

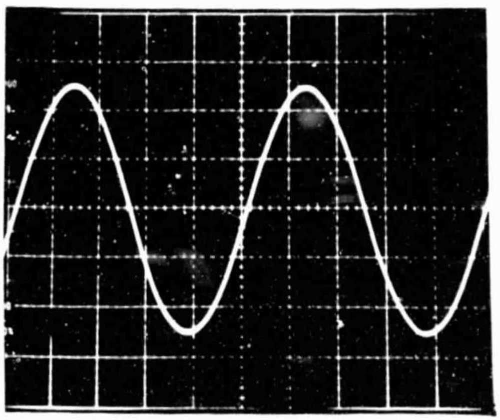

2 KHz - Sine Wave

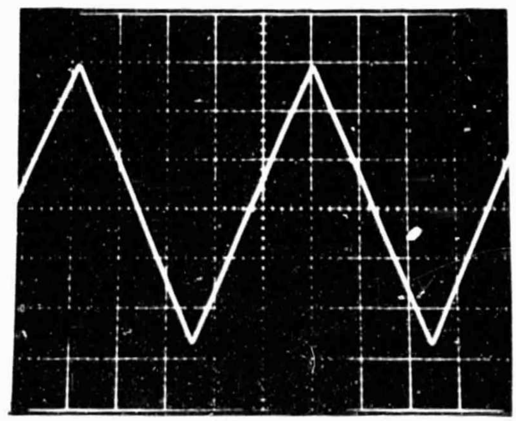

2 KHz - Triangular Waveform

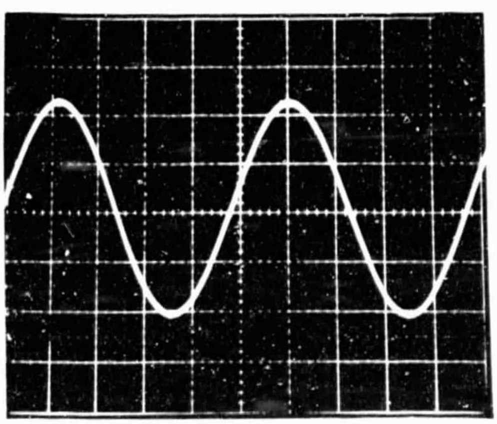

20 KHz - Sine Wave

Figure 2-3(c).

Oscilloscope photos of actual received signals from "Breadboard" phase-locked transmitter-receiver link.

AD/S-082

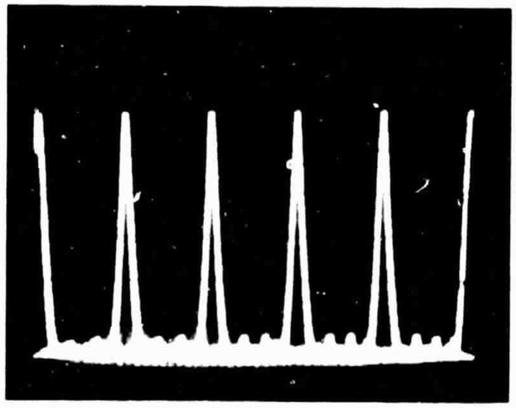

Un-modulated

FM Modulated
+ 75 KHz deviation

Scale = 200 KHz/division (horizontal) and
10 DB/division (vertical)

Figure 2-3(d). Spectral analysis of multiple frequency settings of phase-locked transmitter.

PRECEDING PAGE BLANK NOT FILMED

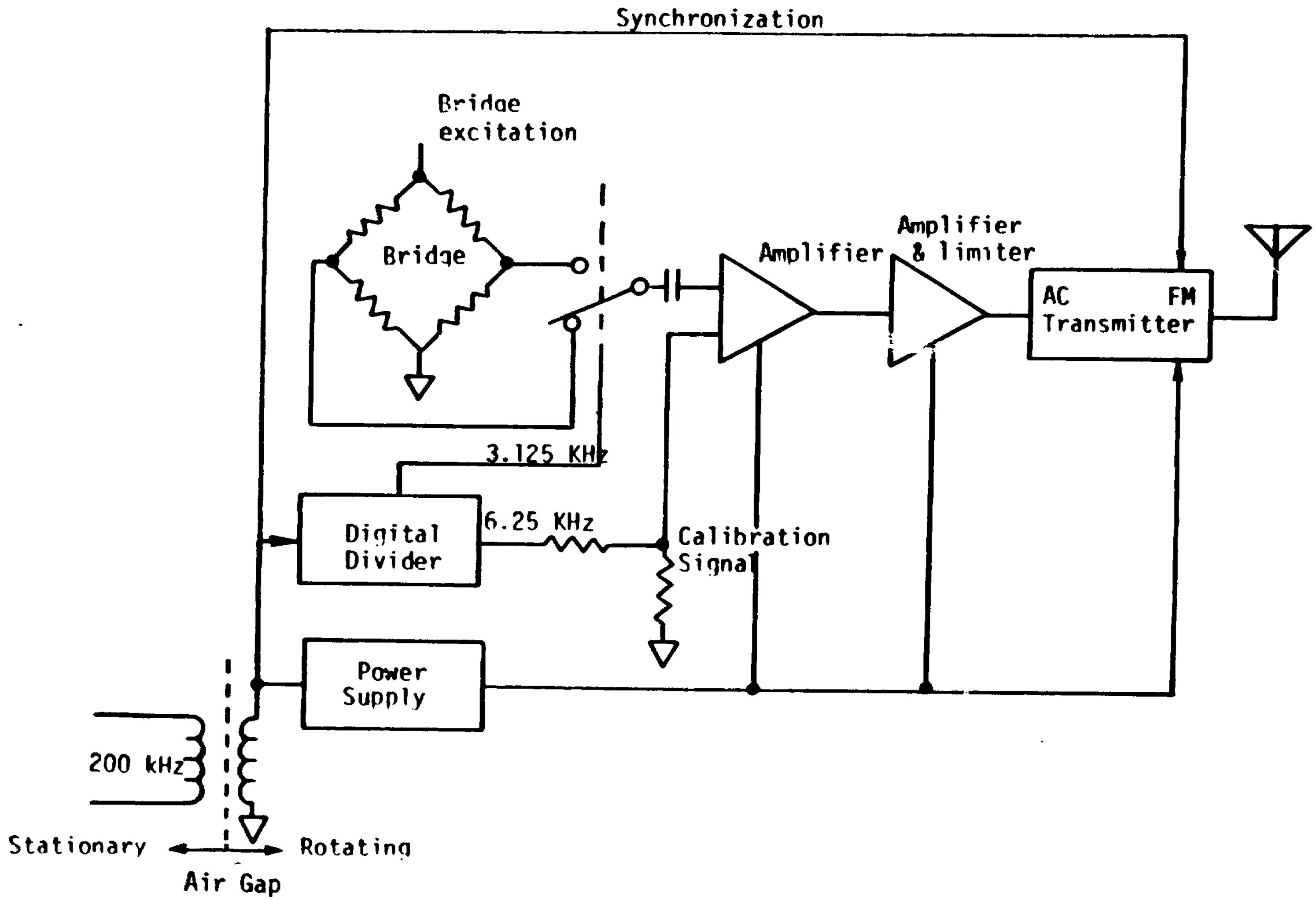

Figure 2-4. Static strain transmitter.

PAGE 18 INTENTIONALLY BLANK

2.4 MODULE C -- TEMPERATURE TRANSMITTER

This module, when used in conjunction with Module A, provides six channels of temperature measurement.

Referring to Figure 2-5, it consists of an analog scanner which sequentially selects 10 separate voltage levels for transmission. Six of the levels are thermocouple outputs. The remaining levels are synchronization, zero, a calibration voltage and a voltage proportional to the module's internal temperature which is used to derive information for automatic cold junction compensation. In order to provide isolation between the channels both the positive and the negative thermocouple leads are switched by the scanner. Each channel is scanned once every 2 milliseconds, which provides a frequency response of DC to 25 Hz for each channel.

2.5 TRANSMITTER PACKAGE DESIGN

Prior experience with Acurex model 218H, 218Q and 215H transmitters had indicated that hybrid microelectronic circuit fabrication methods were suitable for operation in gas turbine engines. Additional studies under Air Force contract number F33615-75-C-2055 probed the feasibility of operating hybrid circuits at temperatures up to 175°C. This study showed 175° operation to be feasible but identified reliability as a significant problem for any type of circuitry at high temperature.

When considering the various circuit construction techniques available today, hybrids continue to be the choice for the gas turbine environment. Perhaps in the future these hybrids may be simplified by greater application of monolithic I.C.'s. But considering the limitations of the monolithic process (such as capacitor size) it is unlikely that the hybrids will be totally replaced.

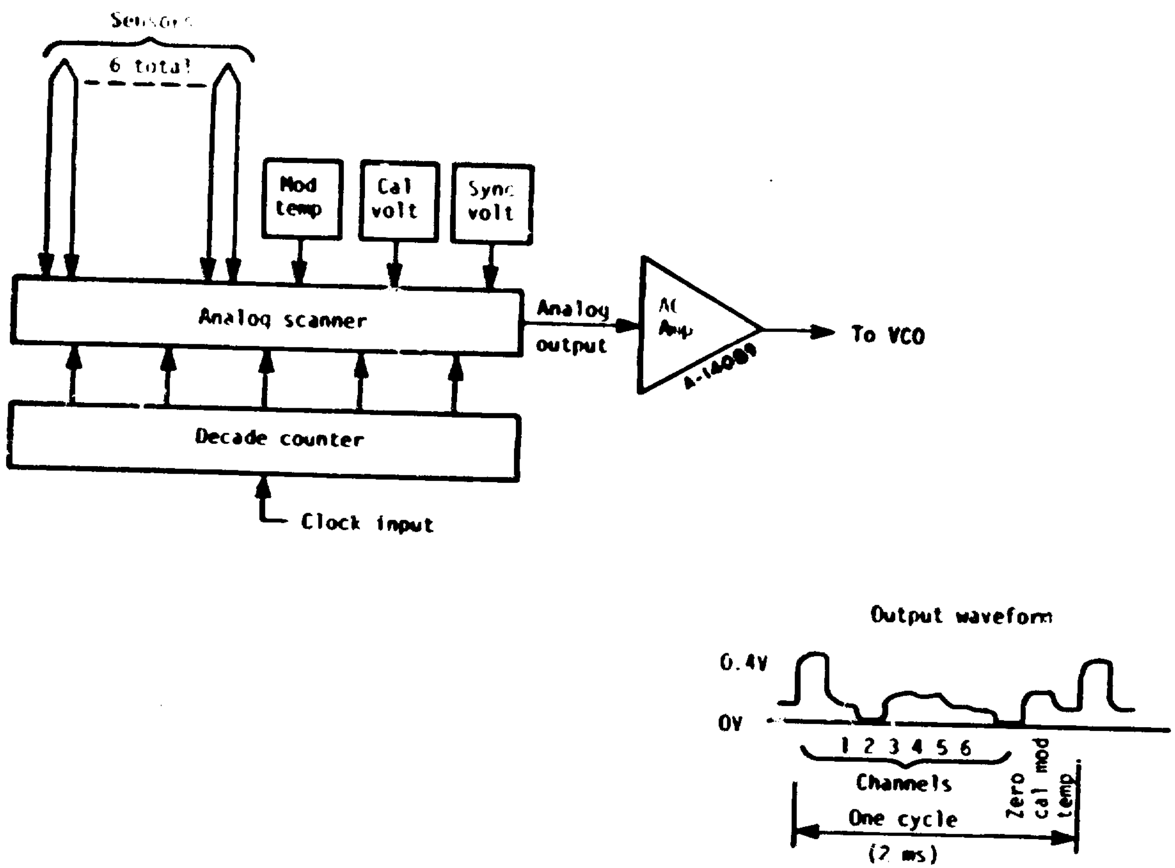

Figure 2-5. Six-channel thermocouple multiplexer/modulator.

The package design of the new transmitter module marks the first case of a design tailored to contain a hybrid circuit. (Note that earlier hybrid transmitter modules were adaptations of existing non-hybrid form-factors.) The hybrid substrate is of a relatively thin, flat configuration. Thus a flat package houses it most efficiently.

The packaging scheme is illustrated in Figure 2-6 which shows a group of transmitters mounted in an engine. Drawings E25506 and E25507 (see Appendix K) show details of the package design. It consists of a shallow metal cavity which houses two hybrid substrates. A support wall in the central area is necessary to reduce stress in the bottom at high centrifugal force (up to 50,000 g's). Some of the sidewalls of the package are drilled to receive feedthrough terminals which connect the circuit to the external transducers, power coil, antenna, and carrier frequency programming jumpers.

Normally these feedthrough terminals would be set in fuzed glass or brazed ceramic sleeves, however, cast epozy sleeves were developed for this application for several reasons:

1. Stress analysis indicated that heat-treated steel was essential. The thermal processes of glass or ceramic sealing and heat-treating are incompatible.
2. Stress analysis indicated that elastic deformation of the metal sidewalls (under high centrifugal loads) would be likely to crack a brittle (glass or ceramic) seal and cause a leak

The epoxy sealing process is performed at 165°C and does not interfere with the (prior) heat-treating of the steel. Furthermore the epoxy seal is relatively elastic and less likely to crack under high g's.

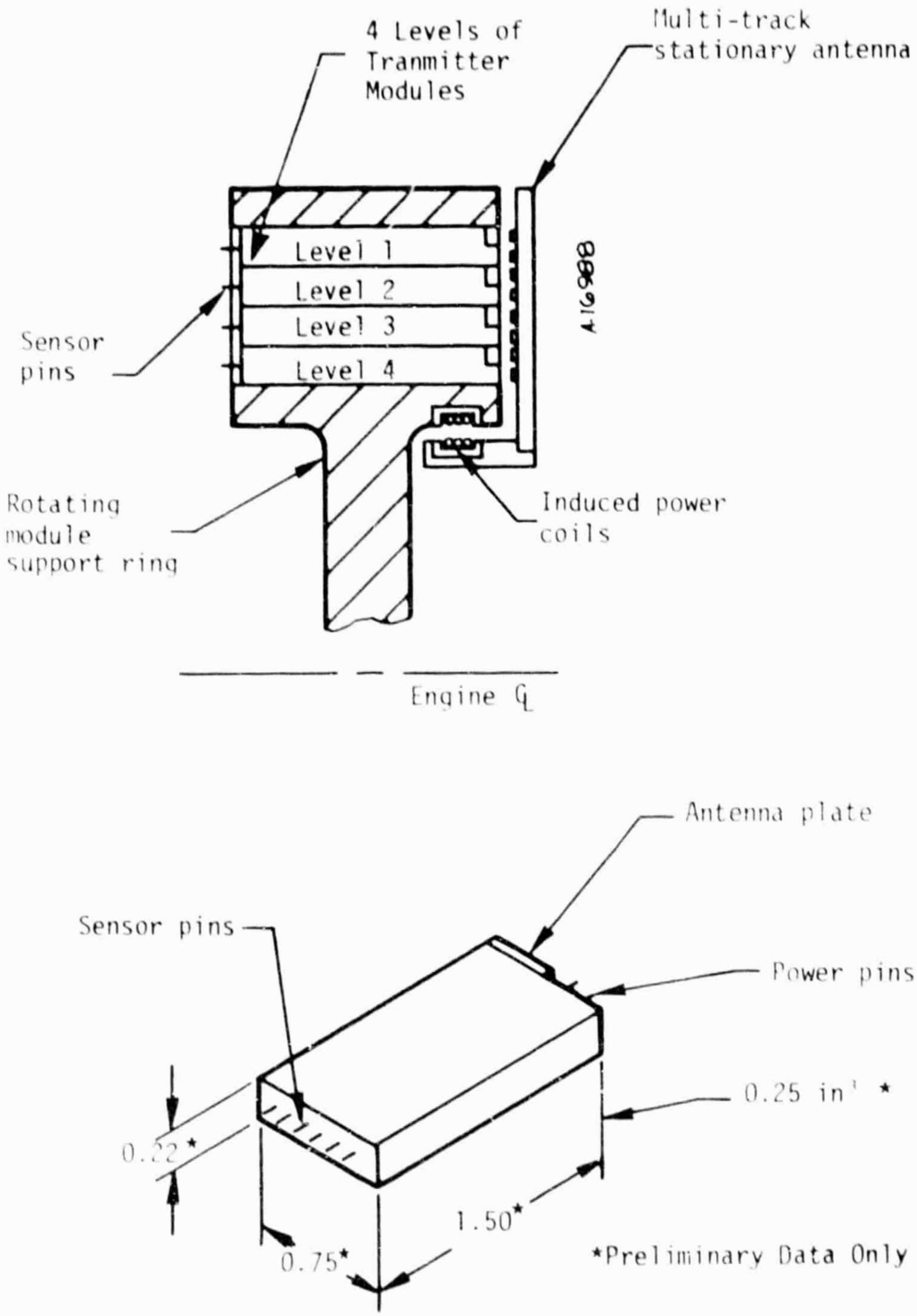

Figure 2-6. Module design and installation.

Although an epoxy seal is not truly hermetic, epoxy lid-seals have proven to be acceptable in other Acurex transmitters which operate in the gas turbine environment.

Pin sealing was performed by temporarily supporting the pin in the center of the hole with a sleeve of glass filled Teflon (Fluorocarbon Corp. "Fluorogold") which extended about halfway into the hole. Epoxy was then applied around the pin and heat cured. After cure the Teflon sleeve was extracted and a second application of epoxy filled the remaining portion of the hole.

Two general families of epoxies were treated for this purpose:

1. High Adhesion Epoxy

   DGEBA resin prereacted with 12 percent CTBN (nitrile rubber) and cured with dicyandiamide. Small amounts of accelerator were also included, to improve high temperature strength rather than to speed up the cure. Also various fillers were tested to enhance high temperature strength.

   All seals made with these materials developed small cracks after the hot spin test (40,000 g's and 175^{o}C for 2 hours). Soldering (to the pins) was also tried with good results.

2. High Temperature -- Low Adhesion Epoxy

   DGEBA resin prereacted with 12 percent CTBN and cured with 50 PHR PMDA (pyromellitic dianhydride). This results in an extremenly hard and temperature resistant cured epoxy, but of relatively low adhesion (as compared to the previous family).

   All seals made with this material successfully passed the hot spin and soldering tests and thus this material was employed in the prototype module and subsequently passed additional hot spin and solder testing.

Despite the initial successful results with this material Acurex still has some reservations about its ability to withstand repeated abuse and soldering and thus further testing and development may be conducted during phase II of this development program.

Appendix F provides details of the stress analysis on this package.

2.5.1 Prototype Module Fabrication and Test

The prototype module was fabricated without the phase-locked VCO due to inavailability of the RCA frequency synthesizer I.C. Figure 2-7 is a photograph of the completed module.

The following environmental tests were conducted.

Spin Test Schedule

Step	Temperature	G's	Duration
1	$20^{o}C$	40,000	1 hr
2	$120^{o}C$	40,000	1 hr
3	$150^{o}C$	40,000	1 hr
4	$175^{o}C$	40,000	1 hr
5	$175^{o}C$	40,000	4 hrs

Module performance recorded after each step was as follows:

Dynamic Strain Module Spin Test Data

Step	DC Supply	Self Test	Amplifier Response		
	Voltage	Signal Output	Gain Stability	f_L (-3db)	f_H (-3db)
1	+ 10.010	0.727 vrms	1	15 Hz	32 kHz
2	+ 10.016	0.881 vrms	-0.4%	15 Hz	32 kHz
3	+ 10.013	0.838 vrms	-0.272%	15 Hz	32 kHz
4	+ 10.013	0.762 vrms	-0.272%	15 Hz	32 kHz
5	--	--	--	--	--

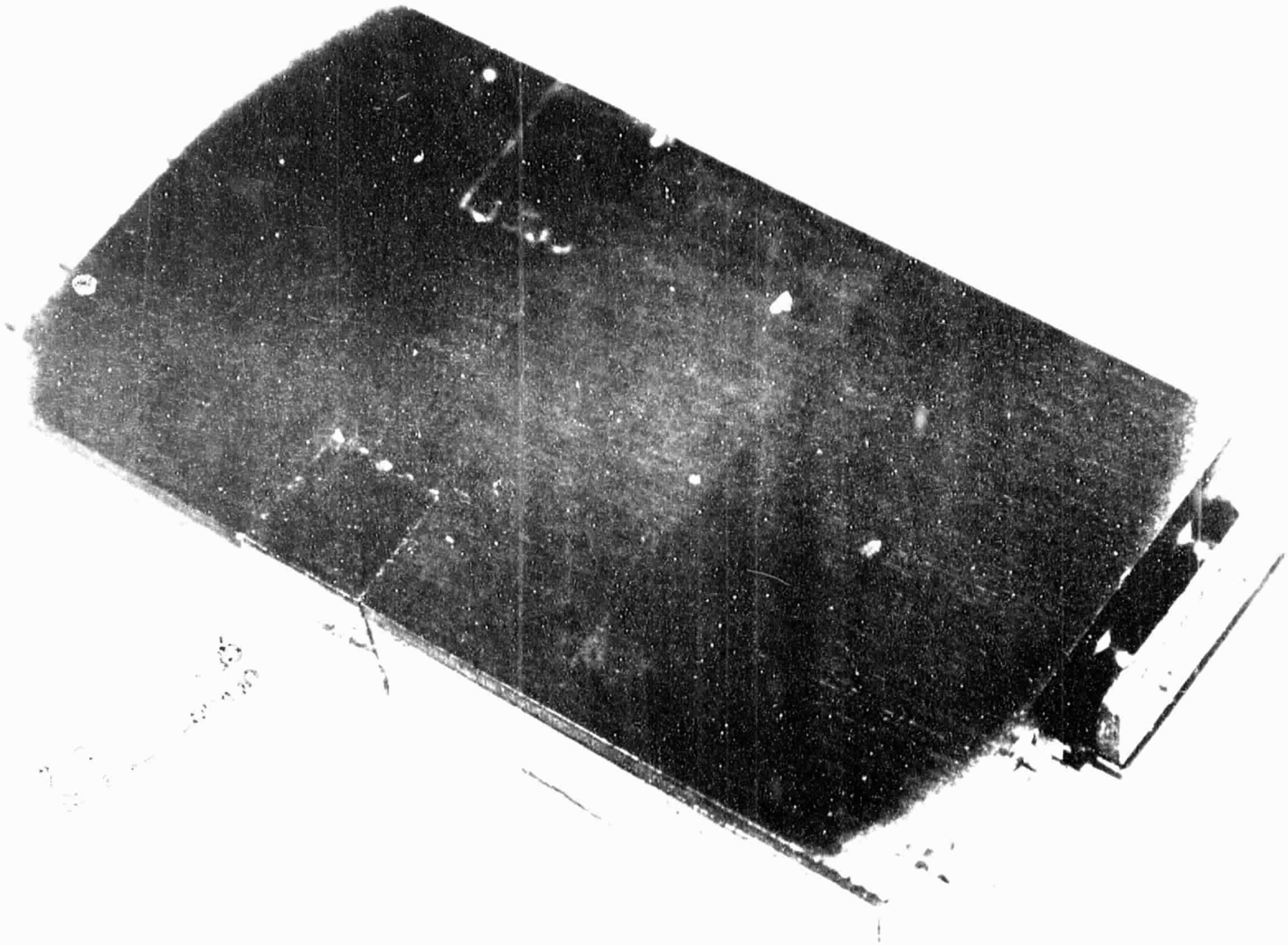

Figure 2-7(a). Exterior view of module.

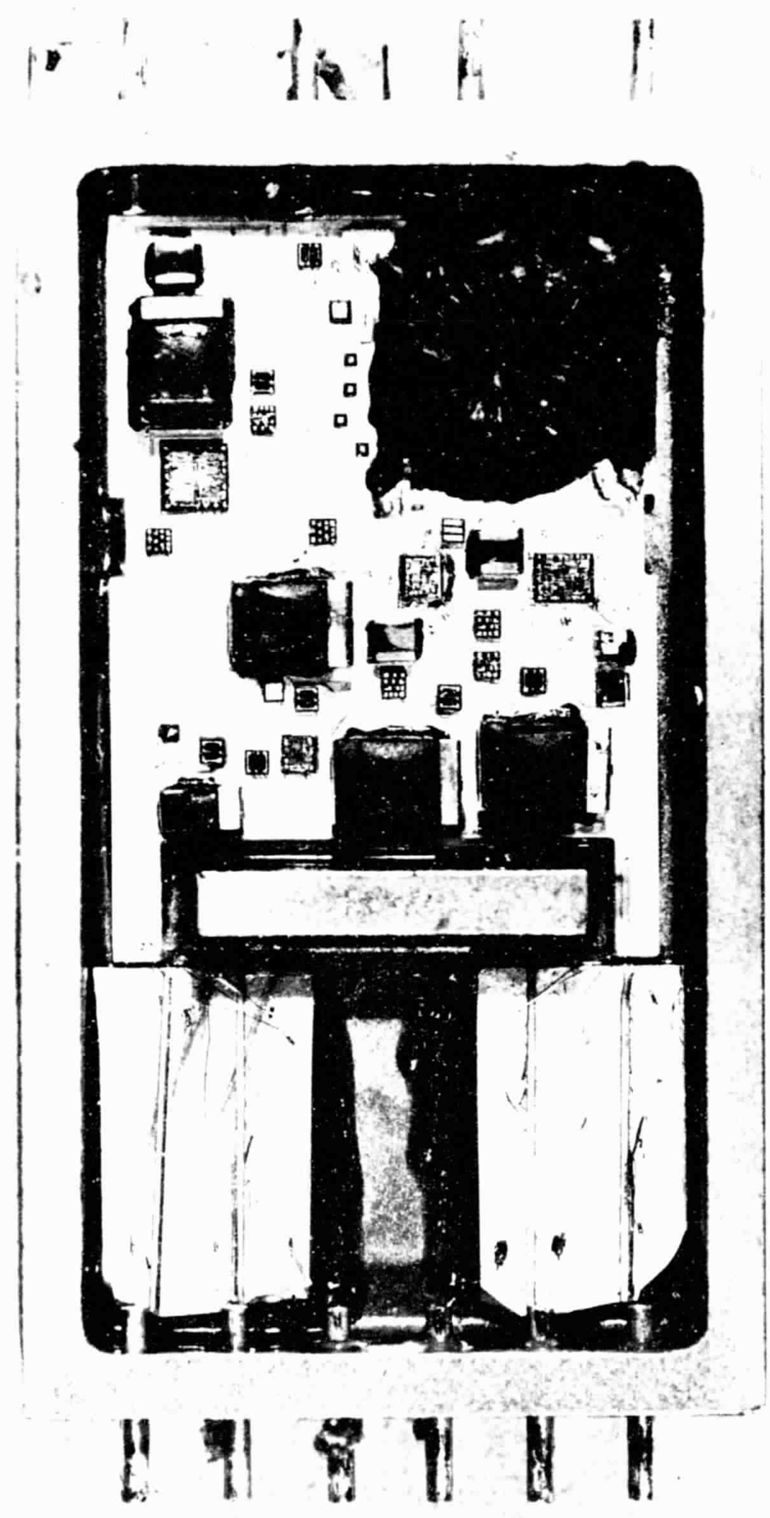

Figure 2-7(b). Interior view of module.

PAGE 28 INTENTIONALLY BLANK

During step 5 the modules' voltage regulator I.C. (A723) lost its internal reference voltage. Subsequent visual inspection revealed that a microscopic (foreign) metal particle had penetrated the device's protective coating and shorted two conductor traces together. The transmitter cover was not sealed during these tests thus this type of failure was not deemed to be characteristic of the overall design and thus the test was judged to be successful. The mechanical integrity of the module was excellent throughout the entire test. Specifically the components, component attachments, wire bonds and feedthrough seals were not visibly affected by the environmental stress.

After replacement of the A723 voltage regulator, an operational amplifier (CA3130) was discovered to be electrically bad. It is not known if this failure occurred during step 5 testing or during subsequent rework handling. However a group of ten CA3130's were subsequently subjected to extensive testing, including 144 hours burn-in at 175^{o}C, with no failures.

2.5.2 <u>Screening of electronic components for improved operation at 175^{o}C in hybrid microelectronic circuits</u>

Assuming that a certain type of component has been determined to be capable of functioning satisfactorily at 175^{o}C and thus designed into a transmitter circuit, a problem remains regarding how to screen these components for use in production assemblies. With conventional "discrete" circuit assemblies, burn-in (active aging at elevated temperature) has been proven to be the most effective screening method. Unfortunately burn-in is not possible with chip components which are used in hybrid microelectronic circuit assemblies. This is because there is no satisfactory method of applying voltages to the chips during aging.

Many manufacturers of hybrid circuits assemble un-screened chip components onto the circuit substrates prior to performing any tests. If a defective component is discovered at this stage it can be replaced, or (rarely) the entire substrate can be discarded.

Other manufacturers test selected critical components by making temporary electronic contact with delicate probes. While probing systems are the industry standard for testing groups of semiconductor devices in wafer form (prior to scribing), their use on individual chips is far more tedious and thus limited. Some people even recommend against the testing of individual chips because this represents a second probing of the delicate aluminum pads (the first probing was performed while the chips were joined together in the wafer) which could cause mechanical degradation. These people sometimes test chips on a lot sample basis only.

Others have developed the art of probing the delicate pads with extreme care and find it worthwhile to perform 100 percent testing on chips. The most notable hybrid manufacturer doing this is Teledyne Microelectronics in Culver City, California. Their large volume of 1 million chips per week has permitted them to develop the chip probing process to a fine art. However, although they are willing to test chips for other manufacturers (such as Acurex) their present methods are limited to 125^{o}C. Also, the cost of setting up screening programs would have to be borne by a relatively small number of devices.

The cost of testing and screening electronic components can easily add orders of magnitude to the component's base price (with standard testing). At present the economics of rotary instrumentation programs can not justify these high added costs. Also the relatively small production volume of these rotary instrumentation systems further hinders the development of optimal screening methods. Acurex has tried to induce semiconductor manufacturers to perform special high temperature screens during wafer probing but when they learn that the quantities required represent less than 0.01 percent of their annual volume they suddenly become very uninterested.

At the present time Acurex employs a variety of screening methods for chips used in hybrid circuits. These methods include:

1. Rigid 100 percent visual inspection
2. Lot sample testing
3. One hundred percent probe testing on critical or problem components
4. Special acceptance criteria during the manufacturer's wafer probe-test (or final test for components other than semiconductors)

(In addition to these component tests, assembled circuits are burned-in.)

Test 3 (chip probe-tests) offers an opportunity for further development tailored to high temperature screening. For example chips might be probed at extreme temperatures (200 - 300^{o}C) and voltages well in excess of normal. This test, nicknamed the "zap test", would be an attempt at condensing the time of a burn-in (normally 168 hours) down to a few seconds (or minutes). However, it is beyond the scope of this present instrumentation development program to pioneer such new testing technologies which would require costly large samples and subsequent life testing to establish meaningful evidence of their value.

SECTION 3

STATIONARY ELECTRONICS

3.1 INTRODUCTION

The units to be discussed are:

- Dynamic strain receiver
- Static strain signal conditioner
- Temperature signal conditioner

Tentative performance specifications for the receiver will be given.

3.2 DYNAMIC STRAIN RECEIVER

A study of several receiver types indicated that the frequency-synthesized superheterodyne and the tracking phase-locked receivers are the most likely candidates. Both have advantages and disadvantages. Briefly, the superheterodyne receiver requires less circuitry but high quality passive filters. On the other hand, the tracking phase-locked receiver utilizes simple filters but a fairly large amount of digital circuitry. It is estimated that the cost of either system is about the same, although the power consumption of the tracking phase-locked receiver may be somewhat higher. Further details will be discussed in the next sections.

3.2.1 Performance Specifications

Tentative dynamic strain receiver performance specifications are shown in Tables 3-1 and 3-2. Whereas the monitor output contains strain

TABLE 3-1. RECEIVER INPUT SPECIFICATIONS

Channel Input	Number of channels Adjacent channel spacing Carrier frequency range Single carrier rms level Combined carrier peak level Type of modulation Frequency deviation Audio frequency range	52 0.2 MHz 10.4 MHz to 20.6 MHz 0.1 mV to 10 mV 400 mV maximum Frequency $\pm$ 75 kHz nominal DC -- 50 kHz
Digital Inputs	Number of channel select line Type of code	2 x 4 2 -- digit complement of 9's complement

TABLE 3-2. RECEIVER OUTPUT SPECIFICATIONS

Analog Outputs	Signal to noise ratio (20 Hz to 50 kHz) Harmonic distortion Voltage level stability Output peak voltage	>40 dB <1 percent $\pm$1 percent $\mp$2V
Composite Output	Frequency range	DC -- 40 kHz (-3 dB)
Monitor Output	Frequency range	DC -- 20 kHz (-3 dB)
Digital Outputs	Carrier strength indicator: yields an "INVALID DATA" output when the desired rms carrier level drops below 0.1 mV	
	Gage failure indicator: yields an "INVALID DATA" output for open gages Level detection of a 40 kHz self-test signal is used for this purpose	

Note: At the time this report was prepared, minor changes of specifications are expected to occur.

data only, the composite output contains also the 40 kHz self-test signal. It is intended that the monitor output be used for visual monitoring only and that the composite output be recorded for analysis after the test. Thus the 40 kHz test signal is also recorded and available for post-test verification of gage continuity and transmitter integrity.

3.2.2 Theoretical Considerations

In relation to the reception of phase or frequency modulated RF carriers, theoretical consideration has been given to the following topics:

- Signal-to-noise (S/N) ratios of phase modulation (PM) versus frequency modulation (FM) (Appendix C)
- Transmission bandwidth (Appendix A)
- Adjacent channel interference (Appendix B)
- Common channel interference (Appenidix B)

Referring to Figure 3-1, it is assumed that the carriers on a given antenna track are separated by 0.4 MHz and that f_c and f_p represent the desired and the undesired channel frequencies, respectively.

Furthermore we define:

$f_c = \omega_c/(2\pi)$

$f_p = \omega_p/(2\pi)$

$f_b = \omega_b/(2\pi)$ = half of the receiver bandwidth

$\Delta f = \Delta\omega/(2\pi)$ = adjacent channel frequency difference

$\Delta f_c = \Delta\omega_c/(2\pi)$ = frequency deviation of f_c

$\Delta f_p = \Delta\omega_p/(2\pi)$ = frequency deviation of f_p

$F_c = \Omega_p/(2\pi)$ = modulating frequency of f_c

$F_p = \Omega_p/(2\pi)$ = modulating frequency of f_p

$\beta_c = \Delta f_c/F_c$ = modulation index of f_c

$\beta_p = f_p/F_p$ = modulation index of f_p

$F_v = \Delta\Omega_v/(2\pi)$ = receiver audio bandwidth

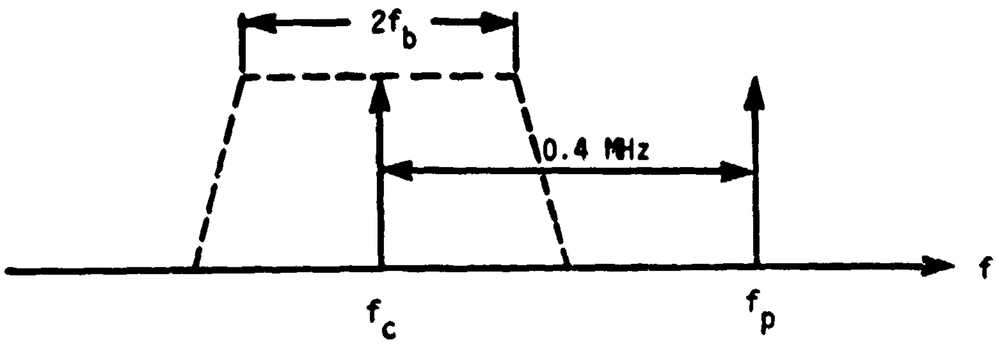

Figure 3-1. RF Spectrum

3.2.2.1 S/N Ratios of PM Versus FM

It has been shown in Appendix C that when the receiver input consists of an angle modulated carrier and white noise of constant spectral density, the S/N ratio of PM is higher than the S/N ratio of FM without frequency deemphasis of the receiver (and emphasis at the transmitter). With deemphasis, however, there exists a value of the modulating (audio) frequency beyond which FM yields an improvement over PM. This value is determined by the total audio bandwidth and by the roll-off frequency of the deemphasis network. FM has been selected over PM due to its simpler implementation and proven performance in these systems.

3.2.2.2 Transmission Bandwidth

It may be shown that when an RF carrier is frequency modulated with a single sinusoidal signal, an infinite array of side bands are generated. Since the actual bandwidth must be finite, it is evident that harmonic distortion of the modulating signal is introduced.

The mathematical determination of this distortion is a complex affair and has not been attempted here. Instead, we utilize an empirical formula known as Carson's rule in which case the half bandwidth is given by:

$$f_b \geq F_c + \Delta f_c$$

For $F_c = 30$ kHz and $\Delta f_c = 75$ kHz, we find $f_b \geq 105$ kHz.

This bandwidth is normally used for high quality FM broadcast receivers.

3.2.2.3 Adjacent Channel Interference

Referring to Figure 3-1, let the receiver be tuned to f_c and consider the interference of the side bands of f_p with the side bands of f_c. It is assumed that f_c is modulated with a very low audio frequency so that virtually all side bands of f_c are contained within a bandwidth which is equal to twice the frequency deviation of f_c.

With F_c and F_p being the modulating (audio) frequencies, the signal-to-noise ratio is defined by:

$$S/N = \left. \frac{\text{RMS audio voltage output due to } F_c}{\text{RMS noise voltage output due to } F_p} \right|_{F_c \rightarrow 0}$$

It is shown in Appendix B that with equal carrier amplitudes, 400 kHz channel separation, ± 75 kHz frequency deviations and a receiver audio frequency range of DC - 40 kHz, the S/N ratios amount to 1000 db with $F_p = 20$ Hz and 146 db with $F_p = 30$ kHz.

Hence, adjacent channel interference may be neglected.

It should be realized that the above results are valid for an ideal discriminator only. Assuming, however, that the discriminator saturates beyond a maximum frequency deviation of ±75 kHz, it is evident that the adjacent carriers located at $\pm$ 400 kHz will cause distortion. Requiring that the discriminator output voltage at 400 kHz amounts to less than one percent of the voltage at 75 kHz, it is found from Appendix B that a bandpass filter is required with an attenuation of more than 50 dB at 800 kHz bandwidth

3.2.2.4 Common Channel Interference

Presently, the undesired (f_p) and desired (f_c) carrier frequencies are assumed to be equal. We distinguish two cases, e.g., Case I: Desired carrier modulated and undesired carrier unmodulated, and Case II: Desired carrier unmodulated and undesired carrier modulated. The analysis assumes that in either case the modulating signals are sinusoidal and that the frequency deviation is $\pm$ 75 kHz.

Case I

This case is the most important of the two since it enables us to study the capture effect of an FM receiver. Let us suppose that the desired carrier amplitude and its modulating signal is held constant and that the undesired carrier amplitude is increased from zero to a value which is less than but near to the value of the desired carrier amplitude. Let us also suppose that the receiver is ideal, i.e., it possesses an infinite RF bandwidth and a linear frequency discriminator of unrestricted dynamic range.

It is then found that the audio output consists of two components. The first component consists of the modulating sinewave. It is essential to note that its amplitude remains constant. The second component consists of a beat frequency whose amplitude increases. The beat frequency depends on both the modulation index and the modulating frequency. Since the average value of the beat frequency is zero and the beat frequency is usually higher than the modulating frequency, it can be removed by lowpass filtering.

This way, the receiver has "captured" the stronger carrier and ignores the weaker carrier. Let us now assume that the discriminator saturates beyond a certain signal level and that the beat frequency peaks are being clipped beyond this level. The results are that the average value of the beat frequency is no longer zero and that the amplitude of the modulating sine wave is reduced by this.

In order to obtain a measure for the capture ability of the receiver, let us define the capture ratio as A/B where A is the desired carrier amplitude and B is the undesired carrier amplitude at which the modulating signal reduces by 1 percent.

In view of the above it can be concluded that the desired small capture ratios can be achieved by:

- Large receiver bandwidth and linear phase response
- Large discriminator bandwidth with good linearity

Further details can be found in Appendix B.

Case II

In this case we consider the maximum allowable crosstalk that can exist between two adjacent antenna tracks operating at the same carrier frequency. It is assumed that only the undesired carrier is modulated. Let D and U represent the amplitudes of the desired and undesired carriers, respectively. Using a sinusoidal modulating signal, the signal-to-noise ratio will be defined as S/N where S and N are the peak audio voltage values at the receiver output with the presence of U and D + U, respectively. Using the standard receiver (Acurex Model 149 with 30 kHz cut-off frequency) and 100 Hz modulating frequency, the measured S/N values as a function of the modulating frequency deviation are given in Table 3-3.

TABLE 3-3. CROSSTALK EFFECTS

Frequency Deviation (kHz)	Audio Output S/N	R.F. Input D/U
$\pm$ 75	20:1	10:1
50	10:1	10:1
25	7.5:1	10:1
10	6:1	10:1

An approximate mathematical analysis (see Appendix B) as well as additional measurements generally showed that:

- S/N $\approx$ D/U when the modulating frequency deviation is less than the receiver audio cut-off frequency
- S/N $\approx$ (D/U) . (frequency deviation/cut-off frequency) when the frequency deviation is larger than the receiver audio cut-off frequency. The value of S/N is practically unaffected by the value of the modulating frequency.

Let us now assume that each of the two adjacent antenna tracks is fed with a carrier of equal amplitude and frequency. It is evident from the above that D/U then represents the required attenuation factor for a given value of S/N. Since the required value of S/N should amount to at least 100 (40 db) in the present system, the minimum attenuation should be equal to this number. Unfortunately, this amount is difficult to achieve for two adjacent tracks.

Thus it was decided to avoid using identical carrier frequencies on adjacent tracks. This is easily accomplished by selecting odd-numbered carrier frequencies for one level or tracks and even-numbered carriers for adjacent levels or tracks. An example of carrier allocations is shown in Table 3-4. With this method of channel separation it was found experimentally with the Model 149 receiver that the undesired carrier amplitude (modulated with $\pm$ 100 kHz frequency deviation) need be only 6 db below the desired carrier amplitude in order to eliminate crosstalk. Twenty-one db is the least signal difference we have ever measured between adjacent tracks, with the preferred antenna design, thus adequate signal separation is easily achieved. (See Appendix I.)

3.2.3 The Superheterodyne Receiver

Referring to Figure 3-2, the operation is as follows. Consider a single channel carrier at frequency $f \pm \Delta f$, where f is the center frequency and Δf is the frequency deviation. After mixing this carrier with f + 10 MHz at MIX 1 and bandpass filtering with BP2, the difference frequency $\mp$ f + 10 MHz results. The frequency f + 10 MHz is a multiple of the 0.2 MHz reference clock. Its value is determined by the frequency division ratio N of a digital counter which forms part of a phase-locked loop. The remaining part of this loop consists of a frequency/phase detector FPD, a lowpass filter LP1, and a voltage - controlled oscillator VCO.

After limiting the amplitude of the output of BP2 at LIM, the signal is mixed with 9.5 MHz at MIX2. The resulting difference frequency $\mp\Delta f$ + 0.5 MHz is then fed to a frequency detector FMD which will

TABLE 3-4. TYPICAL FREQUENCY ASSIGNMENTS FOR A FOUR-TRACK 102-CHANNEL SYSTEM

Carrier Number	Track A (26-Ch)	Track B (25-Ch)	Track C (26-Ch)	Track D (25 Ch)
1	10.2 MHz		10.2 MHz	
2		10.4 MHz		10.4 MHz
3	10.6 MHz		10.6 MHz	
4	↓	10.8 MHz	↓	10.8 MHz
↓		↓		↓
49	19.8 MHz		19.8 MHz	
50		20.0 MHz		20.0 MHz
51	20.2 MHz		20.2 MHz	

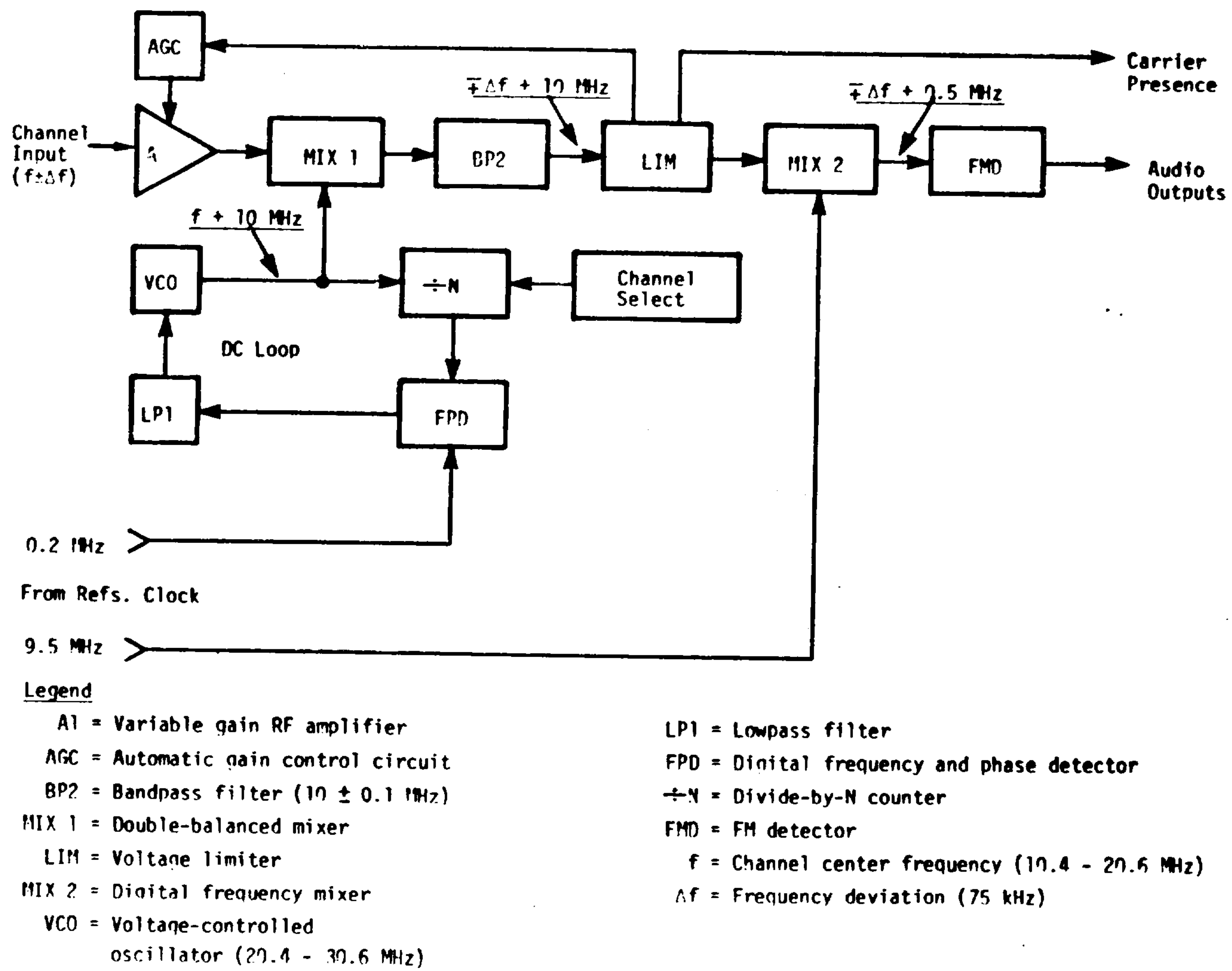

Figure 3-2. Superheterodyne receiver block diagram.

be discussed in Section 3.2.5. In order to optimize the S/N ratio and to prevent overloading, an automatic gain control consisting of AGC and variable gain amplifier A1 is required for each receiver.

3.2.3.1 Analysis

Although this type of receiver is fairly easy to implement, there are a number of items that need careful consideration. These are:

- Image frequency response
- Filter phase and amplitude response

The image frequency response can be reduced by a proper choice of the selectivity of bandpass filters BP1 (see Figure 1-1) and BP2 as well as the value of the intermediate frequency (assumed to be 10 MHz at the present). More work will be required to determine the optimal choice. In order to minimize nonlinear distortion of the frequency modulated signal, the pass band phase and amplitude response of BP1 and BP2 must also be considered. As shown in Appendix A, distortionless transmission requires a constant amplitude and linear phase response (constant group delay). Approximate expressions have been derived which relate third harmonic distortion to the following parameters (defined in the pass band):

- Number of amplitude ripples and ripple amplitude
- Number of phase (or group delay) ripples and ripple amplitude
- Frequency deviation
- Modulating frequency

As an example, consider a bandpass filter with a constant amplitude response and a 0.5 micro-second peak-to-peak group delay ripple amplitude. The ripple consists of a single period of a sinusoid. At modulating frequencies of 15 kHz and 30 kHz, the third harmonic distortions were found to be 1.5 percent and 3 percent, respectively.

3.2.4 The Tracking Phase-Locked Loop Receiver

Referring to Figure 3-3, this receiver essentially consists of three loops.

Loop 1 is a phase-locked loop and consists of voltage-controlled oscillator VCO1, analog phase detector PD1 and lowpass filter LP1. It's purpose is to obtain a digital signal at the output of VCO1 whose instantaneous frequency ($f \pm \Delta f$) is equal to that of the selected channel frequency.

The selection of this frequency is accomplished by loop 2 which consists of VCO1, digital frequency dividers $\div 32$ and $\div N$, digital frequency detector FD, and lowpass filters LP1 and LP2. As shown in Table 3-5, this loop has nonlinear characteristics, i.e., whenever the frequency of VCO1 is within a 0.2 MHz frequency band centered about the selected channel frequency f_0, it is uncontrolled by loop 2. Control is then taken over by loop 1.

TABLE 3-5. FREQUENCY DETECTOR CHARACTERISTICS

VCO1 Frequency f (MHz)	FD Output Voltage	FD Output Impedance
$f<(f_0 - 0.1)$	Low	Low
$(f_0 - 0.1)<f<(f_0 + 0.1)$	X	High
$(f_0 + 0.1)<f$	High	Low

Further details of loop 2 are given in Appendix D.

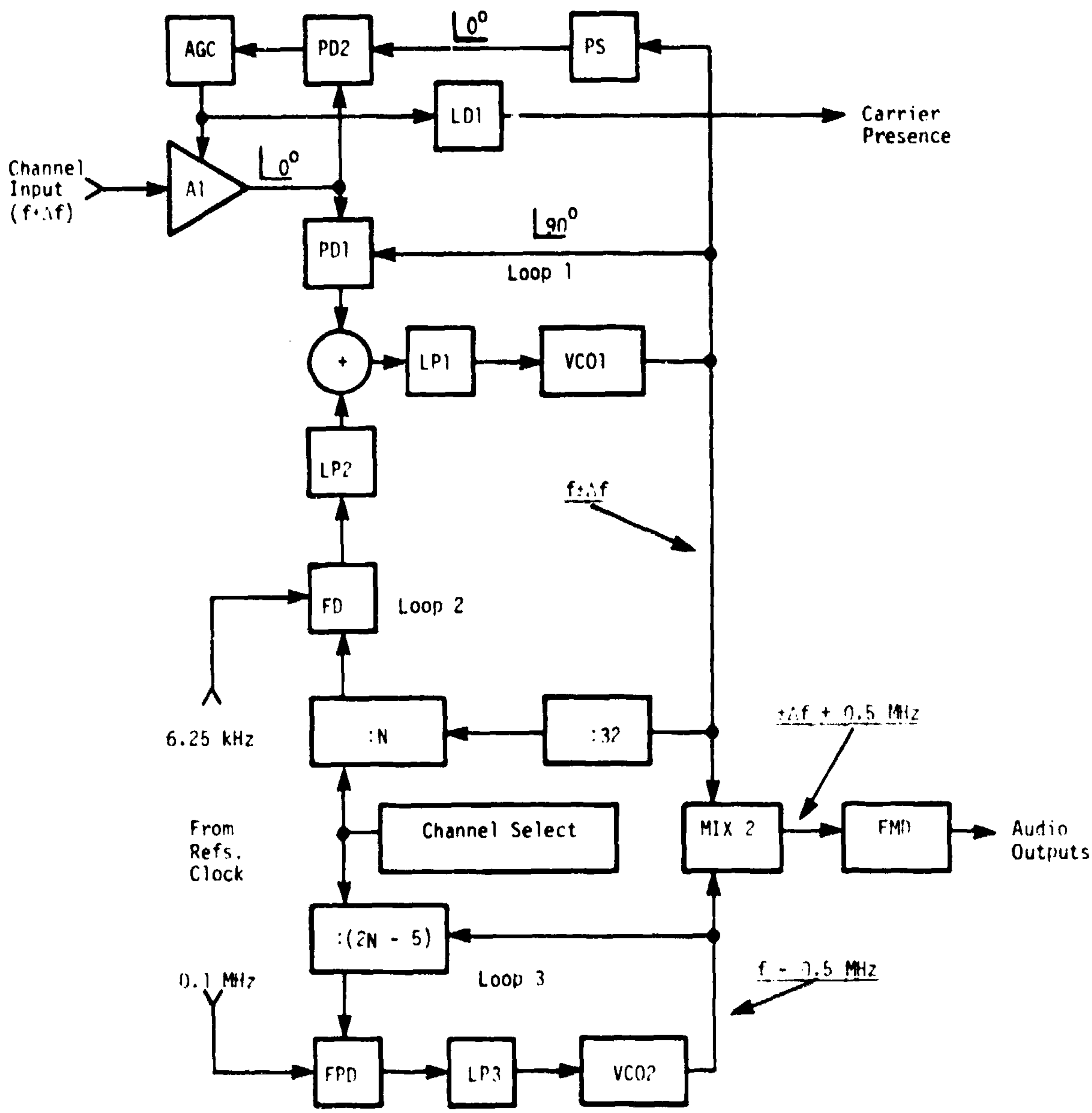

Figure 3-3. Phase-lock loop receiver block diagram.

Phase-locked loop 3 serves the purpose of generating frequency f - 0.5 MHz. It consists of VCO2, digital divider $\div$ (2N-5), digital frequency/phase detector FPD and lowpass filter LP3.

By subtracting the frequency at the output of VCO2 from that at the output of VCO1 by means of digital mixer MIX 2, there results the frequency $\pm \Delta f + 0.5$ MHz, where Δf is the frequency deviation of the modulating signal. Next, this signal is sent to frequency detector FMD which will be discussed in Section 3.2.5.

Since the closed-loop bandwidth of loop 1 (DC-50 kHz) is proportional to the carrier input level of PD 1, it is essential that automatic gain control is included. This part of the receiver consists of phase shifter PS, analog phase detector PD2, gain control circuitry AGC, and variable gain amplifier A1.

Finally, voltage level detector LD1 is included in order to sense the presence of a valid carrier.

3.2.4.1 Test Data

Tentative test data has been obtained by subjecting the receiver to a frequency comb spectrum. Spectrum details and its generation are discussed in Appendix E. The receiver was tuned to either 15.4 MHz or 15.8 MHz. Each carrier was independently modulated by a sine wave and a square wave, respectively. The peak voltage signal-to-noise ratio for either channel amounted to 32 db. It is believed that the S/N ratio can be improved to at least 40 db by applying better lowpass filtering at the audio output.

3.2.5 FM Detector

The frequency detector shown in Figure 3-4 forms part of the dynamic strain receiver. It is indicated by FMD in Figures 3-2 and 3-3. The operation is as follows.

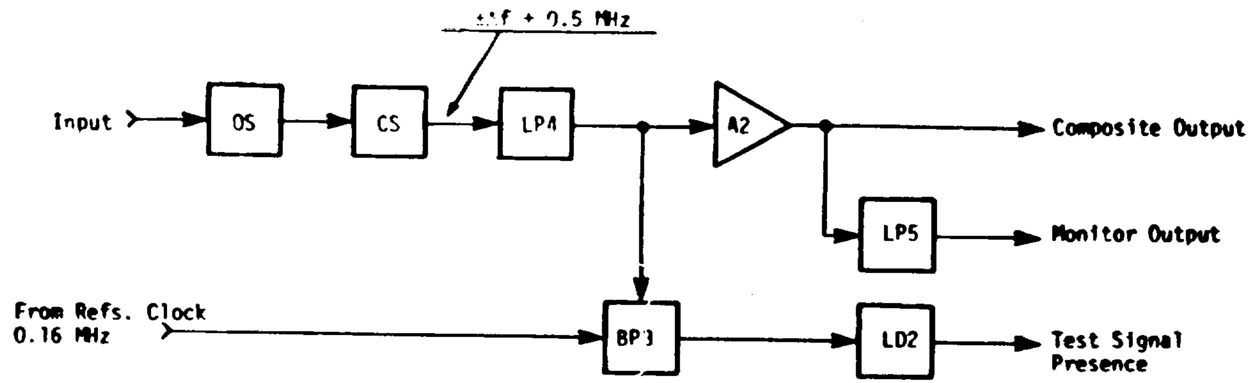

Legend

OS = One-shot (monostable multivibrator)
CS = Switching precision current source
LP4 = Three-pole filter (0-40 kHz)
LP5 = Five-pole filter (0-20 kHz)
BP3 = Commutating bandpass filter (40 kHz ± 10 Hz)
LD = Voltage level detector
A2 = Amplifier with adjustable gain
Δf = Frequency deviation (75 kHz)

Figure 3-4. FM detector (FMD) block diagram.

A frequency modulated 0.5 MHz carrier enters monostable multivibrator OS and is converted to a pulse train of constant pulse width. After passing through switching precision current source CS and lowpass filter LP 4, the average value thus obtained is proportional to the frequency deviation Δf. The composite output signal, consists of both the strain data (20Hz - 40 kHz) and a 40 kHz self-test signal. Strain data and the self-test signal are separated by lowpass filter LP5 (20 kHz cut-off frequency) and by bandpass filter BP3 (40 kHz center frequency), respectively.

In order to avoid the need for tuning, a commutating-type filter has been chosen for BP3. This way, its center frequency is governed by the 0.16 MHz reference clock.

Finally, level detector LD2 provides a digital output indicating the presence of the self-test signal.

Receiver schematics are shown in Appendix K.

CONCLUSION

Analysis and testing of the critical aspects of this phase-locked telemetry system concept have proven it to be well suited to the rotary instrumentation application. No basic system problems have arisen and testing has demonstrated performance in excess of all minimum requirements.

Phase II of the program is scheduled to result in completion of the detailed system design and fabrication and testing of a small protyotype system.

PAGE 52 INTENTIONALLY BLANK

APPENDIX A

FM DISTORTION BY TRANSMISSION NETWORKS

It is well known (Reference 1) that when a frequency modulated carrier is passed through a linear bandpass filter harmonic distortion will result due to:

- Rejection of sidebands outside the passband
- Amplitude and phase variations within the passband

Since the first item has already been discussed in Section 3.2.2 we restrict our attention in this Appendix to the latter item.

Let the filter differential equation

$$v_1(t) \longrightarrow \boxed{F(p)} \longrightarrow v_2(t)$$

be given by

$$v_2(t) = F(p)\, v_1(t) \tag{1}$$

where

$$F(p) = \sum_{i=0}^{\infty} a_i p^i, \; p \equiv \frac{d}{dt}, \; p^{(n)} \equiv \frac{d^n}{dt^n} \tag{2}$$

It should be noted that when p is replaced by $j\omega$, $F(j\omega)$ becomes the complex transfer function.

PRECEDING PAGE BLANK NOT FILMED

Furthermore, let

$$v_2(t) = V_2(t)e^{j\theta_2}, \quad v_1(t) = e^{j\theta_1} \tag{3}$$

where

$$\theta_1(t) = \omega_c t + \int \omega_d(t)dt,$$

$$\theta_1^{(1)}(t) = p\theta_1 = \omega_1(t) = \omega_c + \omega_d(t), \; \theta_2^{(1)} = \omega_2(t) \tag{4}$$

and

$\omega_2(t)$ = instantaneous output carrier frequency (rad/sec)

$\omega_1(t)$ = instantaneous input carrier frequency (rad/sec)

$\omega_d(t)$ = instantaneous input frequency deviation (rad/sec)

ω_c = constant carrier center frequency (rad/sec)

In order to proceed we require the following relation:

$$F(p)e^{f(t)} = e^{f(t)} F(p + \dot{f}), \; \dot{f} = pf = \frac{df}{dt} \tag{5}$$

Proof:

$$p^0 e^{f(t)} = e^{f(t)} = e^{f(t)} (p + \dot{f})^0, \text{ Since } (p + \dot{f})^0 = 1$$

$$p^1 e^{f(t)} = \dot{f}e^{f(t)} = e^{f(t)} (p + \dot{f}), \text{ Since p operates on zero}$$

$$p^2 e^{f(t)} = (\ddot{f} + \dot{f}^2)e^{f(t)} = e^{f(t)} \left[p(p + \dot{f}) + \dot{f}(p + \dot{f})\right] = e^{f(t)}(p + \dot{f})^2$$

$$p^n e^{f(t)} = e^{f(t)} (p + \dot{f})^n$$

thence,

$$F(p)e^{f(t)} = \sum_{i=0}^{\infty} a_i p^i e^{f(t)} = e^{f(t)} \sum_{i=0}^{\infty} a_i (p + \dot{f})^i = e^{f(t)} F(p + \dot{f}) \quad \text{QED}$$

From (1), (3) and (5) we then have

$$V_2(t)e^{j\theta_2} = F(p)e^{j(\omega_c t + \int \omega_d dt)}$$

$$= e^{j\omega_c t} F(p + j\omega_c)\, e^{j\int \omega_d dt}$$

$$= e^{j\omega_c t} \sum_{n=0}^{\infty} \frac{1}{n!} \left[\frac{d^n F(j\omega)}{(dj\omega)^n}\right]_{\omega_c} p^n e^{j\int \omega_d dt}$$

$$= e^{j(\omega_c t + \int \omega_d dt)} \sum_{n=0}^{\infty} \frac{1}{n!} F^{(n)}(j\omega_c)\,(p + j\omega_d)^n \tag{6}$$

Hence

$$V_2(t)e^{j\theta_2} = e^{j(\omega_c t + \int \omega_d dt)}\, F(p + j\omega_d)$$

$$= \left|F(p + j\omega_d)\right| e^{j(\omega_c t + \int \omega_d dt + \phi)} \tag{6a}$$

$$V_2(t) = \left|F(p + j\omega_d)\right| \tag{7}$$

$$\phi(\omega_d) = \tan^{-1} \frac{\mathrm{Im}\, F(p + j\omega_d)}{\mathrm{Re}\, F(p + j\omega_d)} \tag{8}$$

From (2), (6) and (8) we also have

$$\phi(\omega_d) = \tan^{-1} \frac{\operatorname{Im} \sum_{i=0}^{\infty} a_i (p + j\omega_d)^i}{\operatorname{Re} \sum_{i=0}^{\infty} a_i (p + j\omega_d)^i} \tag{9}$$

$$a_n = \frac{1}{n!}\left[\frac{d^n F(j\omega)}{(dj\omega)^n}\right]_{\omega_c} = \frac{1}{n!}\left[\frac{d^n F(j\omega_d)}{(dj\omega_d)^n}\right]_{\omega_d = 0} \tag{10}$$

Evaluating $(p + j\omega_d)^n$ in (9) we have

$$(p + j\omega_d)^0 = 1$$

$$(p + j\omega_d)^1 = j\omega_d$$

$$(p + j\omega_d)^2 = -\omega_d^{\,2} + j\omega_d^{(1)}$$

$$(p + j\omega_d)^3 = -3\omega_d\omega_d^{(1)} + j(\omega_d^{(2)} - \omega_d^{\,3})$$

$$(p + j\omega_d)^4 = (\omega_d^{\,4} - 3\omega_d^{(1)2} - 4\omega_d\omega_d^{(2)}) + j(\omega_d^{(3)} - 6\omega_d^{\,2}\omega_d^{(1)}) \tag{11}$$

<u>Evaluation of a_i</u>

Let

$$F(j\omega_d) = K(\omega_d)e^{j\phi(\omega_d)} = e^{\ln K + j\phi} \tag{12}$$

then from (10) and using (5) we have

$$n!a_n = \left[\frac{d^n F(j\omega_d)}{(dj\omega_d)^n}\right]_{\omega_d = 0}$$

$$= \left\{ e^{\ln K + j\phi} \left[\frac{d}{dj\omega_d} - j\frac{dK/d\omega_d}{K} + \frac{d\phi}{d\omega_d}\right]^n \right\}_{\omega_d = 0}$$

$$n!a_n = F(o) \left[T - j\frac{d}{d\omega_d}\right]^n_{\omega_d = 0} \tag{13}$$

where

$$T(\omega_d) = T_\phi - jT_k \tag{14}$$

$$T_\phi(\omega_d) = \frac{d\phi}{d\omega_d} = \text{group delay time due to phase,} \tag{14a}$$

$$T_K(\omega_d) = \frac{dK/d\omega_d}{K(\omega_d)} = \text{group delay time due to gain} \tag{14b}$$

Now let (See Figures A-1 to A-3)

$$K(\omega_d) = 1 + a\cos(\omega_d\,\tau_K) \tag{15}$$

$$\phi(\omega_d) = \omega_d\,\tau_0 + b\sin(\omega_d\,\tau_\phi)\ , \tag{16}$$

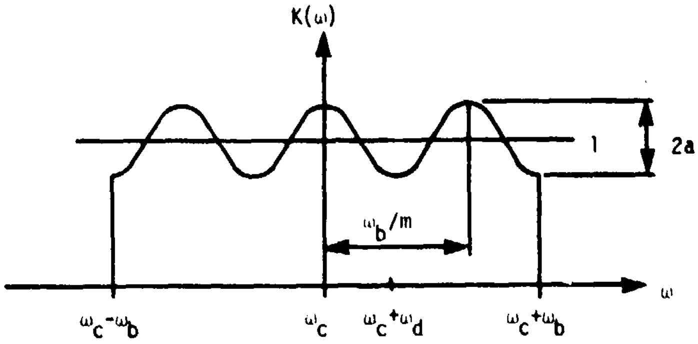

Figure A-1. Gain $K(\omega)$.

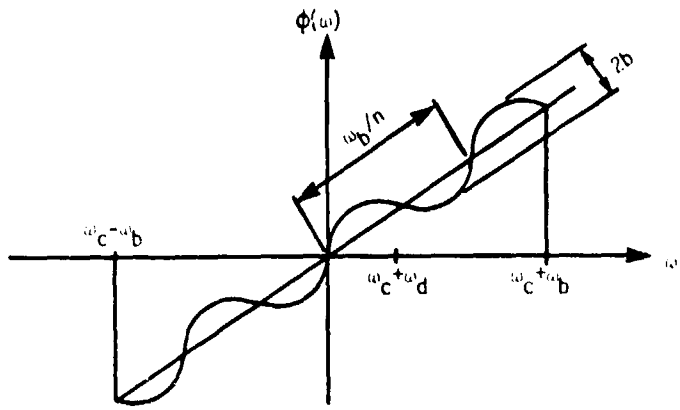

Figure A-2. Phase $\phi(\omega)$.

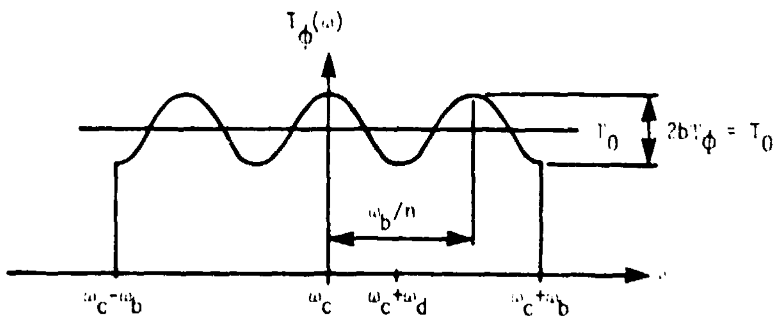

Figure A-3. Phase group delay time $T_{\phi}(\omega)$.

where

$\tau_K = 2m\pi/\omega_b$ = ripple period of $K(\omega_d)$

τ_0 = constant part of $T_\phi(\omega_d)$

$\tau_\phi = 2n\pi/\omega_b$ = ripple period of $\phi(\omega_d)$

a = ripple amplitude of $K(\omega_d)$

b = ripple amplitude of $\phi(\omega_d)$

$b\tau_\phi$ = ripple amplitude of $T_\phi(\omega_d)$

m = number of ripple periods per ω_b for $K(\omega_d)$

n = number of ripple periods per ω_b for $\phi(\omega_d)$

ω_b = half bandwidth (rad/sec)

Noting that

$$F(0) = \left\{\left[1 + a \cos(\omega_d\tau_K)\right] e^{j\left[\omega_d\tau_0 + b \sin(\omega_d\tau_\phi)\right]}\right\}_{\omega_d = 0} \approx 1 ,$$

we have from (13) ,

$a_0 = 1$

$a_1 = T(0)$

$$2!a_2 = T^2 - j\, T^{(1)}$$

$$3!a_3 = T^3 - 3j\, T\, T^{(1)} - T^{(2)}$$

$$4!a_4 = T^4 - 6j\, T^2\, T^{(1)} - 4T\, T^{(2)} - 3\, T^{(3)2} + jT^{(3)} \qquad (17)$$

Since the term $\omega_d\tau_o$ merely delays the waveform and causes no distortion, we shall set $\tau_o = 0$ in (16).

From (14) and (15) - (16) we then have

$$T(0) = b\tau_\phi$$

$$T^{(1)}(0) = ja\tau_K{}^2$$

$$T^{(2)}(0) = -b\tau_\phi{}^3$$

$$T^{(3)}(0) = -ja\tau_K{}^4 \qquad (18)$$

Entering (18) into (17) then yields

$$a_0 = 1$$

$$a_1 = b\tau_\phi$$

$$2!\, a_2 = (b\tau_\phi)^2 + a\tau_K^2$$

$$3!\, a_3 = (b\tau_\phi)^3 + 3ab\tau_K^2\tau_\phi + b\tau_\phi^3$$

$$4!\, a_4 = (b\tau_\phi)^4 + 6ab^2\tau_K^2\tau_\phi^2 + 4b^2\tau_\phi^4 + 3a^2\tau_K^4 + a\tau_K^4 \tag{19}$$

In view of (9) and (11) the phase is given by

$$\phi(\omega_d) = \tan^{-1} \frac{a_1\omega_d + a_2\, \omega_d^{(1)} + a_3(\omega_d^{(2)} - \omega_d^3) + a_4(\omega_d^{(3)} - 6\omega_d^2\, \omega_d^{(1)})}{1 - a_2\omega_d^2 - 3a_3\, \omega_d\, \omega_d^{(1)} - a_4(4\omega_d\, \omega_d^{(2)} + 3\, \omega_d^{(1)2} - \omega_d^4)}$$

In order to get an idea of the magnitude of the terms in (20) let for the time being a = 0 in (18)

and

$$\omega_d = \omega_a\, f(\Omega t)$$

$$\omega_d^{(1)} = \frac{d\omega_d}{dt} = \omega_a\, \Omega\, \frac{df(\Omega t)}{d(\Omega t)} = \omega_a \Omega f^{(1)}$$

$$\omega_d^{(n)} = \omega_a \Omega^n\, f^{(n)} \tag{21}$$

Let us also define the peak-to-peak group delay time variation (See Figure A-3) as

$$T_o = 2b\tau_\phi$$

Then with a = 0 Eqs (19) become

$$a_0 = 1$$

$$a_1 = T_o$$

$$a_2 = \frac{1}{8} T_o^{\,2}$$

$$a_3 = \frac{1}{48} \left(1 + \frac{1}{b^2}\right) T_o^{\,3}$$

$$a_4 = \frac{1}{384} \left(1 + \frac{4}{b^2}\right) T_o^{\,4} \tag{22}$$

Assuming 5% error, the denominator of (20) may be set equal to unity provided

$$0.05 \geq a_2 \omega_d^{\,2} = \frac{T_o^{\,2}}{8} \omega_a^{\,2} \text{ , or}$$

$$\boxed{0.63 \geq T_0 \omega_a} \tag{23}$$

Considering the numerator of (20) we retain only the first term and the largest term generating a third harmonic, i.e., (20) becomes

$$\phi(\omega_d) \approx \tan^{-1}\left[a_1 \omega_d - a_3 \, \omega_d^{\,3}\right]$$

$$\frac{d\phi}{dt} \approx a_1 \, \omega_d^{(1)} - 3a_3 \, \omega_d^{\,2} \, \omega_d^{(1)}$$

$$\approx T_o \omega_a \Omega f^{(1)} - \frac{1}{16} \left(1 + \frac{1}{b^2}\right) T_o^{\,3} \, \omega_a^{\,3} \Omega \, f^2 f^{(1)}$$

Letting

$$f(\Omega t) = \sin \Omega t$$

$$f^{(1)}(\Omega t) = \cos \Omega t$$

$$f^2 f^{(1)} = (\tfrac{1}{2} - \tfrac{1}{2}\cos 2\Omega t)\cos \Omega t = \tfrac{1}{4}\cos \Omega t - \tfrac{1}{4}\cos 3\Omega t,$$

$$\frac{d\phi}{dt} = T_o\omega_a\Omega\left[1 - \frac{T_o^{\,2}\omega_a^{\,2}}{64}\left(1 + \frac{1}{b^2}\right)\right]\cos\Omega\, t \;+$$

$$+ \frac{T_o^{\,3}\omega_a^{\,3}\Omega}{64}\left(1 + \frac{1}{b^2}\right)\cos 3\,\Omega t \tag{24}$$

Hence from (6a) and (24) the total instantaneous frequency at the output of the network is

$$\omega_2 = \omega_c + \omega_d + \frac{d\phi}{dt}$$

$$= \omega_c + \omega_a \sin \Omega t + T_o\omega_a\Omega\left[1 - \frac{T_o^{\,2}\omega_a^{\,2}}{64}\left(1 + \frac{1}{b^2}\right)\right]\cos \Omega t$$

$$+ \frac{T_o^{\,3}\omega_a^{\,3}\Omega}{64}\left(1 + \frac{1}{b^2}\right)\cos 3\,\Omega t \tag{25}$$

One observes that the third term on the right of (25) merely changes the phase of the modulating signal but does not contribute to distortion.

The third harmonic distortion factor is given by

$$D_3 = \frac{\text{factor of } \cos 3\,\Omega t}{\text{factor of } \sin \Omega t} = \frac{T_o^{3}\omega_a^{2}\Omega}{64}\left(1 + \frac{1}{b^2}\right)$$

$$\frac{1}{b} = \frac{2\tau_\phi}{T_o} = \frac{4n\pi}{T_o\omega_b}$$

$$\boxed{D_3 = \frac{(T_o\omega_a)^3}{64}\;\frac{\Omega}{\omega_a}\left[1 + 160\left(\frac{\omega_a}{\omega_b}\right)^2\left(\frac{n}{T_o\omega_a}\right)^2\right]} \tag{26}$$

T_o (sec) = peak-to-peak group delay variations

ω_a (rad/sec) = frequency deviation

Ω (rad/sec) = modulating frequency

ω_b (rad/sec) = half bandwidth

n = number of ripple periods per half bandwidth

Since

$$\frac{\omega_a}{\omega_b} = \frac{75\text{ kHz}}{100\text{ kHz}} = 0.75,$$

$$T_o\omega_a = (0.5\ \mu\text{sec}) \times (2\pi \times 75\text{ kHz}) = 0.236\ ,$$

the second term inside the bracket of (26) is much larger than the first. Hence (26) may be simplified to

$$\boxed{D_3 \approx 2.5\ (T_o\omega_a)\left(\frac{\Omega}{\omega_a}\right)\left(\frac{\omega_a}{\omega_b}\right)^2 n^2} \tag{27}$$

With

$T_o = 0.5\ \mu sec$

$\omega_a/2\pi = 75$ kHz

$\omega_b/2\pi = 100$ kHz

$\Omega/2\pi = 30$ kHz

$n = \frac{1}{2}$

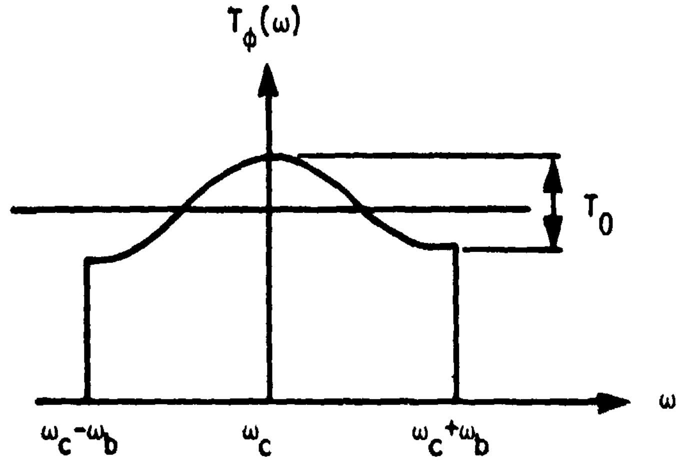

Figure A-4.

$D_3 = 0.03$, or 3% third harmonic distortion assuming constant amplitude over the passband

When amplitude variations are included the third harmonic distortion is given by

$$D_3 = \frac{(T_o\omega_a)^3}{64}\left(\frac{\Omega}{\omega_a}\right)\left[1 + \frac{160n^2}{(T_o\omega_a)^2}\left(\frac{\omega_a}{\omega_b}\right)^2 + \frac{480am^2}{(T_o\omega_a)^2}\left(\frac{\omega_a}{\omega_b}\right)^2\right] \tag{28}$$

If $(T_o\omega_a)$ is small, (28) reduces to

$$D_3 \approx (T_o\omega_a)^2\left(\frac{\Omega}{\omega_a}\right)\left(\frac{\omega_a}{\omega_b}\right)^2\left[2.5\ n^2 + 3.75\ (2a)\ m^2\right] \tag{29}$$

where

n = no. of phase ripple periods per half bandwidth ω_b

m = no. of amplitude ripple periods per half bandwidth ω_b

$2a$ = peak-to-peak amplitude variation

T_o = peak-to-peak group delay variation due to phase

Ω = modulation frequency (rad/sec)

ω_b = half bandwidth (rad/sec)

ω_a = freq. deviation (rad/sec)

APPENDIX B

COMMON-CHANNEL AND ADJACENT-CHANNEL INTERFERENCE

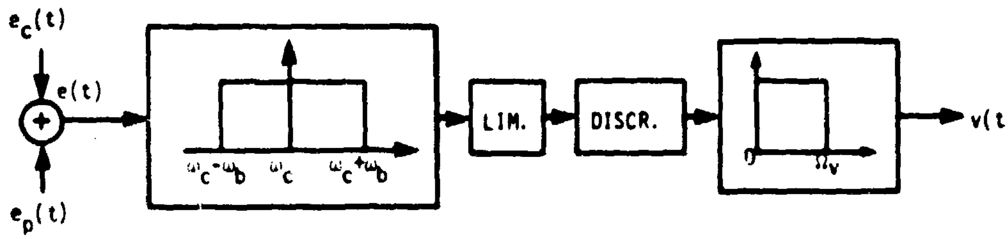

Figure B-1

Referring to Figure B-1 the desired carrier $e_c(t)$ and the undersired carrier $e_p(t)$ enter a bandpass filter of bandwidth $2\omega_b$. After limiting and linear frequency detection the audio signal enters a lowpass filter of cutoff frequency Ω_v. It is assumed that $\omega_b > \Omega_v$ and $\omega_b \approx (\Delta\omega_c + \Omega_{c\ max})$ where $\Delta\omega_c$ is the frequency deviation (75 kHz) and $\Omega_{c\ max}$ is the maximum modulating frequency (30 kHz) of the desired carrier. See References 1, 2 and 3.

B-1 Adjacent-Channel Interference

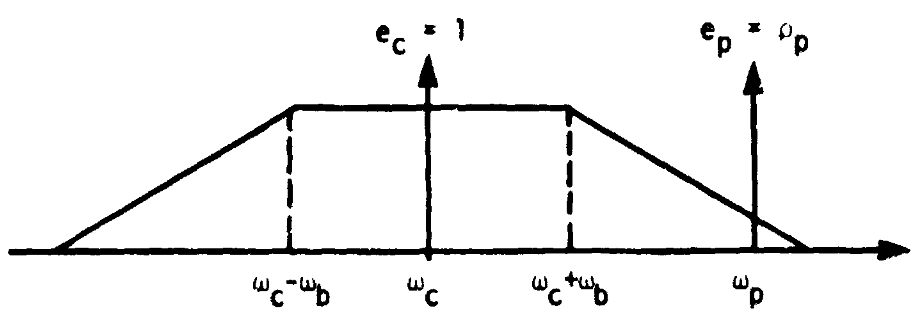

Figure B-2.

Referring to Figure B-2 let

$$e_c = \cos \theta_c \qquad \theta_c = \omega_c t + \beta_c \sin \Omega_c t \tag{1}$$

$$e_p = \rho_p \cos \theta_p \qquad \theta_p = \omega_p t + \beta_p \sin \Omega_p t + \phi_p \tag{2}$$

where

ω_c = desired carrier frequency (rad/sec)

ω_p = undesired carrier frequency (rad/sec)

$\beta_c = \frac{\Delta\omega_c}{\Omega_c}$ = modulation index of desired carrier

$\beta_p = \frac{\Delta\omega_p}{\Omega_p}$ = modulation index of undesired carrier

$\Delta\omega_c$, $\Delta\omega_p$ = frequency deviations (rad/sec)

Ω_c, Ω_p = modulating frequencies (rad/sec)

ϕ_p = constant phase shift (radians)

Expanding $e_p(t)$ we have

$$e_p(t) = \rho_p \cos \theta_p$$

$$= \rho_p \mathrm{Re} \left\{ e^{j(\omega_p t + \phi_p)} e^{j\beta_p \sin \Omega_p t} \right\}$$

$$= \rho_p \mathrm{Re} \left\{ e^{j(\omega_p t + \phi_p)} \cdot \sum_{m=-\infty}^{\infty} J_m (\beta_p) e^{jm\Omega_p t} \right\}$$

$$\rho_p \sum_{-\infty}^{\infty} J_m (\beta_p) \cos (\omega_p t + m\Omega_p + \phi_p) , \tag{3}$$

where $J_m(\beta_p)$ is a Bessel function of the first kind and order m. Adding (3) and (1) the signal e(t) entering the bandpass filter is

$$e(t) = e_c(t) + e_p(t)$$

$$= \cos \theta_c(t) + \rho_p \cos \theta_p$$

$$= \cos \theta_c + \rho_p \sum_{\substack{-\infty \\ m}}^{\infty} J_m (\beta_p) \cos (\omega_p t + m\Omega_p t + \phi_p)$$

$$= \mathrm{Re} \left\{ e^{j\theta_c} \left[1 + \rho_p \sum_{\substack{-\infty \\ m}}^{\infty} J_m (\beta_p) e^{j(\omega_p t + m\Omega_p t + \phi_p - \theta_c)} \right] \right\}$$

$$= (1 + A_p) \cos \theta_c - B_p \sin \theta_c , \tag{4}$$

$$= r \cos (\theta_c + \phi) , \tag{4a}$$

where

$$A_p = \rho_p \sum_{\substack{-\infty \\ m}}^{\infty} J_m(\beta_p) \cos \left[(\omega_p + m\Omega_p - \omega_c)t + \phi_p - \beta_c \sin \Omega_c t \right] \tag{5}$$

$$= \rho_p \sum_{\substack{-\infty \\ m}}^{\infty} \sum_{\substack{-\infty \\ n}}^{\infty} J_m(\beta_p) J_n(\beta_c) \cos \left[(\omega_p + m\Omega_p - \omega_c - n\Omega_c)t + \phi_p \right] \tag{5a}$$

$$B_p = \rho_p \sum_{\substack{-\infty \\ m}}^{\infty} J_m(\beta_p) \sin \left[(\omega_p + m\Omega_p - \omega_c)t + \phi_p - \beta_c \sin \Omega_c t \right] \tag{6}$$

$$= \rho_p \sum_{m=-\infty}^{\infty} \sum_{m=-\infty}^{\infty} J_m(\beta_p)\, J_n(\beta_c) \sin \left[(\omega_p + m\Omega_p - \omega_c - n\Omega_c)t + \phi_p\right] \tag{6a}$$

$$r^2 = (1 + A_p)^2 + B_p{}^2 \tag{7}$$

$$\phi = \tan^{-1} \frac{p}{1 + A_p} \tag{8}$$

A possible expansion for ϕ is

$$\phi = \frac{(1 + A_p)B_p}{r^2} \left\{ 1 + \frac{2}{3} \frac{B_p{}^2}{r^2} + \frac{2.4}{3.5} \frac{B_p{}^4}{r^4} + \ . \ . \ . \right\}$$

Assuming $\left|A_p\right| \ll 1$ and $\left|B_p\right| \ll 1$ so that $r \approx 1$,

Eq. (8) reduces to

$$\phi = B_p \tag{9}$$

Hence in view of (6a)

$$\dot{\phi} = \dot{B}_p$$

$$= \rho_p \sum_{m=-\infty}^{\infty} \sum_{n=-\infty}^{\infty} J_m(\beta_p)\, J_n(\beta_c)\, (\Delta\omega + m\Omega_p - n\Omega_c) \cos \left[(\Delta\omega + m\Omega_p - n\Omega_c)t + \phi_p\right] \tag{10}$$

where

$$\Delta\omega = \omega_p - \omega_c = \text{beat frequency (rad/sec)} \tag{11}$$

Now let the bandpass filter be given by

$$F(j\omega) = K(\omega) \quad e^{-j\phi(\omega)} \tag{12}$$

where $\phi(\omega)$ is the nonlinear part of the phase shift (the linear part merely delays the signal undistorted).

Defining

$$\omega_{mn} = \Delta\omega + m\Omega_p - n\Omega_c \tag{13}$$

$$K_{mn} = K(\omega_{mn}) \tag{14a}$$

$$\phi_{mn} = \phi(\omega_{mn}) \;, \tag{14b}$$

Eq. (10) should be modified to

$$\dot{\phi} = \rho_p \sum_{m=-\infty}^{\infty} \sum_{n=-\infty}^{\infty} J_m(\beta_p)\, J_n(\beta_c)\, K_{mn}\omega_{mn} \cos\left[\omega_{mk}t + \phi_p - \phi_{mn}\right] \tag{15}$$

Assuming a linear discriminator and an ideal audio lowpass filter with cutoff frequency Ω_v (rad/sec), the audio output is given by

$$\begin{aligned} v(t) &= \dot{\theta}_c + \dot{\phi} - \omega_c \\ &\approx \Delta\omega_c \cos\Omega_c t + \rho_p \sum_m \sum_n \; J_m(\beta_p)\, J_n(\beta_c)\, K_{mn}\omega_{mn}\cos\;\left[\omega_{mn}t + \phi_p - \phi_{mn}\right] \end{aligned} \tag{16}$$

where

$\Omega_c < \Omega_v$ = audio filter bandwidth (rad/sec)

$\Delta\omega_c < \omega_b$ = bandpass filter half bandwidth (rad/sec)

$$-\Omega_v \leq \omega_{mn} \leq \Omega_v,\ \omega_b > \Omega_v \tag{16a}$$

Equivalent statements of (16a) are

$$(\Delta\omega - \Omega_v) \leq (n\Omega_c - m\Omega_p) \leq (\Delta\omega + \Omega_v) \tag{16b}$$

$$\frac{\Delta\omega + m\Omega_p - \Omega_v}{\Omega_c} \leq n \leq \frac{\Delta\omega + m\Omega_p + \Omega_v}{\Omega_c} \tag{16c}$$

$$\frac{n\Omega_c - \Delta\omega - \Omega_v}{\Omega_p} \leq m \leq \frac{n\Omega_c - \Delta\omega + \Omega_v}{\Omega_p} \tag{16d}$$

In what follows we shall assume that

a) the desired carrier modulating frequency is very low so that

$\Omega_c \approx 0$, $n \approx 0$, and

b) the undesired carrier e_p is modulated with Ω_p. Eqs. (16) and (16d) then reduce to

$$v(t) \approx \Delta\omega_c \cos \Omega_c t + \rho_p \sum_m J_m(\beta_p) K_m \omega_m \cos(\omega_m t + \phi_p - \phi_m), \tag{17}$$

where

$K_m = K(\omega_m),\ \phi_m = \phi(\omega_m)$

$$\boxed{\begin{aligned} &\omega_m = \Delta\omega + m\Omega_p \qquad (17a) \\ &\frac{-\Delta\omega - \Omega_v}{\Omega_p} \le m \le \frac{-\Delta\omega + \Omega_v}{\Omega_p} \qquad (17b) \end{aligned}}$$

The RMS signal/noise ratio is given by

$$S/N = \frac{\text{RMS value of } \Delta\omega_c \cos\Omega_c t}{\text{RMS value of } \dot{\phi}(t)}$$

Using (17) we have

$$\boxed{S/N = \frac{\Delta\omega_c}{\rho_p \left\{ \sum_m [J_m(\beta_p) K_m \omega_m]^2 \right\}^{1/2}}} \qquad (18)$$

As an example let

$K_m = 1$ (uniform gain in the pass band),

$\rho_p = 1$ (equal carrier amplitudes),

$\Delta\omega/(2\pi) = 0.4$ MHz,

$\Delta\omega_c/(2\pi) = \Delta\omega_p/(2\pi) = 75$ kHz,

$\Omega_v/(2\pi) = 40$ kHz, (19)

$\Omega_c/(2\pi) = 0$ Hz,

and consider the following two cases.

<u>Case I</u>: $\Omega_p/(2\pi) = 20$ Hz (20)

$$\beta_p = \frac{\Delta\omega_p}{\Omega_p} = \frac{75000}{20} = 3750 \tag{21}$$

From (17b), (19) and (20)

$$\frac{-400-40}{0.02} \leq m \leq \frac{-400 + 40}{0.02}$$

$$-22000 \leq m \leq 18000 \tag{22}$$

From (18), (21) and (22),

$$S/N = \frac{75}{\left\{\sum_{m=18000}^{22000} [J_m(3750) \cdot 1 \cdot (400 - m \times 0.02)]^2\right\}^{1/2}}$$

$$= \frac{75}{\left\{[J_{18000}(3750) \times 40]^2 + \cdot \cdot \cdot \cdot + [J_{22000}(3750) \times 40]^2\right\}^{1/2}} \tag{23}$$

Now, for m is large,

$$J_m(mx) \approx \frac{x^m e^m \sqrt{1-x^2}}{\sqrt{2\pi m}\,(1 - x^2)^{1/4}\,[1 + \sqrt{1 - x^2}]^m} \tag{24}$$

Since $mx = \beta_p$, $x = \frac{\beta_p}{m} \approx \frac{3750}{20000} = 0.19$

Therefore, (24) reduces to

$$J_m(mx) \approx \frac{1}{\sqrt{2\pi m}} \left(\frac{xe}{2}\right)^m \text{, or}$$

$$J_m(\beta_p) \approx \frac{1}{\sqrt{2\pi m}} \left(\frac{\beta_p e}{2m}\right)^m \qquad (25)$$

For $\beta_p = 3750$ and $m = 18000$,

$$J_m(\beta_p) = \frac{1}{\sqrt{2\pi \times 18000}} \left(\frac{3750 \times 2.718}{18000}\right)^{18000}$$

$$= \frac{(0.566)^{18000}}{\sqrt{2\pi \times 18000}} \ll 1 \qquad (26)$$

Hence values for m greater than 18000 need not be considered

so that from (23) and (26)

$$\frac{S}{N} \approx 1.9 \sqrt{2\pi \times 18000} \cdot (1.765)^{18000}$$

$$= 640 \times (1.765)^{18000}$$

$$\boxed{\frac{S}{N} \gg 1000 \text{ dB}} \qquad (27)$$

<u>Case II</u>: $\Omega_p/(2\pi) = 30$ kHz (28)

$$\beta_p = \frac{\Delta\omega_p}{\Omega_p} = \frac{75}{30} = 2.5$$

From (17b), (19) and (28)

$$\frac{-400-40}{30} \leq m \leq \frac{-400+40}{30}, \text{ or}$$

$$-14 \leq m \leq -12 \tag{29}$$

From (18) and (29),

$$\frac{S}{N} = \frac{75}{\left\{\sum_{m=12}^{14} [J_m(2.5)(400 - m \times 30)]^2\right\}^{1/2}}$$

or

$$\frac{S}{N} = \frac{75}{\left\{\left[J_{12}(2.5) \times 40\right]^2 + \left[J_{13}(2.5) \cdot 10\right]^2 + \cdot \cdot \cdot \cdot + \left[J_{14}(2.5) \cdot 20\right]^2\right\}^{1/2}} \tag{30}$$

In order to see if we can make the large order approx. we have

$$J_n(x) = \sum_{r=0}^{\infty} \frac{(-1)^r}{(n+r)!} \left(\frac{x}{2}\right)^{n+2r}$$

$$= \frac{1}{n!}\left(\frac{x}{2}\right)^n - \frac{1}{(n+1)!}\left(\frac{x}{2}\right)^{n+2} + \cdot \cdot \cdot \tag{31}$$

The ratio of the second and first terms is

$$y = \frac{x^2}{4(n+1)} = \frac{6.25}{4(12+1)} = \frac{6.25}{52} < 0.2.$$

We can therefore keep only the first term.

Using Stirling's approx., we have for large n,

$n! = \sqrt{2\pi n}\left(\frac{n}{e}\right)^n$ (which is already 1.5 percent accurate for n = 4)

so that (31) becomes

$$J_n(x) = \frac{1}{\sqrt{2\pi n}}\left(\frac{xe}{2n}\right)^n \tag{32}$$

which is the usual approx. of $J_n(x)$ for large n.

Hence

$$J_{12}(2.5) = \frac{1}{\sqrt{24\pi}}\left(\frac{2.5 \times 2.718}{24}\right)^{12} = \frac{1}{\sqrt{24\pi}(3.54)^{12}} \tag{33}$$

Referring to (30) and (33) orders larger than 12 may be omitted

so that (30) becomes

$\frac{S}{N} = 16.5 \times (3.54)^{12}$, or

$$\boxed{\frac{S}{N} = 146 \text{ dB}} \tag{34}$$

We conclude that adjacent channel interference may be neglected.

B-2 Bandpass Filter Selectivity

In what follows we consider the approximate attenuation the bandpass filter should have at ω_p (see Figure B-2). Neglecting the sidebands of the interfering carrier, it follows from (17) that the discriminator output is given by

$$v(t) = \Delta\omega_c \cos \Omega_c t + J_o(\beta_p)K_o \,\Delta\omega \cos(\Delta\omega t + \phi_p - \phi_o) \tag{35}$$

where we have set $\rho_p = 1$ and where

K_o = Bandpass attenuation factor at ω_p.

The maximum value of v(t) will occur when

$\beta_p = 0$ (i.e., e_p unmodulated), $t = 0$ and $\phi_p - \phi_o = 0$,

i.e.,

$$v_{max} = \Delta\omega_c + K_o\Delta\omega \tag{36}$$

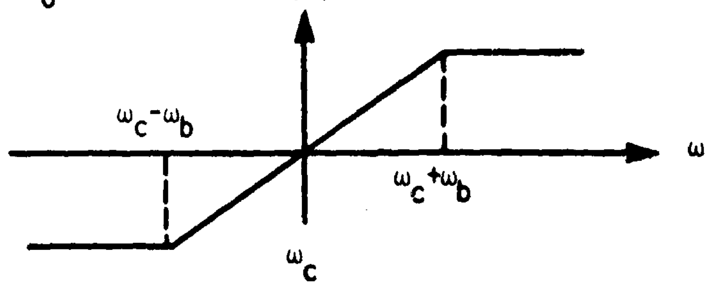

Figure B-3

Since most discriminators saturate beyond $\omega_c \pm \omega_b$ as shown in Figure B-3 it is in view of (36) essential that $|K_o\Delta\omega| \leq 0.01 \, |\Delta\omega_c|$, i.e.,

$$\boxed{K_o = 0.01 \frac{\Delta\omega_c}{\Delta\omega} = \frac{0.01 \times 75 \text{ kHz}}{400 \text{ kHz}} \sim -50 \text{ dB}} \tag{37}$$

B-3 Common-Channel Interference

The S/N ratio as given by Equation (18) can also be used in this case provided ρ_p <<1. But because ρ_p can be near unity a different derivation must be considered. Also, we are presently more interested in the capture ratio than in the S/N ratio. Hence Equation (18) will no longer be considered.

B-3.1 <u>Desired Channel Modulated</u>

Let us again have (See Figure B-1)

$$e(t) = e_c(t) + e_p(t)$$

$$= \cos \theta_c + \rho_p \cos \theta_p, \tag{38}$$

where

ρ_p = amplitude of undesired carrier

$$\theta_c = \omega_c t + \beta_c \sin \Omega_c t \tag{39a}$$

$$\theta_p = \omega_p t + \phi_p \tag{39b}$$

ω_c = desired carrier freq. (rad/sec)

ω_p = undesired carrier freq. (rad/sec)

ϕ_p = constant phase shift (rads)

$\beta_c = \dfrac{\Delta\omega_c}{\Omega_c}$ = modulation index

$\Delta\omega_c$ = freq. deviation (rad/sec)

Ω_c = modulating freq. (rad/sec)

From (38) we have

$$e(t) = \mathrm{Re}\, e^{j\theta_c} \left[1 + \rho_p e^{j(\theta_p - \theta_c)}\right]$$

$$= \mathrm{Re}\, e^{j\theta_c} \left\{\left[1 + \rho_p \cos(\theta_p - \theta_c)\right] + j\left[\rho_p \sin(\theta_p - \theta_c)\right]\right\}$$

$$= [1 + \rho_p \cos(\theta_p - \theta_c)] \cos\theta_c - [\rho_p \sin(\theta_p - \theta_c)] \sin\theta_c \tag{40}$$

$$= r \cos\phi \cos\theta_c - r \sin\phi \sin\theta_c \tag{40a}$$

$$= r \cos(\theta_c + \phi), \tag{40b}$$

where

$$\theta_p - \theta_c = \Delta\omega t + \phi_p - \beta_c \sin\Omega_c t \tag{41a}$$

$$\Delta\omega = \omega_p - \omega_c \tag{41b}$$

$$r = \left[1 + 2\rho_p \cos(\theta_p - \theta_c) + \rho_p^2\right]^{1/2}$$

$$\phi = \tan^{-1} \frac{\rho_p \sin(\theta_p - \theta_c)}{1 + \rho_p \cos(\theta_p - \theta_c)} \tag{43}$$

Using a perfect limiter, the discriminator output is given by

$$v_1(t) = \dot{\theta}_c + \dot{\phi} - \omega_c$$

$$= \Delta\omega_c \cos\omega_c t + (\Delta\omega - \Delta\omega_c \cos\Omega_c t) \frac{\rho_p \cos(\theta_p - \theta_c) + \rho_p^2}{1 + 2\rho_p \cos(\theta_p - \theta_c) + \rho_p^2} \tag{44}$$

In what follows we shall assume that

$$\Delta\omega = \omega_p - \omega_c = 0, \ \phi_p = 0$$

Hence (42) and (44) become

$$r = [1 + 2\rho_p \cos(\beta_c \sin \Omega_c t) + \rho_p^2], \tag{45}$$

$$v_1(t) = \Delta\omega_c \cos \Omega_c t - \Delta\omega_c \cos \Omega_c t \cdot f_1(t), \tag{46a}$$

where

$$f_1(t) = \frac{\rho_p \cos(\beta_c \sin \Omega_c t) + \rho_p^2}{1 + 2\rho_p \cos(\beta_c \sin \Omega_c t) + \rho_p^2} \tag{46b}$$

Let us first consider the carrier envelope r.

From (45) we have

$$r_{max} = 1 + \rho_p$$

$$r_{min} = 1 - \rho_p$$

For $\rho_p = 0.95$, the limiter should be capable of covering a dynamic range of at least $\frac{r_{max}}{r_{min}} = \frac{1 + \rho_p}{1 - \rho_p} = 40$, or 32 dB.

A plot of r vs. $\Omega_c t$ (Eq. 45) has been given by Corrington (Reference 2) in Figure B-4 for $\beta_c = 10$ and several values of ρ_p.

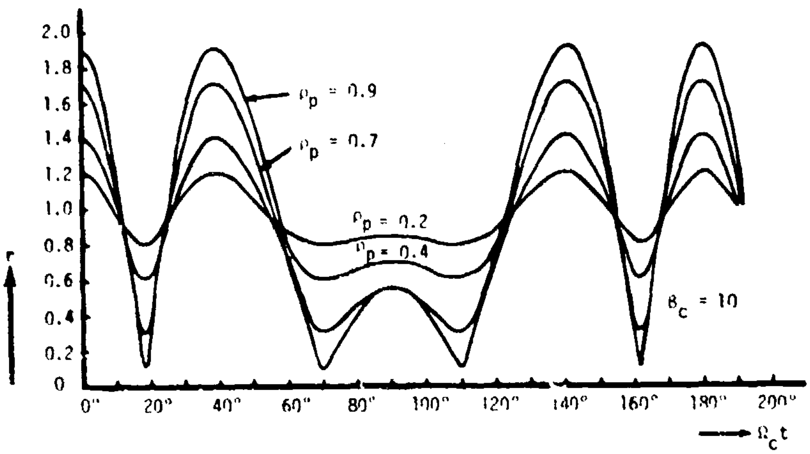

Figure B-4.

Let us next consider (46a) and (46b). Values of v(t) vs. $\Omega_c t$ for $\rho_p = 0.5$ and several values of β_c are also given by Corrington in Figures B-5 and B-6. Now suppose that the waveform of Figure B-6 is passed through a low-pass filter which passes Ω_c but rejects the indicated high frequency waveform. It will then be found that the output of the lowpass filter amounts to

$$v(t) = \Delta\omega_c \cos \omega_c t + \Delta\omega_c f_{1\ avg} \cos \omega_c t = \Delta\omega_c \cos \omega_c t$$

because it has been shown by Corrington that

$$f_{1\ avg} = \frac{1}{\pi} \int_0^{\pi} f_1(\theta)\, d\theta = 0 \text{ for } \rho_p \leq 1. \tag{47}$$

It may further be found that

$$\left| f_{1max} \right| = \frac{\rho_p}{1 - \rho_p}, \tag{48a}$$

$$\left| f_{1min} \right| = \frac{\rho_p}{1 + \rho_p}, \tag{48b}$$

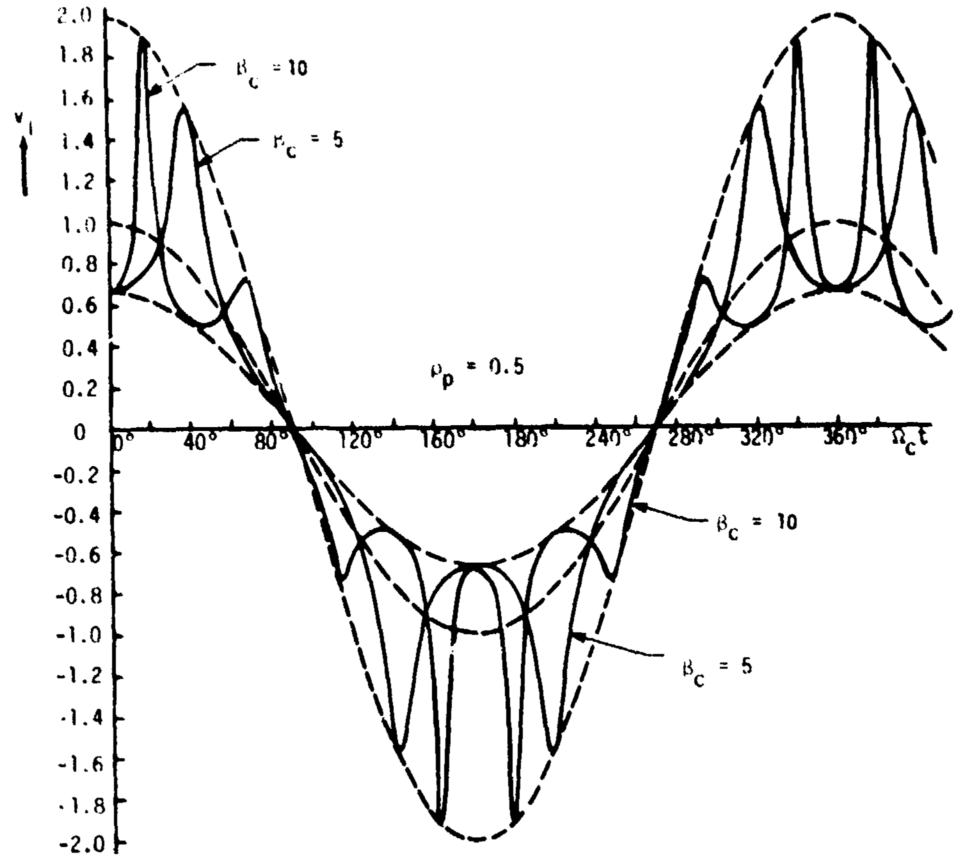

Figure B-5

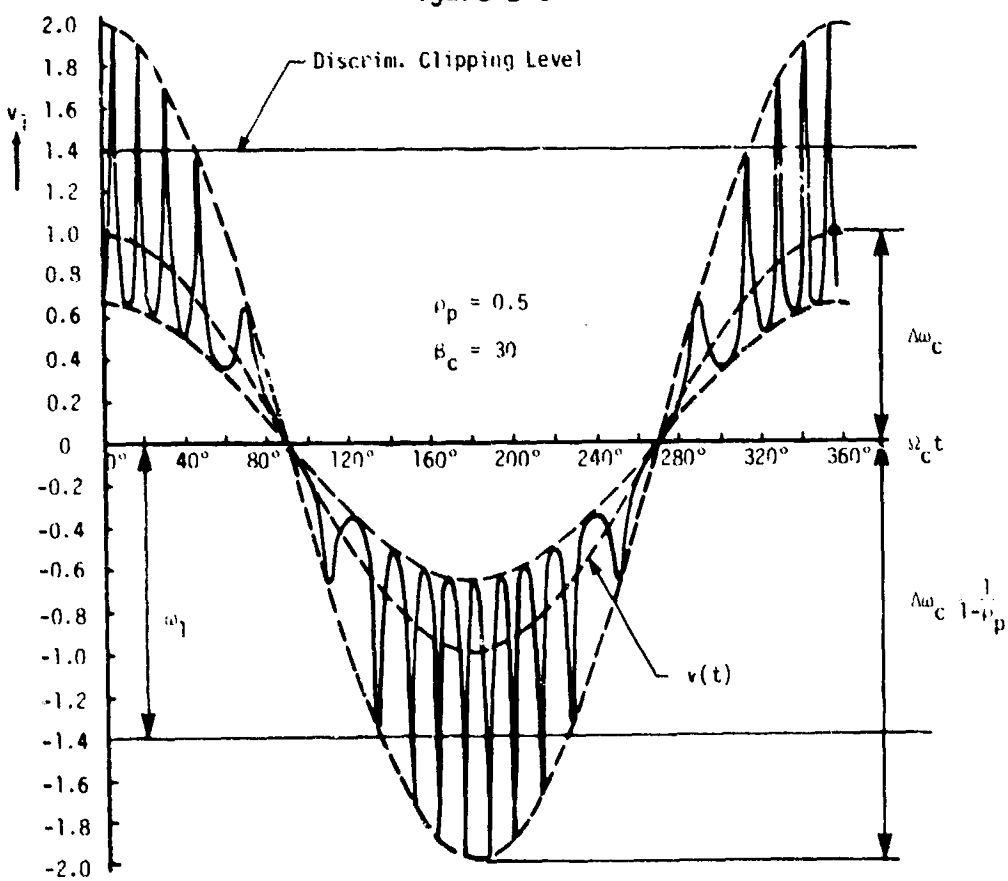

Figure B-6.

Therefore, the maximum and minimum values of the envelopes in Figure B-6 are

$$\left|v_{1max}\right| = \left|\Delta\omega_c\left(1 + \frac{\rho_p}{1 - \rho_p}\right)\right| = \Delta\omega_c \frac{1}{1 - \rho_p}, \tag{49a}$$

$$\left|v_{1min}\right| = \left|\Delta\omega_c\left(1 - \frac{\rho_p}{1 + \rho_p}\right)\right| = \Delta\omega_c \frac{1}{1 + \rho_p}, \tag{49b}$$

Let us now suppose that the bandwidth of the bandpass filter is sufficiently large so that $v_1(t)$ is passed without distortion but that the discriminator saturates beyond $\pm\ \omega_1$ as shown in Figures B-6 and B-7.

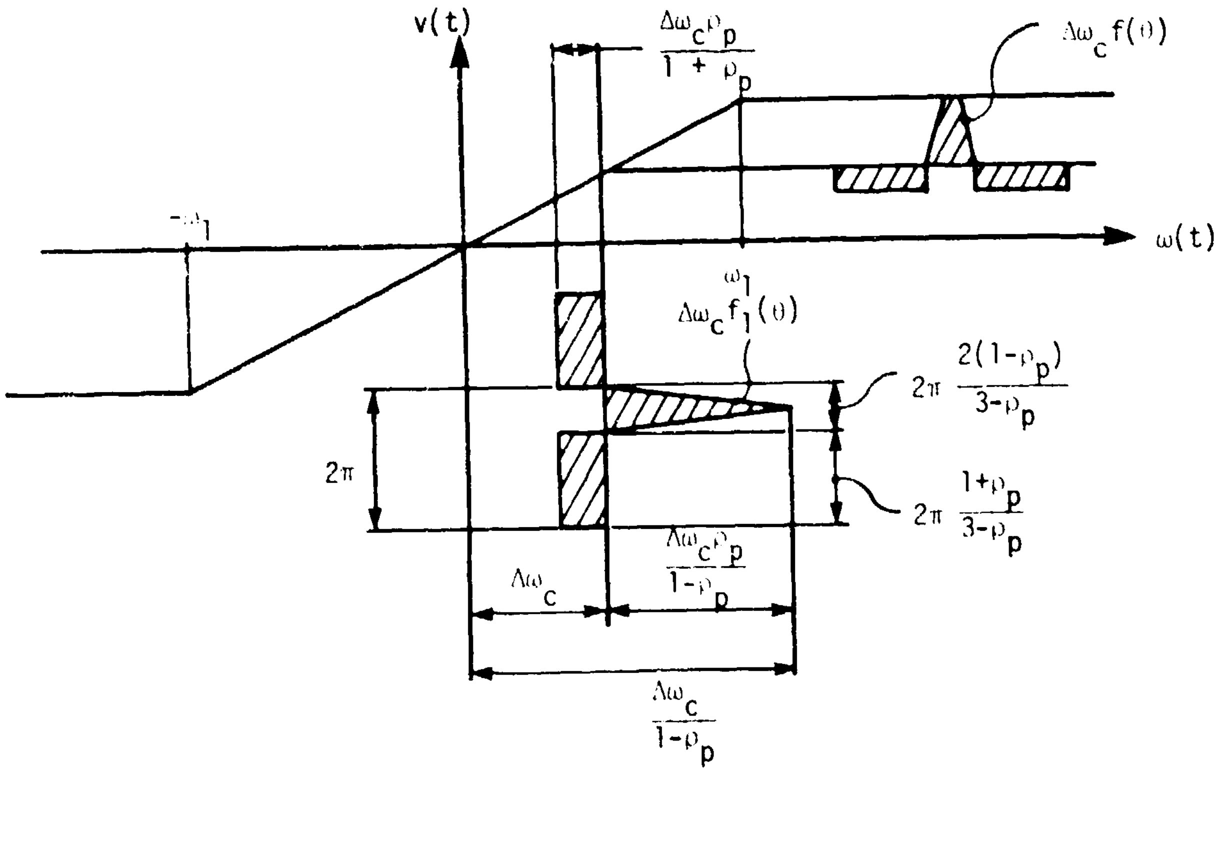

Figure B-7.

It is evident that when

$$\Delta\omega_c < \omega_1 < \frac{\Delta\omega_c}{1 - \rho_p} \tag{50}$$

a portion of the high frequency waveform is clipped and (47) no longer holds, i.e., a reduction of the average amplitude of cos $\Omega_c t$ results. In order to obtain an approximate expression for the amplitude reduction we make two assumptions:

a) period of modulating frequency Ω_c large compared to the period of the superimposed frequency,

b) replace the superimposed waveform by a waveform which is square below the axis and triangular above the axis (see Figure B-7) and which has zero average value, i.e.,

$$f_1 avg = - \frac{1 + \rho_p}{3 - \rho_p} \frac{\rho_p}{1 + \rho_p} + \frac{2(1 - \rho_p)}{2\,(3 - \rho_p\,)} \frac{\rho_p}{1 - \rho_p} = 0 \tag{51}$$

for

$$\omega_1 \geq \frac{\Delta\omega_c}{1 - \rho_p} \tag{52}$$

Now when

$$\Delta\omega_c \leq \omega_1 \leq \frac{\Delta\omega_c}{1 - \rho_p} \tag{53a}$$

it may be found that

$$f_{avg} = - \frac{\left[1 - (1 - \rho_p)\,\frac{\omega_1}{\Delta\omega_c}\right]^2}{\rho_p(3 - \rho_p)} \tag{53b}$$

After lowpass filtering the audio output is thus given by

$$v(t) = \Delta\omega_c \left[1 + f_{avg}\right] \cos \Omega_c t \tag{53c}$$

Let us now define the capture ratio R as follows.

R(dB) = (Desired Carrier Amplitude)/(Undesired Carrier Amplitude at

which the frequency deviation amplitude $\Delta\omega_c$ reduces by K dB) (54)

Hence,

$$R = 20 \log \left(\frac{1}{\rho_p}\right) \tag{55a}$$

$$K = 20 \log \frac{\Delta\omega_c}{\Delta\omega_c \, [1 + f_{avg}]} = - 20 \log [1 + f_{avg}] \tag{55b}$$

where f_{avg} is given by (53b).

Hence from a knowledge of R and K, ω_1 can be approximately determined. So far it has been assumed that the bandpass filter has a large bandwidth. Unfortunately the calculation of the response due to the waveform in Figure B-7 is a complicated affair. We can say at best that if the frequency of this waveform is relatively low, a quasi-static approximation may be used. In this case Figure B-7 may also be used except that ω_1 is replaced by ω_b, where ω_b is the half bandwidth of the IF filter.

It is evident that if $\omega_b < \omega_1$, ω_1 should be replaced by ω_b in Figure B-7 and Equations (53b) and (55). We conclude this section by stating that small capture ratios can be achieved by having:

a) large IF bandwidth with uniform amplitude and linear phase response, and

b) large discriminator bandwidth with good linearity.

B-3.2 Undesired Channel Modulated

Instead of (39a) and (39b) we set

$$\theta_c = \omega_c t \tag{56a}$$

$$\theta_p = \omega_c t + \beta_p \sin \Omega_p t + \phi_p \tag{56b}$$

We now find a Fourier expansion for (43) as follows.

Comparing (40) and (40a) we have

$$1 + \rho_p \cos (\theta_p - \theta_c) = r \cos \phi \tag{57}$$

$$\rho_p \sin (\theta_p - \theta_c) = r \sin \phi \tag{58}$$

Multiplying (58) by $j = \sqrt{-1}$ and adding the result to (57) yields

$$1 + \rho_p e^{j(\theta_p - \theta_c)} = r e^{j\phi},$$

or

$$\ln \left[1 + \rho_p e^{j(\theta_p - \theta_c)}\right] = \ln r + j\phi \tag{59}$$

Since

$$\ln (1 + x) = - \sum_{k=1}^{\infty} \frac{(-x)^k}{k}, \; -1 < x \leq 1,$$

we have from (59) and by equating the imaginary parts,

$$\phi = - \sum_{k=1}^{\infty} \frac{(-\rho_p)^k}{k} \sin k(\phi_p + \beta_p \sin \Omega_p t) , \ 0 \leq \rho_p \leq 1 \tag{60}$$

Hence the discriminator output is given by

$$v_1(t) = \dot{\theta}_c + \dot{\phi} - \omega_c$$

$$= - \Delta\omega_p \cos(\Omega_p t) \sum_{k=1}^{\infty} (-\rho_p)^k \cos k(\phi_p + \beta_p \sin \Omega_p t). \tag{61}$$

Without the presence of the desired unmodulated carrier, the discriminator output is

$$v_{1p}(t) = \dot{\theta}_p - \omega_c$$

$$= \Delta\omega_p \cos (\Omega_p t). \tag{62}$$

In order to obtain an approximate expression for*

$$\frac{v_{p\ max}}{v_{max}} = \frac{\text{receiver peak output without desired carrier}}{\text{receiver peak output with desired carrier}}$$

we shall assume that

$$\rho_p = \frac{\text{amplitude of undesired carrier}}{\text{amplitude of desired carrier}} \leq 0.1$$

Thus, (61) reduces to

$$v_1(t) \approx \Delta\omega_p \ \rho_p \cos(\Omega_p t) \cos (\phi_p + \beta_p \sin \Omega_p t). \tag{63}$$

*Although $v_{p\ max}/v_{max}$ represents a receiver output level reduction factor due to the presence of the unmodulated desired carrier, it may (for small values of ρ_p) also be interpreted as a signal-to-noise ratio for the case the desired carrier is modulated and the frequency deviations of the desired and undesired carriers are equal.

As shown in Figure B-8, $v_1(t)$ comprises a variable frequency of period T_2 with an envelope of period T_1.

After lowpass filtering v(t) as shown in Figure B-9 is obtained.

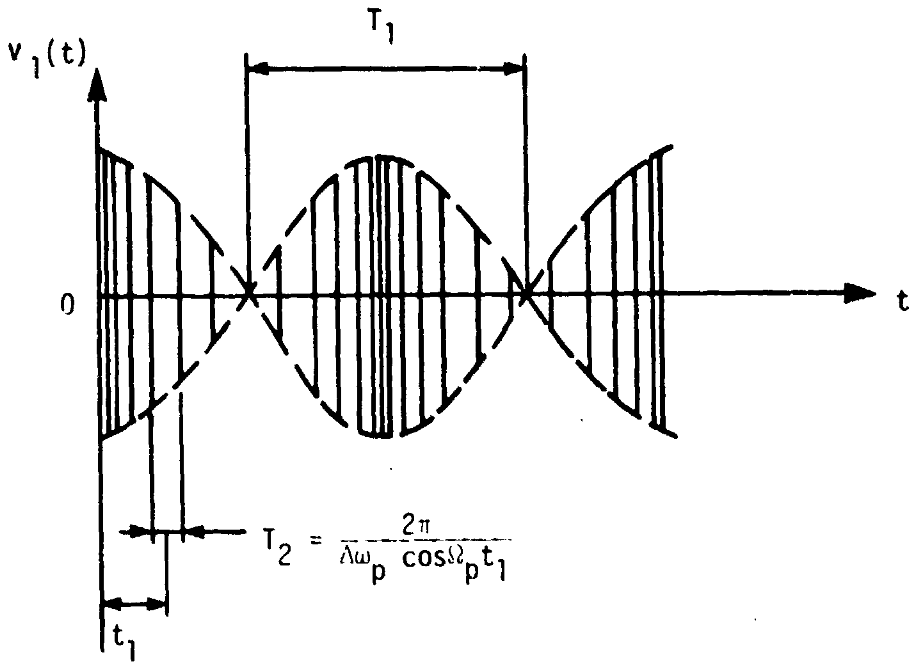

Figure B-8.

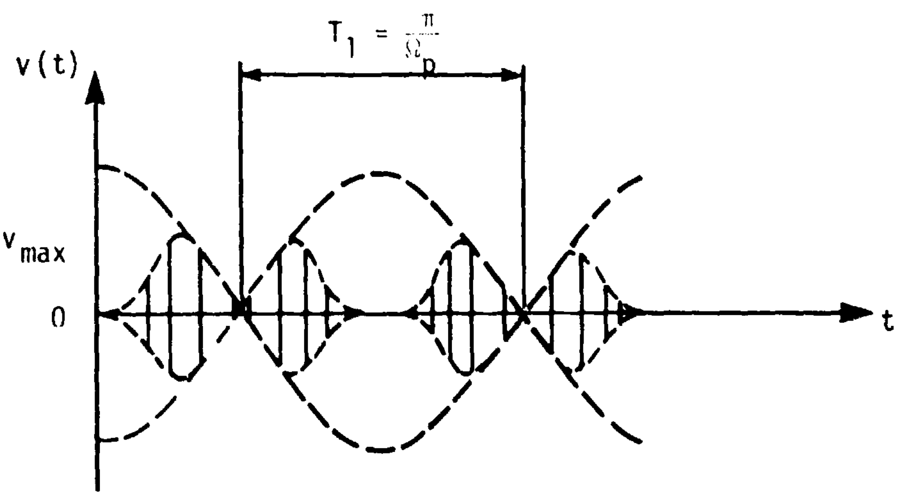

Figure B-9. Band limited version of Figure B-8.

We proceed by assuming that

$\Omega_p < \Omega_v$,

where

Ω_p = angular modulating frequency, and

Ω_v = angular lowpass cutoff frequency.

From (62) we then have

$$v_{p\ max} = v_{1p\ max} = \Delta\omega_p \tag{64}$$

Referring to (63) we consider two cases.

<u>Case I: $\Delta\omega_p > \Omega_v$</u>

Assuming a steep lowpass filter rolloff it may be seen from Figure B-8 that

$$\frac{1}{T_2} = \frac{\Delta\omega_p \cos \Omega_p t_1}{2\pi} = \frac{\Omega_v}{2\pi}, \text{ or}$$

$$\cos \Omega_p t_1 = \frac{\Omega_v}{\Delta\omega_p} < 1 \tag{65}$$

But according to (63), the positive value of the envelope at t_1 equals

$$v_{max} = v_{1\ max} = \Delta\omega_p\ \rho_p \cos(\Omega_p t_1). \tag{66}$$

Hence from (65) and (66)

$$v_{max} \approx \Omega_v\ \rho_p, \tag{67}$$

and from (67) and (64)

$$\boxed{\frac{v_{p\ max}}{v_{max}} \approx \frac{\Delta\omega_p}{\Omega_v\ \rho_p}} \tag{68}$$

Case II: $\Delta\omega_p \leq \Omega_v$

As a first-order approximation we may assume that all frequencies of $v_1(t)$ pass the lowpass filter, i.e.,

$$v(t) \approx v_1(t) \tag{69}$$

The maximum positive value of the envelope is in view of (63)

$$v_{max} = \Delta\omega_p \, \rho_p. \tag{70}$$

Hence, from (70) and (64) we have

$$\boxed{\frac{v_{p\,max}}{v_{max}} = \frac{1}{\rho_p}} \tag{71}$$

Experimental Observations

It should be evident that (68) and (71) are only approximate due to the fact that we neglected

a) the response sluggishness of the IF bandpass and audio lowpass filter, and

b) the effects of the higher-order sidebands.

Referring to (68) it is found that with

$\frac{1}{2\pi} \; \Delta\omega_p = 75$ kHz,

$$\frac{1}{2\pi}\,\Omega_v = 30\ \text{kHz},$$

$$\frac{1}{2\pi}\,\Omega_p = 100\ \text{Hz}$$

$$\rho_p = 0.225,$$

the calculated and measured values are 11 and 6, respectively.

It was also found that (68) showed very little dependency upon the value of the modulating frequency Ω_p.

APPENDIX C

SIGNAL-TO-NOISE RATIOS FOR AM, PM AND FM

In this report we derive expressions (References 1, 3) for the signal-to-noise power ratios for amplitude (AM), phase (PM) and frequency (FM) modulated receivers. Effects of frequency empahsis at the transmitter and de-emphasis at the receiver will be included. It is assumed that the receiver input contains white noise with uniform spectral density and zero mean value.

Let in what follows:

C = carrier power (Watts),

S = signal power (Watts),

N = noise power (Watts),

[illegible] = noise spectral density (Watts/Hz),

e = RF signal voltage (Volts),

[illegible] = modulating signal, and

n = noise voltage (Volts).

It is further assumed that g(t) is band-limited and of zero mean value.

C-1 Amplitude Modulation

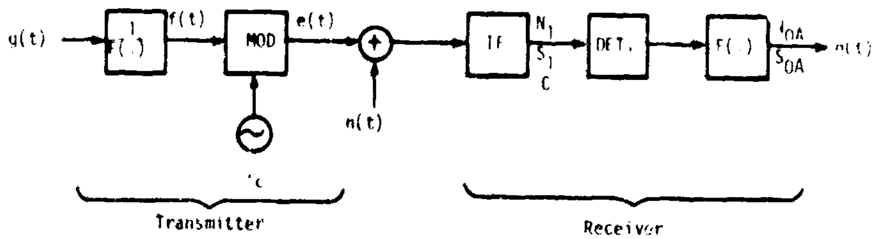

Figure C-1

Referring to Figure C-1, video signal g(t) enters pre-emphasis filter $1/F(\omega)$ and is then amplitude modulated, i.e.,

$$e(t) = E[1 + mf(t)] \cos (\omega_c t + \phi_c), \tag{1}$$

where

E = carrier amplitude (Volts),

m = modulation factor,

ω_c = carrier frequency (rad/sec),

ϕ_c = constant phase shift (rads) and

$|f(t)| \leq 1.$

For reasons of simplicity ω_c has been made equal to the center frequency of the IF bandpass filter of the receiver whose idealized magnitude characteristics are shown in Figure C-2. Assuming that f(t) is band-limited, the signal power after the IF filter equals

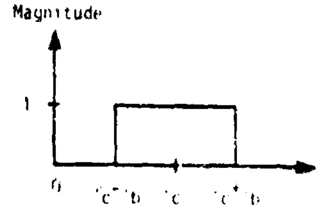

Figure C-2

$$S_1 = \frac{E^2}{2} + Em\,\overline{f(t)} + \frac{E^2}{2} m^2\,\overline{f^2(t)}$$

$$= \frac{E^2}{2}\left[1 + m^2\,\overline{f^2(t)}\right], \tag{2}$$

where

$$\overline{f(t)} = \lim_{T\to\infty} \frac{1}{2T}\int_{-T}^{T} f(t)dt = 0 \tag{3}$$

is the mean value of f(t) which is zero when f(t) contains no DC component and

$$\overline{f^2(t)} = \lim_{T\to\infty} \frac{1}{2T}\int_{-T}^{T} f^2(t)dt \tag{4}$$

is the power of f(t).

Let the noise voltage n(t) possess a constant spectral density η. Then after the bandpass filter, the spectral density equals (See Figure C-2)

$$W_1(\omega) = \eta[u(\omega - \omega_c + \omega_b) - u(\omega - \omega_c - \omega_b)], \tag{5}$$

where u(x) is a step function defined by

$u(x) = 0$ for $x < 0$

$u(x) = 1$ for $x \geq 0$

The power N_1 is then given by

$$N_1 = \frac{1}{2\pi}\int_0^\infty W_1(\omega)\, d\omega \tag{6}$$

$$= \frac{1}{2\pi}\int_0^\infty \eta[u(\omega - \omega_c + \omega_b) - u(\omega - \omega_c - \omega_b]\, d\omega$$

$$= \frac{\eta}{2\pi}\int_{\omega_c-\omega_b}^{\omega_c+\omega_b} d\omega \quad \text{, or}$$

$$N_1 = 2\eta\,\frac{\omega_b}{2\pi} \tag{7}$$

From (2) and (7) we then have

$$\frac{S_1}{N_1} = \frac{E^2/2}{2\eta\,\frac{\omega_b}{2\pi}}\,[1 + m^2\,\overline{f^2(t)}] = \frac{C}{N_1}\,[1 + m^2\overline{f^2(t)}]\ , \tag{8}$$

where the carrier-to-noise ratio is

$$\frac{C}{N_1} = \frac{E^2/2}{2\eta\,\frac{\omega_b}{2\pi}} \tag{9}$$

Referring to Figure C-1 it is evident that after envelope detection and de-emphasis with $F(\omega)$, the modulating signal $f(t)$ is converted back to the original signal $g(t)$.

Hence in view of (1) the signal power at the receiver output equals

$$S_{oA} = E^2 m^2 \overline{g^2(t)} \tag{10}$$

In order to determine the noise power output, the noise spectral density at the receiver output must be known. In terms of $W_1(\omega)$ we have

$$W_{oA}(\omega) = |F(\omega)|^2 W_1(\omega) \tag{11}$$

Making use of (5) and (11) yields

$$N_{oA} = \frac{\eta}{2\pi} \int_{\omega_c - \omega_b}^{\omega_c + \omega_b} |F(\omega)|^2 d\omega = \frac{\eta}{2\pi} \int_{-\omega_b}^{\omega_b} |F(\Omega)|^2 d\Omega \tag{12}$$

Hence

$$\frac{S_{oA}}{N_{oA}} = 2 \frac{\frac{E^2}{2} m^2 \overline{g^2(t)}}{\frac{\eta}{2\pi} \int_{-\omega_b}^{\omega_b} |F(\Omega)|^2 d\Omega} = \frac{C}{N_1} \frac{2m^2 \overline{g^2(t)}}{\frac{1}{2\omega_b} \int_{-\omega_b}^{\omega_b} |F(\Omega)|^2 d\Omega}, \tag{13}$$

where C/N_1 is defined by (9). In the above as well as in the next derivations it has been assumed that C/N_1 is large.

C-2 Phase and Frequency Modulation

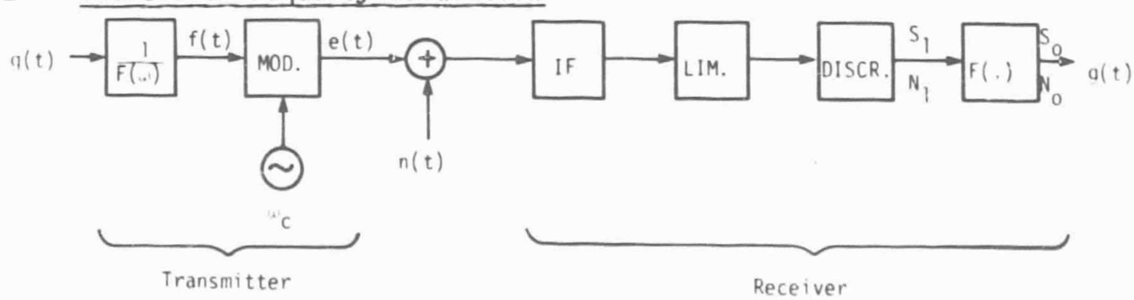

Figure C-3

In the block diagram of Figure C-3 we may now either have phase or frequency modulation and demodulation. It is assumed that perfect limiting occurs. The RF signals are given by

$$e_P(t) = E \cos [\omega_c t + \phi_c + \Delta\phi_c f(t)] \qquad \text{for PM,} \tag{14}$$

$$e_F(t) = E \cos [\omega_c t + \phi_c + \Delta\omega_c \int_0^t f(t)dt] \qquad \text{for FM,} \tag{15}$$

where

ω_c = carrier frequency = IF center frequency (rad/sec)

ϕ_c = constant phase shift (radians)

$\Delta\phi_c$ = phase deviation amplitude (radians)

$\Delta\omega_c$ = frequency deviation amplitude (rad/sec)

$|f(t)| \leq 1.$

Without noise and by taking the de-emphasis filter $F(\omega)$ into account, the audio output power is given by

$$S_{oP} = \overline{[\Delta\phi_c \; g(t)]^2} = (\Delta\phi_c)^2 \; \overline{g^2(t)} \qquad \text{for PM} \tag{16}$$

$$S_{oF} = \overline{[\Delta\omega_c \; g(t)]^2} = (\Delta\omega_c)^2 \; \overline{g^2(t)} \qquad \text{for FM} \tag{17}$$

In order to find the noise power N_1 after the discriminator we must first determine the special density $W_1(\omega)$. We start by considering the noise contribution of the narrow strip in Figure C-4. It has been shown elsewhere that for this case the noise voltage may be represented by

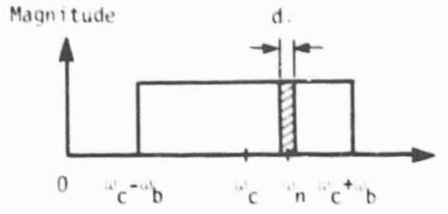

Figure C-4

$$e_n(t) = E_n(t) \cos(\omega_n t + \phi_n) , \tag{18}$$

where $E_n(t)$ is a slowly varying function.

Furthermore,

$$\overline{e_n^2(t)} = \frac{1}{2} E_n^2 = \frac{1}{2\pi} \int_{\omega_n}^{\omega_n + d\omega} \eta d\omega = \frac{\eta d\omega}{2\pi} \tag{19}$$

where η is the constant spectral density of the noise.

Let us now add the unmodulated carrier voltage $e(t)$ to the noise voltage $e_n(t)$. Hence in view of (14) and (18)

$$e(t) + e_n(t) = E \cos(\omega_c t + \phi_c) + E_n \cos(\omega_n t + \phi_n)$$

$$= V_n \cos[\omega_c t + \phi_c + \theta_n(t)], \tag{20}$$

where

$$V_n = E\left[1 + 2\frac{E_n}{E} \cos \psi_n + \frac{E_n^2}{E^2}\right]^{\frac{1}{2}}, \tag{20a}$$

$$\theta_n = \tan^{-1} \frac{E_n \sin \psi_n}{E + E_n \cos \psi_n} \quad , \text{ and} \tag{20b}$$

$$\psi_n = (\omega_n - \omega_c)t + \phi_n - \phi_c. \tag{20c}$$

Now for $E_n/E << 1$, (20b) reduces to

$$\theta_n = \frac{E_n}{E} \sin \psi_n \qquad \text{for PM} \tag{21}$$

so that

$$\dot{\theta}_n = \frac{E_n}{E} (\omega_n - \omega_c) \cos \psi_n \quad , \qquad \text{for FM} \tag{22}$$

where (21) and (22) represent the noise outputs at the phase and frequency discriminators, respectively. Hence for the infinitesimal frequency band in Figure C-4, the corresponding infinitesimal noise powers are

$$dN_p = \overline{\theta_n^{\,2}} = \frac{1}{2} \frac{E_n^{\,2}}{E^2} = \frac{\eta}{E^2} \frac{d\omega}{2\pi} \quad , \text{ and} \qquad \text{for PM} \tag{23}$$

$$dN_F = \overline{\dot{\theta}_n^{\,2}} = \frac{1}{2} \frac{E_n^2}{E^2} (\omega_n - \omega_c)^2 = \frac{\eta}{E^2} (\omega_n - \omega_c)^2 \frac{d\omega}{2\pi} \quad \text{for FM} \tag{24}$$

where we have made use of (19).

Since the spectral density amounts to

$$W(\omega) = 2\pi \frac{dN}{d\omega} \quad , \tag{25}$$

we have from (23) - (25) just after the discriminator,

$$W_{1P}(\omega) = \frac{\eta}{E^2} \qquad \text{for PM} \tag{26}$$

$$W_{1F}(\omega) = \frac{\eta}{E^2}(\omega - \omega_c)^2 \qquad \text{for FM} \tag{27}$$

The spectral densities after the de-emphasis filter $F(\omega)$ are

$$W_{oP}(\omega) = \frac{\eta}{E^2}|F(\omega - \omega_c)|^2 \qquad \text{for PM} \tag{28}$$

$$W_{oF}(\omega) = \frac{\eta}{E^2}(\omega - \omega_c)^2 |F(\omega - \omega_c)|^2 \qquad \text{for FM} \tag{29}$$

With ω_b being half the bandpass filter bandwidth the output noise power will generally be given by

$$N_o = \frac{1}{2\pi}\int_{\omega_c - \omega_b}^{\omega_c + \omega_b} W_o(\omega)\, d\omega = \frac{1}{2\pi}\int_{-\omega_b}^{\omega_b} W_o(\omega_c + \Omega)\, d\Omega \tag{30}$$

Using (28) - (30) the noise power output is

$$N_{oP} = \frac{\eta}{2\pi E^2}\int_{-\omega_b}^{\omega_b} |F(\Omega)|^2\, d\Omega \qquad \text{for PM} \tag{31}$$

$$N_{oF} = \frac{\eta}{2\pi E^2}\int_{-\omega_b}^{\omega_b} \Omega^2 |F(\Omega)|^2\, d\Omega\,. \qquad \text{for FM} \tag{32}$$

Recalling from (9) that the carrier-to-noise ratio amounts to

$$\frac{C}{N_1} = \frac{E^2/2}{2\eta \frac{\omega_b}{2\pi}} , \tag{9}$$

it may be found from (16), (17), (31) and (32) that

$$\frac{S_{oP}}{N_{oP}} = \frac{C}{N_1} \cdot \frac{2(\Delta\phi_c)^2 \; \overline{g^2(t)}}{\frac{1}{2\omega_b} \int\limits_{-\omega_b}^{\omega_b} |F(\Omega)|^2 \, d\Omega} , \quad \text{for PM} \tag{33}$$

$$\frac{S_{oF}}{N_{oF}} = \frac{C}{N_1} \cdot \frac{2(\Delta\omega_c)^2 \; \overline{g^2(t)}}{\frac{1}{2\omega_b} \int\limits_{-\omega_b}^{\omega_b} \Omega^2 |F(\Omega)|^2 d\Omega} . \quad \text{for FM} \tag{34}$$

C-3 Comparison of PM and FM

From (33) and (34) it follows that

$(S_{oP}/N_{oP})/(S_{oF}/N_{oF}) =$

$$(\Delta\phi_c/\Delta\omega_c)^2 \left[\int\limits_{-\omega_b}^{\omega_b} \Omega^2 \; |F(\Omega)|^2 d\Omega\right] \Big/ \left[\int\limits_{-\omega_b}^{\omega_b} |F(\Omega)|^2 \; d\Omega\right] \tag{35}$$

In order to evaluate (35) let us first assume that the output of the receiver contains an ideal lowpass filter with radian cutoff frequency Ω_v, i.e., we set $\omega_b = \Omega_v$. Assuming a sinusoidal modulating signal we also set $\Delta\omega_c = \Omega\Delta\phi_c$ where Ω is the radian signal frequency.

Without frequency de-emphasis we then obtain from (35) with $|F(\Omega)| = 1$,

$$(S_{oP}/N_{oP})/(S_{oF}/N_{oF}) = \Omega_v^2/(3\Omega^2). \tag{36}$$

With frequency de-emphasis we set

$$|F(\Omega)|^2 = 1/[1 + (\Omega/\Omega_d)^2] \tag{37}$$

where Ω_d is the radian cutoff frequency. Assuming $\Omega_c << \Omega_v$ we obtain

$$(S_{oP}/N_{oP})/(S_{oF}/N_{oF}) \approx (2\Omega_d\Omega_v)/(\pi\Omega^2). \tag{38}$$

Expressions (36) and (38) show that the S/N ratios of PM are higher than FM provided

$$\Omega < (\Omega_v/\sqrt{3}), \text{ without de-emphasis,} \tag{39}$$

and

$$\Omega < (2\Omega_d\Omega_v/\pi)^{\frac{1}{2}} \text{ , with de-emphasis} \tag{40}$$

APPENDIX D

NONLINEAR FREQUENCY DETECTOR

It is the objective of this detector to digitally program the frequency $f_V = 1/T_V$ of a voltage-controlled oscillator (VCO) as shown in Table D-1 where

$f_R = 1/T_R$ = reference frequency,

N_1 = channel select number, and

N_2 = dead zone select number.

TABLE D-1

Region	VOC Frequency f_V	Detector	
		Output Voltage E(v)	Output Impedance Z(Ω)
1	$2(N_1 + N_2)f_R < f_V'$	High	Low
2	$2(N_1 - N_2)f_R < f_V'' < 2(N_1 + N_2)f_R$	X	High
3	$f_V''' < 2(N_1 - N_2)f_R$	Low	Low

One observes from the conditions of the detector output voltage and impedance that the VCO is controlled only in regions 1 and 3 and that in region 2 (the dead zone) the VCO can assume any frequency within the band $4N_2f_R$. The center frequency of this band is given by $2N_1f_R$.

Referring to Figures D-1 and D-2, the operation is as follows:

Note first that delay flip-flops FF1, FF2 and synchronous up-counters CR1, CR2 clock on the positive edges of output V of the voltage-controlled oscillator (VCO). The period of V equals $T_V = 1/f_V$. Next, consider the reference clock R of half-period $T_R/2$ which is shifted through FF1 and FF2. By combining Q_1 and $Q_2 = D_3$ at gate G1 a load pulse L of width T_V is generated. When L is low, a channel select number is loaded into counter CR1. After N_1 up-counts, CR1 stops counting and D_4 goes high. This is accomplished by feeding the carry output back to its T input. Furthermore, by combining $Q_2 = D_3$ and D_4 at gate G2, a second load pulse H of variable width T_H is generated. When H is low, a dead zone select number is loaded into counter CR2. After N_2 up-counts CR2 stops counting by feeding back its carry output to its P input. At this instant K goes high and both delay flip-flops FF3 and FF4 are being clocked at CK. The states of Q_3 and $\overline{Q}_4$ therefore depend on the states of D_3 and D_4 prior to the arrival of the positive edge of K. An inspection of Figure D-2 is facilitated by consulting Table D-2 simultaneously. This table has been derived from Table D-1 by using the relations $T_R = 1/f_R$ and $T_V = 1/f_V$. One observes that the output states of Q_3 and $\overline{Q}_4$ are directly related to the inequality signs.

As an example, a detailed description of region 1 will now be given.

After the positive edge of load pulse L, output D'_4 of counter CR1 remains high during N_1 counts, i.e., $T_4' = N_1 T_V'$. Next, load pulse H' of length T_H' is obtained from D_3 and D'_4. Since T_3 is

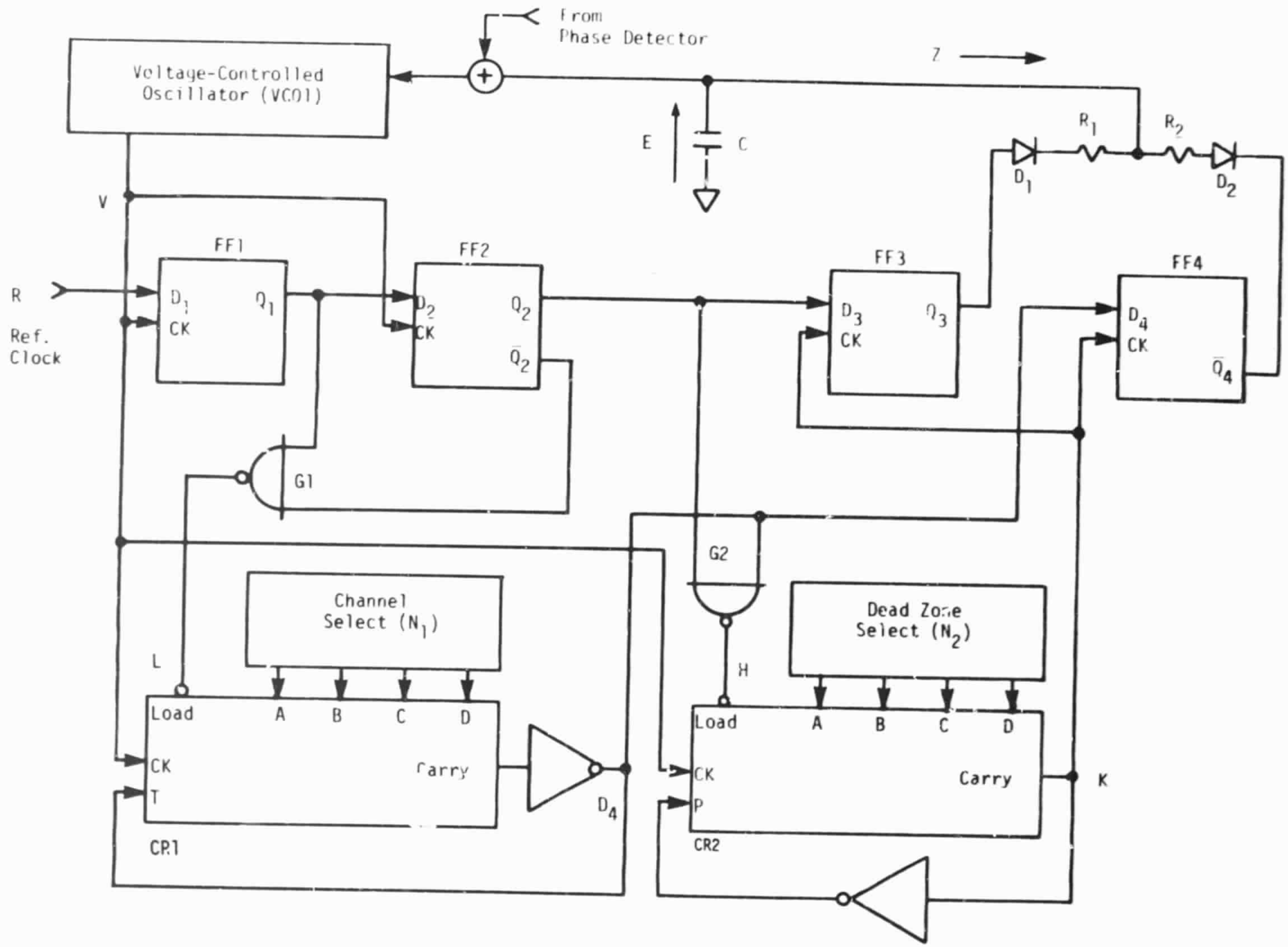

Figure D-1. Frequency-lock loop with dead zone.

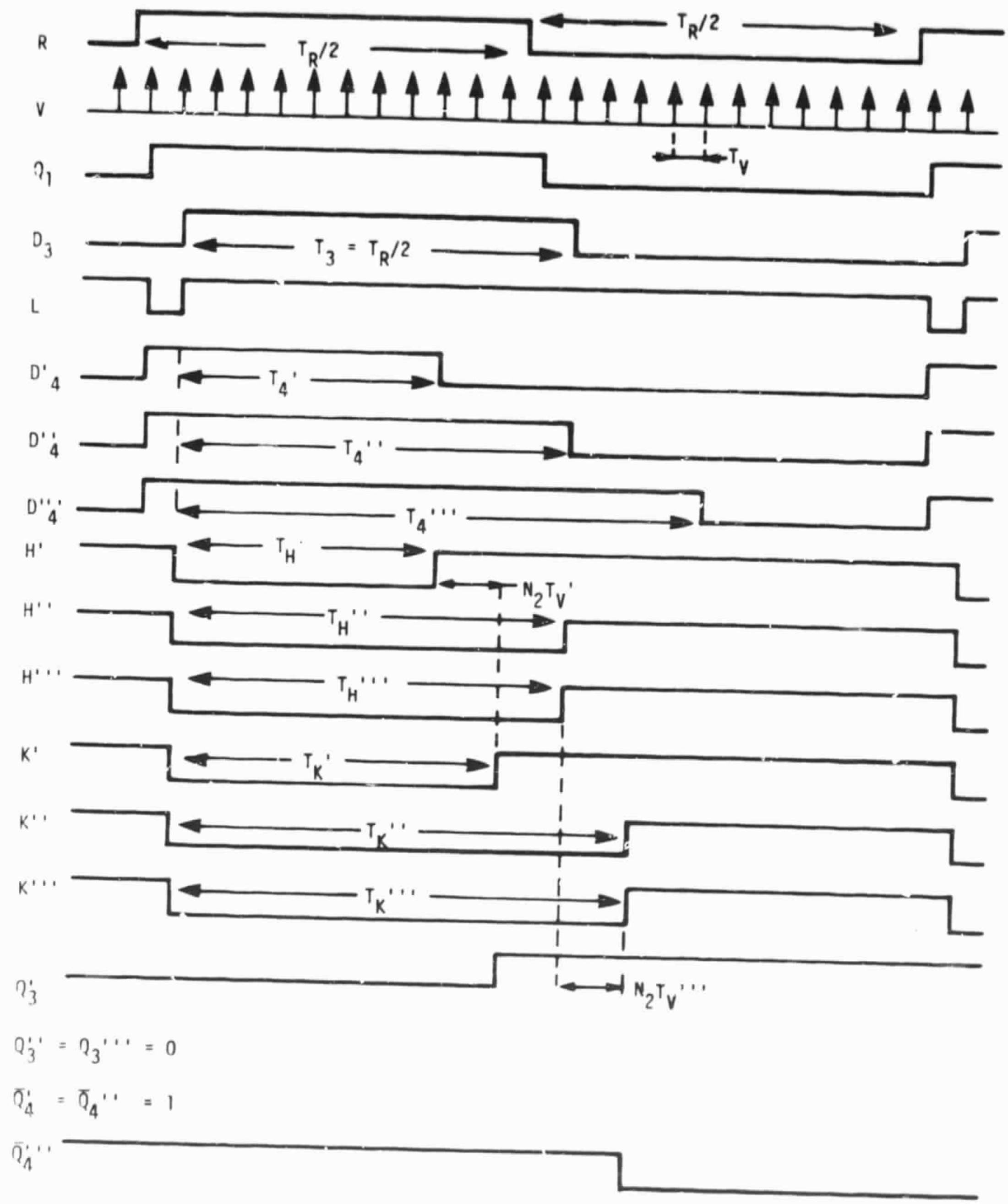

Figure D-2. Timing diagram.

TABLE D-2.

Region	T_3		$T_K = T_H + N_2T_V$		T_4	T_H	Q3	$\overline{Q4}$
1	$T_R/2$	>	$(N_1 + N_2)T_V'$	>	N_1T_V'	N_1T_V'	1	1
2a	$T_R/2$	<	$(N_1 + N_2)T_V''$	>	N_1T_V''	N_1T_V''	0	1
2b	$T_R/2$	<	$(T_R/2) + N_2T_V''$	>	N_1T_V''	$T_R/2$	0	1
3	$T_R/2$	<	$(T_R/2) + N_2T_V'''$	<	N_1T_V'''	$T_R/2$	0	0

greater than T_4', it follows that $T_H' = T_4' = N_1T_V'$. After the positive edge of H', output K' of counter CR2 goes high after N_2 counts, i.e.,

$$T_K' = T_H' + N_2T_V' = (N_1 + N_2)T_V'$$

Now since $T_3 = T_R/2$ is greater than T_K', D_3 will be high when FF3 is clocked, i.e., Q_3 goes high. Furthermore, since $T_4' = N_1T_V'$ is smaller than T_K', D_4 will be low when FF4 is clocked, i.e., $\overline{Q_4}$ goes high. This completes the description of region 1. It remains to be shown how the states of Q_3 and $\overline{Q_4}$ of Table D-2 are related to the voltage and impedance requirements of Table D-1.

In region 1 both Q_3 and $\overline{Q_4}$ are high so that diode D_1 conducts (low impedance) and E goes high. In region 2, Q_3 is low and $\overline{Q_4}$ is high. As long as the value of E remains between the high and low voltage values of Q_3 and $\overline{Q_4}$, neither diode D_1 or D_2 conducts so that the impedance is high. Finally, in region 3 both Q_3 and $\overline{Q_4}$ are low so that now only diode D_2 conducts and E becomes low.

APPENDIX E

COMB FREQUENCY SPECTRUM GENERATOR

It is the purpose of this instrument to test the performance of the multichannel receiver by simulating an array of frequency modulated transmitter carriers.

Referring to Figure E-1, the primary carriers received on a particular antenna track are indicated by 'A' and 'B'. In addition, the secondary carriers 'a' are generated which simulate crosstalk from the adjacent antenna tracks. The receiver under test is normally tuned to carrier 'B' at 15.4 MHz.

The present design includes the following features (see also Figure E-2):

- All 'A' and 'a' carriers simultaneously frequency modulated by audio input 1
- 'B' carrier frequency modulated by audio input 2
- Maximum frequency deviation: ± 200 kHz
- Audio response: 10 Hz to 150 kHz, ± 1 dB
- Carrier response: 10.4 MHz to 20.6 MHz, ± 1 dB
- Load impedance: 50 Ohms

Referring to Figure E-2, the comb frequency spectrum generator operates as follows.

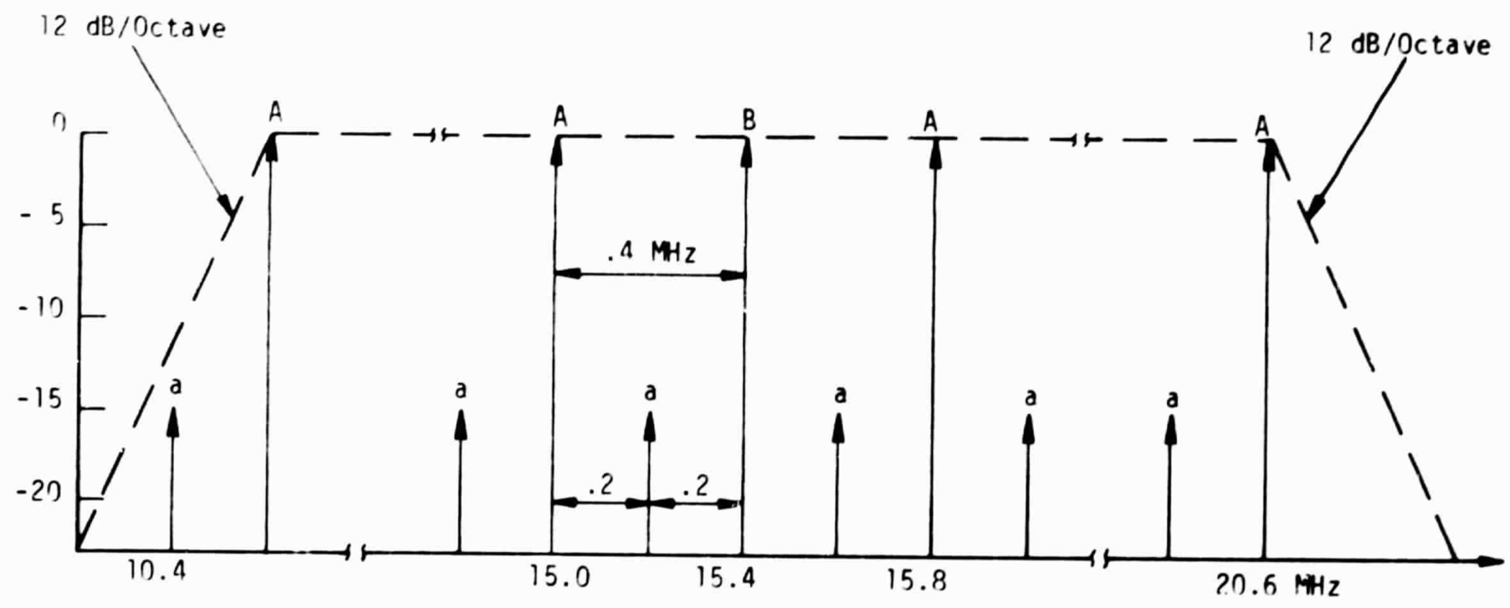

Legend

A, B = Primary Carriers

a = Secondary Carriers

Amplitude of 'a' adjustable from -15 dB to -35 dB.

Carriers 'A' and 'a' modulated by audio input 1.

Carrier 'B' modulated by audio input 2.

Figure E-1. Frequency Spectrum

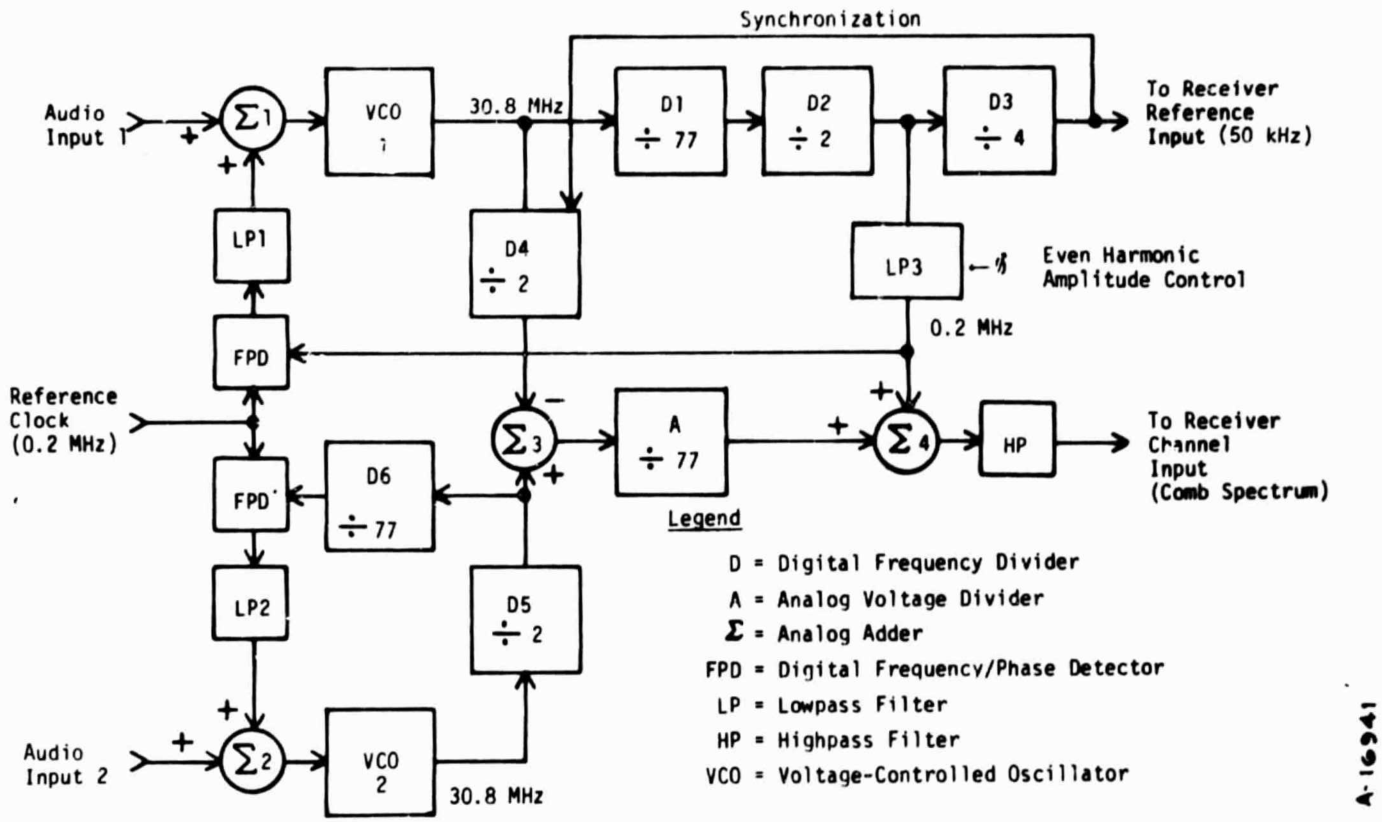

Figure E-2. Block diagram -- comb generator.

First, the 0.2 MHz reference clock frequency is multiplied by a factor 154 in order to obtain the 30.8 MHz carriers at the outputs of voltage-controlled oscillators VCO 1 and VCO 2. This is accomplished by two phase-lock loops. One loop consists of VCO 1, the digital frequency dividers D1, D2, frequency and phase detector FPD and lowpass filter LP1. The other loop contains VCO2, frequency dividers D5, D6, frequency and phase detector FPD and lowpass filter LP2. The two loops serve also as frequency modulators. Audio input 1 modulates carriers 'A' and 'a' and Audio input 2 modulates carrier 'B'.

Next, the discrete 'A' (odd harmonics) and 'a' (even harmonics) spectra are generated from the square wave at the output of D2. Lowpass filter LP3 serves to control the amplitude of the 'a' carriers.

Before the 'B' carrier at the output of D5 can be added to the 'A' spectrum, it is evident that the 15.4 MHz component of this spectrum must be removed first. In the present design this has been accomplished by subtracting the 15.4 MHz carrier at the output of D4 from the 'A' spectrum by means of analog adders $\sum 3$ and $\sum 4$ and analog attenuator A.

Finally, highpass filter HP shapes the spectrum for uniform response between 10.4 MHz and 20.6 MHz and provides a frequency rolloff of 12 dB/octave outside this band.

APPENDIX F

STRESS ANALYSIS OF TRANSMITTER PACKAGE

INTRODUCTION

As part of the design task, the transmitter cases were stress analyzed for operation in a stacked configuration at acceleration levels of 50,000 g's. The direction of the acceleration is normal to the case (vertical) and in a downward configuration, such that circuit components are pressed against their supporting substrates. The calculations are made for the transmitter at the bottom of the stack. The most severely stressed areas of the transmitter were analyzed for stress and deflection. Areas whose stress levels were obviously lower were not included in the calculations.

Stress Analysis Summary, Flat Pack Transmitters

A. Basic Case Configuration and Material Properties

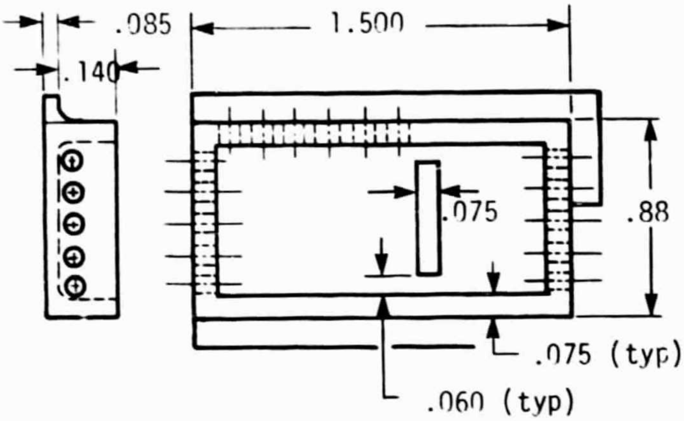

Material: 17-4PH SST (H900)

$E = 3 \times 10^7$

$\mu = .3$

$\sigma_{yield} = 165$ ksi

$\sigma_{ult} = 190$ ksi

B. Bottom of Large Compartment, Bending Stresses

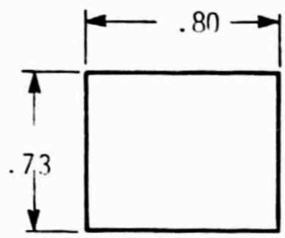

a_r = Radial acceleration, g's

W_B = Effective weight of bottom

$W_B = \ell \omega t \rho a_r$

$W_B = 0.73(0.80)0.085(0.287)50000 = 712$ lbs

$w_B = \frac{W}{A} = \rho t a_r = 0.287(0.085)50000 = 1220$ psi

Effective substrate Weight $W_s = 0.63(0.70)0.034(0.137)50000 = 106$ lbs

$w_s = \frac{W}{A} = \rho t a_r = 0.137(0.035(50000 = 240$ psi

Assuming a uniform load and simply supported edges, the maximum bending stress in the bottom, σ_{max} is:

$w = w_B + w_S = 1220 + 240 \quad = 1460$ psi

$b = .73$ in $\qquad \alpha = \frac{a}{b} = \frac{.73}{.80} = .9125$

$$\sigma_{max} = \frac{0.75\ wb^2}{t^2(1 + 1.61\ \alpha^3)} \qquad \mu = 0.3$$

$$= \frac{.75(1460).73^2}{.085^2(1 + 1.61(.9125)^3)} = \underline{36,327 \text{ psi}}$$

σ_{yield} = 165 ksi

Safety factor = $\frac{165}{36.3}$ = 4.55

However, the thickness of the bottom must be determined by its maximum deflection, since a crack in the alumina substrate of the hybrid circuit will fail the transmitter.

The maximum deflection, y_{max}, of the case bottom

$$y_{max} = \frac{.1422\ \omega b^4}{Et^3(1 + 2.21\alpha^3)} = \frac{.1422(1460).73^4}{3 \times 10^7(.085)^3(1 + 2.21(.9125)^3)} = \underline{.00119 \text{ in.}}$$

It is felt that deflections on the order of .001 - .002 inches could be safely tolerated without substrate damage.

C. Wall Stresses for Bottom Xmitter in a Stack of Four

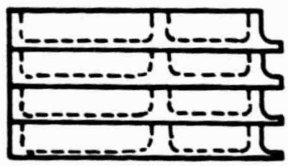

1. Effective Weights @ 50,000 g's

Xmitter bottom:	1.5(.88).085(.287)50000 =	1610 lbs
Substrates:	[.63(.70) + .38(.63)].035(.137)50000 =	163
Walls:	5.07(.140).075(.287)50000 =	764
Top:	1.5(.88).040(.287)50000 =	758
Shelf:	[.10(.035) + 7.73 x 10^{-4}]1.9(.287)50000 =	117
	TOTAL XMITTER WT	3412

2. Load carried by walls of bottom xmtr

3 xmtrs @ 3412	=	10236 lbs
1 wall + 1 top @ 1522	=	1522
TOTAL LOAD		11758 lbs

Assuming a uniform distribution of load over the 5.07 inches of wall length, the distributed load, w, is:

$$w = \frac{11758}{5.07} = 2319 \text{ lbs/in}$$

3. <u>End Wall Compressive Stresses</u>

For the end wall containing 5 electrical feedthroughs,

ℓ = .73 in, W = 2319(.73) = 1693 lbs

<u>Effects of Stress Concentration on Compressive Wall Stresses</u>

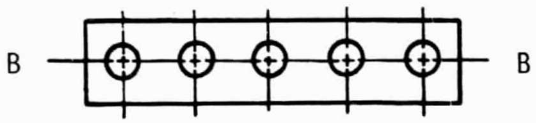

Net area along plane B-B = [.73 - 5(.063)].075 = <u>.03113 in^2</u>.

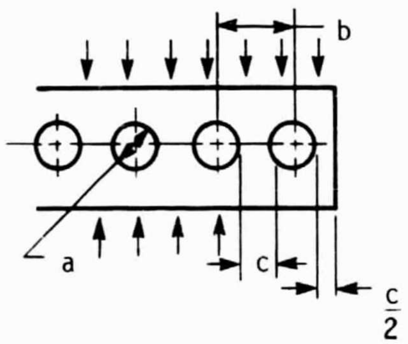

Hole Spacing

$$c = \frac{.73 - 5(.063)}{5} = .083$$

$$b = .083 + .063 = .146$$

$$a = .063, \ \frac{a}{b} = \frac{.063}{.146} = .431$$

For an infinite wall with uniformly spaced holes, $\frac{a}{b} = .431$,

$$K_{tn} = 1.8 \qquad \sigma_{max} = K_{tn} \frac{W}{A_{net}} = 1.8 \ \frac{1693}{.03113} = \underline{97,893 \text{ psi}}$$

σ_{yield} = 165 ksi

Safety factor = $\frac{165}{97.9}$ = 1.69

4. Side Wall Compressive Stresses

Repeating the same calculations on the side wall containing 6 electrical feedthroughs

Supported load, W = 2319(.80) = 1855 lbs

Net area, A_{net} = [.80 - 6(.063)].075 = .03165

Hole Spacing Parameters

$$c = \frac{.80 - .378}{6} = .070$$

$$b = .070 + .063 = .133$$

$$\frac{a}{b} = \frac{.063}{.133} = .474$$

Effects of Stress Concentration

For an infinitely long wall with uniformly spaced holes,

K_{tn} = 1.68

$$\sigma_{max} = 1.68 \frac{1855}{.03165} = \underline{.98{,}464 \text{ psi}}$$

$$\text{Safety factor} = \frac{165}{98.5} = 1.68$$

D. Top Cover Stresses

Material thickness, t = .040 inches

Largest unsupported span = .73 x .80, $\omega = \rho t a_r$ = .287(.040)50000 = 574 psi

$W = 574(.73 \times .80) = 335$ lbs

$$\sigma_{max} = \frac{.75(574).73^2}{.04^2(1 + 1.61(.9125)^3)} = \underline{64{,}492 \text{ psi}} \quad \text{(74K psi if .035 thk)}$$

$$y_{max} = \frac{.1422(574).73^4}{3 \times 10^7(.04)^3(1 + 2.21\alpha^3)} = \underline{.00451 \text{ in}} \quad \text{(.0052 if .035 thk)}$$

Max Shear Stress, $\tau = \frac{W}{2(\ell+w)t} = \frac{335}{2(.08+.73).040} = 2736$ psi, $\tau_{yield} = 94$ ksi

E. <u>Shelf Bending Stresses</u>

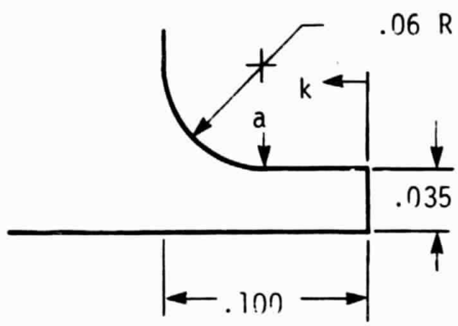

(Maximum stress occurs at Point a)

Per unit width $M = .035(1)x.287(50000)\frac{x}{2} = 502.3\,\frac{x^2}{2}$ lb-in

For $0 \leq x \leq 0.04$ in

$$I = \frac{1(.035)^3}{12} = 3.57 \times 10^{-6} \text{in}^4$$

@$x = .04$ in $\quad M = 502.3\frac{(.04)^2}{2} = .4018$ lb-in

For a beam in bending with fillet radius r,

For $\frac{r}{d} = \frac{.06}{.035} = 1.71$, $K_t < 1.4$

Maximum Bending Stress, $\sigma_{max} = K_t \frac{Mc}{I} < 1.4 \frac{.4018(.0175)}{3.57 \times 10^{-6}} = 1970$ psi

Safety Factor = 83

APPENDIX G

TRANSMITTER RELIABILITY ANALYSIS

Note:

Failure rate calculations in this report make no allowance for centrifugal force. Acurex experience indicates that centrifugal force is considerably less of a factor than ambient temperature (which is factored into these calculations) - provided that appropriate packaging techniques and components are employed.

MULTICHANNEL WIRELESS DATA TRANSMITTER

RELIABILITY PREDICTION

25 APRIL, 1977

FOR

NASA

BY

ACUREX CORPORATION

485 Clyde Avenue

Mountain View, California 94042

Prepared by: ______________________
L. Leichter
Reliability Consultant

Approved by: ______________________
Sam Toy
Project Engineer

1.0 SCOPE

This Reliability Prediction Report has been prepared at the request of Sam Toy, Project Engineer on the Multichannel Wireless Data Transmitter (MWDT).

2.0 APPLICABLE DOCUMENTS

The following documents, of the issue in effect on the date of contract award, form a part of the requirements of this document to the extent specified herein:

RADC-TR-67-108	RADC Reliability Notebook (1967, Vol. II).
RADAC	Tymshare Tymcom-IX Manual.

3.0 REQUIREMENTS

There are no definitive reliability requirements for the MWDT. However, it is important that it survive a 30-hour test period with a high probability of success.

4.0 RELIABILITY PREDICTION MODEL

A reliability model for the MWDT is shown in Figure 1. This model is a conservative series model; i.e., if any one component within the system fails, the entire system is considered failed. In addition, each of the components within the Hybrid Circuit Modules were considered in series.

5.0 FAILURE RATES

The part failure rates used in this prediction are from RADC Reliability Notebook RADC-TR-67-108. The failure rates were calculated at 25% stress for temperatures of 125°C, 150°C, and 175°C. A list of the part types, quantities and failure rates used is shown for each module in Tables I, II, and III. For the chip components used in the Hybrid Modules, the nearest standard component equivalent failure rate was used. This approach should result in a slightly conservative estimate since the standard components are slightly more complex and, therefore, should have a higher failure rate than the chip component. All failure rates were calculated by a TYMSHARE computer program called "RADAC" which is a computerized version of the RADC Reliability Notebook RADC-TR-67-108. The failure rates were calculated considering both upper quality and lower quality parts. Upper quality parts are defined as those that receive burn-in and parts screening including 100% high-temperature screening. Lower quality parts are defined as those which do not receive burn-in or 100% high-temperature testing. Acurex is burning in and 100% high-temperature testing the hybrid circuits used in the MWDT and, therefore, the upper quality grade failure rates and MTBF should apply.

6.0 RELIABILITY PREDICTION

A parts count estimate for each module at 125°C, 150°C, and 175°C is shown in Tables I, II, and III. Combining these failure rates in accordance with the reliability prediction model shown in Figure 1, the predicted MTBF's for each module was calculated as shown in Figure 2 at 125°C, 150°C, and 175°C. The total MTBF for the three hybrid modules as a system is 1,462,784 and 125 hours at temperatures of 125°C, 150°C, and 175°C, respectively.

The probability of success for a 30-hour test from Figure 2 is 97.9% (@ 125°C), 96.2% (@ 150°C), and 78.7% (@ 175°C).

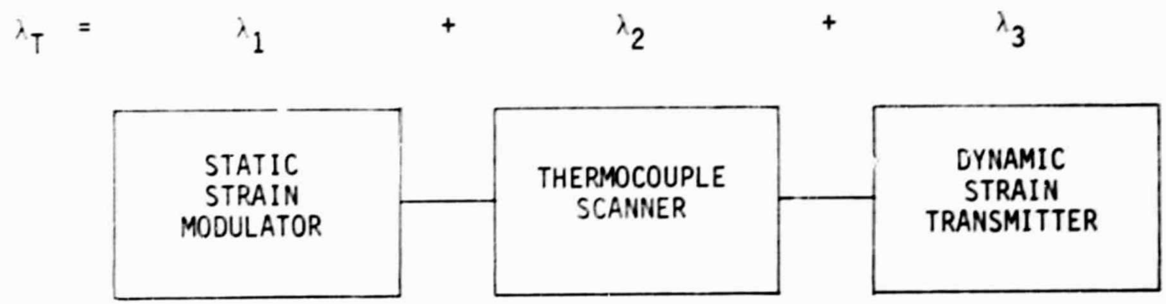

Figure G-1. Multichannel Wireless Data Transmitter Reliability Prediction Model.

Note: System changes, since this work was performed, have simplified the Static Strain and Thermocouple models so that their reliability is now comparable to that of the Dynamic Strain transmitter when considered alone (EG, MTBF = 3,573 hrs @ 125°C). The "series" model, illustrated here, is no longer applicable.

ASSEMBLY	MTBF - Hours 125°C	150°C	175°C
1. Static Strain Modulator	4,486	2,748	503
2. Thermocouple Scanner	5,524	2,121	239
3. Dynamic Strain Transmitter	3,573	2,269	549
TOTAL SYSTEM	1,462	784	125

Probability of Success = Reliability = $e^{-\lambda T}$

where λ = Failure Rate = $\frac{1}{MTBF}$

T = Test Time

ASSEMBLY	% Reliability 125°C	150°C	175°C
1. Static Strain Modulator	99.3%	98.9%	94.2%
2. Thermocouple Scanner	99.4%	98.6%	88.2%
3. Dynamic Strain Transmitter	99.2%	98.7%	94.7%
TOTAL SYSTEM*	97.9%	96.2%	78.7%

*See note in Figure G-1.

Figure G-2. MWDT MTBF and Reliability Summary.

TABLE G-1. MULTICHANNEL WIRELESS DATA TRANSMITTER MTBF @ 125°C

MODULE # 1 STATIC STRAIN MODULATOR

CIRCUIT REF DESIG	PART CODE	QUANTITY	FAILURES/MILLION HRS UPPER QUAL	FAILURES/MILLION HRS LOWER QUAL	DERATING	STRESS
R1	RN50C	1.000	.051509	.214623	.250	.250
R2	RN50C	1.000	.051509	.214623	.250	.250
R3	RN50C	1.000	.051509	.214623	.250	.250
R4	RN50C	1.000	.051509	.214623	.250	.250
R5	RN50C	1.000	.051509	.214623	.250	.250
R6	RN50C	1.000	.051509	.214623	.250	.250
R7	RN50C	1.000	.051509	.214623	.250	.250
R8	RC05	1.000	.162807	.437016	.250	.250
R9	RC05	1.000	.162807	.437016	.250	.250
R10	RC05	1.000	.162807	.437016	.250	.250
R11	RC05	1.000	.162807	.437016	.250	.250
R12	RC05	1.000	.162807	.437016	.250	.250
R13	RC05	1.000	.162807	.437016	.250	.250
R14	RN50C	1.000	.051509	.214623	.250	.250
R15	RC05	1.000	.162807	.437016	.250	.250
R16	RN50C	1.000	.051509	.214623	.250	.250
R17	RC05	1.000	.162807	.437016	.250	.250
R18	RN50C	1.000	.051509	.214623	.250	.250
R19	RC05	1.000	.162807	.437016	.250	.250
R20	RC05	1.000	.162807	.437016	.250	.250
R21	RN50C	1.000	.051509	.214623	.250	.250
R22	RC05	1.000	.162807	.437016	.250	.250
R23	RN50C	1.000	.051509	.214623	.250	.250
C1	CSR	1.000	.012850	.128497	.250	.250
C2	CSR	1.000	.012850	.128497	.250	.250
C3	CK	1.000	.173601	.888005	.250	.250
C4	CSR	1.000	.012850	.128497	.250	.250
C5	CSR	1.000	.012850	.128497	.250	.250
C6	CK	1.000	.173601	.888005	.250	.250
C7	CK	1.000	.173601	.888005	.250	.250
C8	CSR	1.000	.012850	.128497	.250	.250
C9	CSR	1.000	.012850	.128497	.250	.250
C10	CK	1.000	.173601	.888005	.250	.250
C11	CSR	1.000	.012850	.128497	.250	.250
C12	CK	1.000	.173601	.888005	.250	.250
C13	CSR	1.000	.012850	.128497	.250	.250
C14	CSR	1.000	.012850	.128497	.250	.250
C15	CSR	1.000	.012850	.128497	.250	.250
C16	CSR	1.000	.012850	.128497	.250	.250
C17	CK	1.000	.173601	.888005	.250	.250
C18	CK	1.000	.173601	.888005	.250	.250
Q1	FET	1.000	10.436877	205.137543	.917	.250
Q2	FET	1.000	10.436877	205.137543	.917	.250
Q3	FET	1.000	10.436877	205.137543	.917	.250
A1	IC	1.000	52.663966	394.979742	1.020 ^^	1.020 ^^
A2	IC	1.000	78.995948	592.469614	1.020 ^^	1.020 ^^
A3	IC	1.000	52.663966	394.979742	1.020 ^^	1.020 ^^
A4	IC	1.000	1.755466	13.165991	1.020 ^^	1.020 ^^
A5	IC	1.000	1.755466	13.165991	1.020 ^^	1.020 ^^

TABLE G-1. MULTICHANNEL WIRELESS DATA TRANSMITTER MTBF @ 125°C (continued)

MODULE # 2 THERMOCOUPLE SCANNER

CIRCUIT REF DESIG	PART CODE	QUANTITY	FAILURES/MILLION HRS UPPER QUAL	LOWER QUAL	DERATING	STRESS
R1	RC05	1.000	.162807	.437016	.250	.250
R2	RC05	1.000	.162807	.437016	.250	.250
R3	RC05	1.000	.162807	.437016	.250	.250
R4	RC05	1.000	.162807	.437016	.250	.250
R5	RC05	1.000	.162807	.437016	.250	.250
R6	RC05	1.000	.162807	.437016	.250	.250
R7	RC05	1.000	.162807	.437016	.250	.250
R8	RC05	1.000	.162807	.437016	.250	.250
R9	RC05	1.000	.162807	.437016	.250	.250
R10	RC05	1.000	.162807	.437016	.250	.250
C1	CK	1.000	.173601	.888005	.250	.250
C2	CK	1.000	.173601	.888005	.250	.250
C3	CK	1.000	.173601	.888005	.250	.250
C4	CK	1.000	.173601	.888005	.250	.250
C5	CK	1.000	.173601	.888005	.250	.250
C6	CK	1.000	.173601	.888005	.250	.250
C7	CK	1.000	.173601	.888005	.250	.250
C8	CK	1.000	.173601	.888005	.250	.250
C9	CK	1.000	.173601	.888005	.250	.250
C10	CK	1.000	.173601	.888005	.250	.250
C11	CK	1.000	.173601	.888005	.250	.250
C12	CK	1.000	.173601	.888005	.250	.250
C13	CK	1.000	.173601	.888005	.250	.250
Q1	FET	1.000	10.436877	205.137543	.917	.250
Q2	FET	1.000	10.436877	205.137543	.917	.250
Q3	FET	1.000	10.436877	205.137543	.917	.250
Q4	FET	1.000	10.436877	205.137543	.917	.250
Q5	FET	1.000	10.436877	205.137543	.917	.250
Q6	FET	1.000	10.436877	205.137543	.917	.250
Q7	FET	1.000	10.436877	205.137543	.917	.250
Q8	FET	1.000	10.436877	205.137543	.917	.250
Q9	FET	1.000	10.436877	205.137543	.917	.250
Q10	FET	1.000	10.436877	205.137543	.917	.250
Q11	FET	1.000	10.436877	205.137543	.917	.250
Q12	FET	1.000	10.436877	205.137543	.917	.250
Q13	FET	1.000	10.436877	205.137543	.917	.250
Q14	FET	1.000	10.436877	205.137543	.917	.250
Q15	FET	1.000	10.436877	205.137543	.917	.250
Q16	FET	1.000	10.436877	205.137543	.917	.250
Q17	QSP	1.000	4.018585	39.735852	.917	.250
A1	IC	1.000	2.633198	19.748987	1.020 ^^	1.020 ^^
A2	IC	1.000	3.510931	26.331983	1.020 ^^	1.020 ^^

ORIGINAL PAGE IS OF POOR QUALITY

TABLE G-1. MULTICHANNEL WIRELESS DATA TRANSMITTER MTBF @ 125°C (continued)

MODULE # 3 DYNAMIC STRAIN TRANSMITTER

CIRCUIT REF DESIG	PART CODE	QUANTITY	FAILURES/MILLION HRS UPPER QUAL	LOWER QUAL	DERATING	STRESS
R1	RN50C	1.000	.051509	.214623	.250	.250
R2	RN50C	1.000	.051509	.214623	.250	.250
R3	RC05	1.000	.162807	.437016	.250	.250
R4	RN50C	1.000	.051509	.214623	.250	.250
R5	RN50C	1.000	.051509	.214623	.250	.250
R6	RC05	1.000	.162807	.437016	.250	.250
R8	RN50C	1.000	.051509	.214623	.250	.250
R9	RC05	1.000	.162807	.437016	.250	.250
R10	RC05	1.000	.162807	.437016	.250	.250
R11	RN50C	1.000	.051509	.214623	.250	.250
R12	RN50C	1.000	.051509	.214623	.250	.250
R13	RN50C	1.000	.051509	.214623	.250	.250
R14	RN50C	1.000	.051509	.214623	.250	.250
R17	RC05	1.000	.162807	.437016	.250	.250
R18	RC05	1.000	.162807	.437016	.250	.250
R19	RC05	1.000	.162807	.437016	.250	.250
R20	RN50C	1.000	.051509	.214623	.250	.250
R21	RC05	1.000	.162807	.437016	.250	.250
R22	RN50C	1.000	.051509	.214623	.250	.250
R23	RN50C	1.000	.051509	.214623	.250	.250
R25	RC05	1.000	.162807	.437016	.250	.250
C1	CSR	1.000	.012850	.128497	.250	.250
C2	CSR	1.000	.012850	.128497	.250	.250
C3	CSR	1.000	.012850	.128497	.250	.250
C4	CSR	1.000	.012850	.128497	.250	.250
C5	CSR	1.000	.012850	.128497	.250	.250
C6	CK	1.000	.173601	.888005	.250	.250
C7	CSR	1.000	.012850	.128497	.250	.250
C8	CK	1.000	.173601	.888005	.250	.250
C9	CSR	1.000	.012850	.128497	.250	.250
C10	CSR	1.000	.012850	.128497	.250	.250
C11	CK	1.000	.173601	.888005	.250	.250
C12	CK	1.000	.173601	.888005	.250	.250
C13	CSR	1.000	.012850	.128497	.250	.250
C15	CSR	1.000	.012850	.128497	.250	.250
C16	CK	1.000	.173601	.888005	.250	.250
Q1	QSP	1.000	4.018585	39.735852	.917	.250
D1	CRS	1.000	.233060	1.248359	.917	.250
D2	CRS	1.000	.233060	1.248359	.917	.250
D3	ZEN	1.000	2.059603	20.056030	.917	.250
D4	VAR	1.000	26.250964	126.754818	.917	.250
A1	IC	1.000	52.663966	394.979742	1.020 ^^	1.020 ^^
A2	IC	1.000	78.995948	592.469614	1.020 ^^	1.020 ^^
A3	IC	1.000	78.995948	592.469614	1.020 ^^	1.020 ^^
A4	IC	1.000	7.899595	59.246961	1.020 ^^	1.020 ^^
A5	IC	1.000	25.454250	190.906876	1.020 ^^	1.020 ^^

TABLE G-1. MULTICHANNEL WIRELESS DATA TRANSMITTER MTBF @ 125°C (continued)

<<< EQUIPMENT FAILURE TABLE >>>

- EQUIPMENT NAME

MULTICHANNEL WIRELESS DATA TRANSMITTER

- ENVIRONMENTAL SERVICE CONDITION AIRBORNE UNINHABITED

MODULE NAME		QUANTITY	FAILURE/MILLION HRS QUALITY GRADE (UQG)	(LQG)
STATIC STRAIN MODULATOR		1	222.91098	2039.18587
THERMOCOUPLE SCANNER		1	181.03763	3383.93174
DYNAMIC STRAIN TRANSMITTER		1	279.88485	2031.34984
	TOTAL	---	--------	--------
		3	683.83346	7454.46745

<<< EQUIPMENT MTBF >>>

UQG - 1,462 HRS LQG - 134 HRS

<<< FAILURE RATE DISTRIBUTION >>>
(RANKED ORDER, UQG)

PART CODE	QUANTITY	FAILURE RATE	PERCENT CONTRIBUTION
IC	12.000	437.98865	64.049 %
FET	19.000	198.30067	28.998 %
VAR	1.000	26.25096	3.839 %
QSP	2.000	8.03717	1.175 %
RC05	30.000	4.88420	.714 %
CK	25.000	4.34003	.635 %
ZEN	1.000	2.05960	.301 %
RN50C	24.000	1.23623	.181 %
CRS	2.000	.46612	.068 %
CSR	21.000	.26984	.039 %
	---	-------	-------
TOTAL	137.000	683.83346	100.000 %

TABLE G-2. MULTICHANNEL WIRELESS DATA TRANSMITTER MTBF @ 150°C

MODULE # 1 STATIC STRAIN MODULATOR

CIRCUIT REF DESIG	PART CODE	QUANTITY	FAILURES/MILLION HRS UPPER QUAL	LOWER QUAL	DERATING	STRESS
R1	RN50C	1.000	.063363	.264013	.250	.250
R2	RN50C	1.000	.063363	.264013	.250	.250
R3	RN50C	1.000	.063363	.264013	.250	.250
R4	RN50C	1.000	.063363	.264013	.250	.250
R5	RN50C	1.000	.063363	.264013	.250	.250
R6	RN50C	1.000	.063363	.264013	.250	.250
R7	RN50C	1.000	.063363	.264013	.250	.250
R8	RC05	1.000	.408188	1.050471	.250	.250
R9	RC05	1.000	.408188	1.050471	.250	.250
R10	RC05	1.000	.408188	1.050471	.250	.250
R11	RC05	1.000	.408188	1.050471	.250	.250
R12	RC05	1.000	.408188	1.050471	.250	.250
R13	RC05	1.000	.408188	1.050471	.250	.250
R14	RN50C	1.000	.063363	.264013	.250	.250
R15	RC05	1.000	.408188	1.050471	.250	.250
R16	RN50C	1.000	.063363	.264013	.250	.250
R17	RC05	1.000	.408188	1.050471	.250	.250
R18	RN50C	1.000	.063363	.264013	.250	.250
R19	RC05	1.000	.408188	1.050471	.250	.250
R20	RC05	1.000	.408188	1.050471	.250	.250
R21	RN50C	1.000	.063363	.264013	.250	.250
R22	RC05	1.000	.408188	1.050471	.250	.250
R23	RN50C	1.000	.063363	.264013	.250	.250
C1	CSR	1.000	.072922	.729222	.250	.250
C2	CSR	1.000	.072922	.729222	.250	.250
C3	CK	1.000	2.295604	11.498018	.250	.250
C4	CSR	1.000	.072922	.729222	.250	.250
C5	CSR	1.000	.072922	.729222	.250	.250
C6	CK	1.000	2.295604	11.498018	.250	.250
C7	CK	1.000	2.295604	11.498018	.250	.250
C8	CSR	1.000	.072922	.729222	.250	.250
C9	CSR	1.000	.072922	.729222	.250	.250
C10	CK	1.000	2.295604	11.498018	.250	.250
C11	CSR	1.000	.072922	.729222	.250	.250
C12	CK	1.000	2.295604	11.498018	.250	.250
C13	CSR	1.000	.072922	.729222	.250	.250
C14	CSR	1.000	.072922	.729222	.250	.250
C15	CSR	1.000	.072922	.729222	.250	.250
C16	CSR	1.000	.072922	.729222	.250	.250
C17	CK	1.000	2.295604	11.498018	.250	.250
C18	CK	1.000	2.295604	11.498018	.250	.250
Q1	FET	1.000	26.147970	519.359408	1.083 ^^	.250 ^^
Q2	FET	1.000	26.147970	519.359408	1.083 ^^	.250 ^^
Q3	FET	1.000	26.147970	519.359408	1.083 ^^	.250 ^^
A1	IC	1.000	73.837936	553.784518	1.270 ^^	1.270 ^^
A2	IC	1.000	110.756904	830.676778	1.270 ^^	1.270 ^^
A3	IC	1.000	73.837936	553.784518	1.270 ^^	1.270 ^^
A4	IC	1.000	2.461265	18.459484	1.270 ^^	1.270 ^^
A5	IC	1.000	2.461265	18.459484	1.270 ^^	1.270 ^^

TABLE G-2. MULTICHANNEL WIRELESS DATA TRANSMITTER MTBF @ 150°C (continued)

MODULE # 2 THERMOCOUPLE SCANNER

CIRCUIT REF DESIG	PART CODE	QUANTITY	FAILURES/MILLION HRS UPPER QUAL	LOWER QUAL	DERATING	STRESS
R1	RC05	1.000	.408188	1.050471	.250	.250
R2	RC05	1.000	.408188	1.050471	.250	.250
R3	RC05	1.000	.408188	1.050471	.250	.250
R4	RC05	1.000	.408188	1.050471	.250	.250
R5	RC05	1.000	.408188	1.050471	.250	.250
R6	RC05	1.000	.408188	1.050471	.250	.250
R7	RC05	1.000	.408188	1.050471	.250	.250
R8	RC05	1.000	.408188	1.050471	.250	.250
R9	RC05	1.000	.408188	1.050471	.250	.250
R10	RC05	1.000	.408188	1.050471	.250	.250
C1	CK	1.000	2.295604	11.498018	.250	.250
C2	CK	1.000	2.295604	11.498018	.250	.250
C3	CK	1.000	2.295604	11.498018	.250	.250
C4	CK	1.000	2.295604	11.498018	.250	.250
C5	CK	1.000	2.295604	11.498018	.250	.250
C6	CK	1.000	2.295604	11.498018	.250	.250
C7	CK	1.000	2.295604	11.498018	.250	.250
C8	CK	1.000	2.295604	11.498018	.250	.250
C9	CK	1.000	2.295604	11.498018	.250	.250
C10	CK	1.000	2.295604	11.498018	.250	.250
C11	CK	1.000	2.295604	11.498018	.250	.250
C12	CK	1.000	2.295604	11.498018	.250	.250
C13	CK	1.000	2.295604	11.498018	.250	.250
Q1	FET	1.000	26.147970	519.359408	1.083 ^^	.250 ^^
Q2	FET	1.000	26.147970	519.359408	1.083 ^^	.250 ^^
Q3	FET	1.000	26.147970	519.359408	1.083 ^^	.250 ^^
Q4	FET	1.000	26.147970	519.359408	1.083 ^^	.250 ^^
Q5	FET	1.000	26.147970	519.359408	1.083 ^^	.250 ^^
Q6	FET	1.000	26.147970	519.359408	1.083 ^^	.250 ^^
Q7	FET	1.000	26.147970	519.359408	1.083 ^^	.250 ^^
Q8	FET	1.000	26.147970	519.359408	1.083 ^^	.250 ^^
Q9	FET	1.000	26.147970	519.359408	1.083 ^^	.250 ^^
Q10	FET	1.000	26.147970	519.359408	1.083 ^^	.250 ^^
Q11	FET	1.000	26.147970	519.359408	1.083 ^^	.250 ^^
Q12	FET	1.000	26.147970	519.359408	1.083 ^^	.250 ^^
Q13	FET	1.000	26.147970	519.359408	1.083 ^^	.250 ^^
Q14	FET	1.000	26.147970	519.359408	1.083 ^^	.250 ^^
Q15	FET	1.000	26.147970	519.359408	1.083 ^^	.250 ^^
Q16	FET	1.000	26.147970	519.359408	1.083 ^^	.250 ^^
Q17	QSP	1.000	10.561813	105.168127	1.083 ^^	.250 ^^
A1	IC	1.000	3.691897	27.689226	1.270 ^^	1.270 ^^
A2	IC	1.000	4.922529	36.918968	1.270 ^^	1.270 ^^

ORIGINAL PAGE IS OF POOR QUALITY

TABLE G-2. MULTICHANNEL WIRELESS DATA TRANSMITTER MTBF @ 150°C (continued)

MODULE # 3 DYNAMIC STRAIN TRANSMITTER

CIRCUIT REF DESIG	PART CODE	QUANTITY	FAILURES/MILLION HRS UPPER QUAL	FAILURES/MILLION HRS LOWER QUAL	DERATING	STRESS
R1	RN50C	1.000	.063363	.264013	.250	.250
R2	RN50C	1.000	.063363	.264013	.250	.250
R3	RC05	1.000	.408188	1.050471	.250	.250
R4	RN50C	1.000	.063363	.264013	.250	.250
R5	RN50C	1.000	.063363	.264013	.250	.250
R6	RC05	1.000	.408188	1.050471	.250	.250
R8	RN50C	1.000	.063363	.264013	.250	.250
R9	RC05	1.000	.408188	1.050471	.250	.250
R10	RC05	1.000	.408188	1.050471	.250	.250
R11	RN50C	1.000	.063363	.264013	.250	.250
R12	RN50C	1.000	.063363	.264013	.250	.250
R13	RN50C	1.000	.063363	.264013	.250	.250
R14	RN50C	1.000	.063363	.264013	.250	.250
R17	RC05	1.000	.408188	1.050471	.250	.250
R18	RC05	1.000	.408188	1.050471	.250	.250
R19	RC05	1.000	.408188	1.050471	.250	.250
R20	RN50C	1.000	.063363	.264013	.250	.250
R21	RC05	1.000	.408188	1.050471	.250	.250
R22	RN50C	1.000	.063363	.264013	.250	.250
R23	RN50C	1.000	.063363	.264013	.250	.250
R25	RC05	1.000	.408188	1.050471	.250	.250
C1	CSR	1.000	.072922	.729222	.250	.250
C2	CSR	1.000	.072922	.729222	.250	.250
C3	CSR	1.000	.072922	.729222	.250	.250
C4	CSR	1.000	.072922	.729222	.250	.250
C5	CSR	1.000	.072922	.729222	.250	.250
C6	CK	1.000	2.295604	11.498018	.250	.250
C7	CSR	1.000	.072922	.729222	.250	.250
C8	CK	1.000	2.295604	11.498018	.250	.250
C9	CSR	1.000	.072922	.729222	.250	.250
C10	CSR	1.000	.072922	.729222	.250	.250
C11	CK	1.000	2.295604	11.498018	.250	.250
C12	CK	1.000	2.295604	11.498018	.250	.250
C13	CSR	1.000	.072922	.729222	.250	.250
C15	CSR	1.000	.072922	.729222	.250	.250
C16	CK	1.000	2.295604	11.498018	.250	.250
Q1	QSP	1.000	10.561813	105.168127	1.083 ^^	.250 ^^
D1	CRS	1.000	.766280	4.447680	1.083 ^^	.250 ^^
D2	CRS	1.000	.766280	4.447680	1.083 ^^	.250 ^^
D3	ZEN	1.000	4.895974	48.419744	1.083 ^^	.250 ^^
D4	VAR	1.000	65.004994	320.524968	1.083 ^^	.250 ^^
A1	IC	1.000	73.837936	553.784518	1.270 ^^	1.270 ^^
A2	IC	1.000	110.756904	830.676778	1.270 ^^	1.270 ^^
A3	IC	1.000	110.756904	830.676778	1.270 ^^	1.270 ^^
A4	IC	1.000	11.075690	83.067678	1.270 ^^	1.270 ^^
A5	IC	1.000	35.688336	267.662517	1.270 ^^	1.270 ^^

TABLE G-2. MULTICHANNEL WIRELESS DATA TRANSMITTER MTBF @ 150°C (continued)

<<< EQUIPMENT FAILURE TABLE >>>

- EQUIPMENT NAME

MULTICHANNEL WIRELESS DATA TRANSMITTER

- ENVIRONMENTAL SERVICE CONDITION AIRBORNE UNINHABITED

MODULE NAME		QUANTITY	FAILURE/MILLION HRS QUALITY GRADE (UQG)	(LQG)
STATIC STRAIN MODULATOR		1	363.92101	3636.47391
THERMOCOUPLE SCANNER		1	471.46849	8639.50578
DYNAMIC STRAIN TRANSMITTER		1	440.75240	3126.28117
	TOTAL	---	--------	--------
		3	1276.14191	15402.26086

<<< EQUIPMENT MTBF >>>

UQG - 784 HRS LQG - 65 HRS

<<< FAILURE RATE DISTRIBUTION >>>
(RANKED ORDER, UQG)

PART CODE	QUANTITY	FAILURE RATE	PERCENT CONTRIBUTION
IC	12.000	614.08550	48.120 %
FET	19.000	496.81144	38.931 %
VAR	1.000	65.00499	5.094 %
CK	25.000	57.39009	4.497 %
QSP	2.000	21.12363	1.655 %
RC05	30.000	12.24565	.960 %
ZEN	1.000	4.89597	.384 %
CRS	2.000	1.53256	.120 %
CSR	21.000	1.53137	.120 %
RN50C	24.000	1.52071	.119 %
	---	-------	-------
TOTAL	137.000	1276.14191	100.000 %

TABLE G-3. MULTICHANNEL WIRELESS DATA TRANSMITTER MTBF @ 175°C

MODULE # 1 STATIC STRAIN MODULATOR

CIRCUIT REF DESIG	PART CODE	QUANTITY	FAILURES/MILLION HRS UPPER QUAL	FAILURES/MILLION HRS LOWER QUAL	DERATING	STRESS
R1	RN50C	1.000	.078304	.326268	.250	.250
R2	RN50C	1.000	.078304	.326268	.250	.250
R3	RN50C	1.000	.078304	.326268	.250	.250
R4	RN50C	1.000	.078304	.326268	.250	.250
R5	RN50C	1.000	.078304	.326268	.250	.250
R6	RN50C	1.000	.078304	.326268	.250	.250
R7	RN50C	1.000	.078304	.326268	.250	.250
R8	RC05	1.000	1.075205	2.718013	.250	.250
R9	RC05	1.000	1.075205	2.718013	.250	.250
R10	RC05	1.000	1.075205	2.718013	.250	.250
R11	RC05	1.000	1.075205	2.718013	.250	.250
R12	RC05	1.000	1.075205	2.718013	.250	.250
R13	RC05	1.000	1.075205	2.718013	.250	.250
R14	RN50C	1.000	.078304	.326268	.250	.250
R15	RC05	1.000	1.075205	2.718013	.250	.250
R16	RN50C	1.000	.078304	.326268	.250	.250
R17	RC05	1.000	1.075205	2.718013	.250	.250
R18	RN50C	1.000	.078304	.326268	.250	.250
R19	RC05	1.000	1.075205	2.718013	.250	.250
R20	RC05	1.000	1.075205	2.718013	.250	.250
R21	RN50C	1.000	.078304	.326268	.250	.250
R22	RC05	1.000	1.075205	2.718013	.250	.250
R23	RN50C	1.000	.078304	.326268	.250	.250
C1	CSR	1.000	19.011041	190.110409	.250	.250
C2	CSR	1.000	19.011041	190.110409	.250	.250
C3	CK	1.000	140.702060	703.530301	.250	.250
C4	CSR	1.000	19.011041	190.110409	.250	.250
C5	CSR	1.000	19.011041	190.110409	.250	.250
C6	CK	1.000	140.702060	703.530301	.250	.250
C7	CK	1.000	140.702060	703.530301	.250	.250
C8	CSR	1.000	19.011041	190.110409	.250	.250
C9	CSR	1.000	19.011041	190.110409	.250	.250
C10	CK	1.000	140.702060	703.530301	.250	.250
C11	CSR	1.000	19.011041	190.110409	.250	.250
C12	CK	1.000	140.702060	703.530301	.250	.250
C13	CSR	1.000	19.011041	190.110409	.250	.250
C14	CSR	1.000	19.011041	190.110409	.250	.250
C15	CSR	1.000	19.011041	190.110409	.250	.250
C16	CSR	1.000	19.011041	190.110409	.250	.250
C17	CK	1.000	140.702060	703.530301	.250	.250
C18	CK	1.000	140.702060	703.530301	.250	.250
Q1	FET	1.000	142.281087	2842.021734	1.250 ^^	.250 ^^
Q2	FET	1.000	142.281087	2842.021734	1.250 ^^	.250 ^^
Q3	FET	1.000	142.281087	2842.021734	1.250 ^^	.250 ^^
A1	IC	1.000	99.709882	747.824116	1.520 ^^	1.520 ^^
A2	IC	1.000	149.564823	1121.736175	1.520 ^^	1.520 ^^
A3	IC	1.000	99.709882	747.824116	1.520 ^^	1.520 ^^
A4	IC	1.000	3.323663	24.927471	1.520 ^^	1.520 ^^
A5	IC	1.000	3.323663	24.927471	1.520 ^^	1.520 ^^

TABLE G-3. MULTICHANNEL WIRELESS DATA TRANSMITTER MTBF @ 175°C (continued)

MODULE # 2 THERMOCOUPLE SCANNER

CIRCUIT REF DESIG	PART CODE	QUANTITY	FAILURES/MILLION HRS UPPER QUAL	FAILURES/MILLION HRS LOWER QUAL	DERATING		STRESS	
R1	RC05	1.000	1.075205	2.718013	.250		.250	
R2	RC05	1.000	1.075205	2.718013	.250		.250	
R3	RC05	1.000	1.075205	2.718013	.250		.250	
R4	RC05	1.000	1.075205	2.718013	.250		.250	
R5	RC05	1.000	1.075205	2.718013	.250		.250	
R6	RC05	1.000	1.075205	2.718013	.250		.250	
R7	RC05	1.000	1.075205	2.718013	.250		.250	
R8	RC05	1.000	1.075205	2.718013	.250		.250	
R9	RC05	1.000	1.075205	2.718013	.250		.250	
R10	RC05	1.000	1.075205	2.718013	.250		.250	
C1	CK	1.000	140.702060	703.530301	.250		.250	
C2	CK	1.000	140.702060	703.530301	.250		.250	
C3	CK	1.000	140.702060	703.530301	.250		.250	
C4	CK	1.000	140.702060	703.530301	.250		.250	
C5	CK	1.000	140.702060	703.530301	.250		.250	
C6	CK	1.000	140.702060	703.530301	.250		.250	
C7	CK	1.000	140.702060	703.530301	.250		.250	
C8	CK	1.000	140.702060	703.530301	.250		.250	
C9	CK	1.000	140.702060	703.530301	.250		.250	
C10	CK	1.000	140.702060	703.530301	.250		.250	
C11	CK	1.000	140.702060	703.530301	.250		.250	
C12	CK	1.000	140.702060	703.530301	.250		.250	
C13	CK	1.000	140.702060	703.530301	.250		.250	
Q1	FET	1.000	142.281087	2842.021734	1.250	^^	.250	^^
Q2	FET	1.000	142.281087	2842.021734	1.250	^^	.250	^^
Q3	FET	1.000	142.281087	2842.021734	1.250	^^	.250	^^
Q4	FET	1.000	142.281087	2842.021734	1.250	^^	.250	^^
Q5	FET	1.000	142.281087	2842.021734	1.250	^^	.250	^^
Q6	FET	1.000	142.281087	2842.021734	1.250	^^	.250	^^
Q7	FET	1.000	142.281087	2842.021734	1.250	^^	.250	^^
Q8	FET	1.000	142.281087	2842.021734	1.250	^^	.250	^^
Q9	FET	1.000	142.281087	2842.021734	1.250	^^	.250	^^
Q10	FET	1.000	142.281087	2842.021734	1.250	^^	.250	^^
Q11	FET	1.000	142.281087	2842.021734	1.250	^^	.250	^^
Q12	FET	1.000	142.281087	2842.021734	1.250	^^	.250	^^
Q13	FET	1.000	142.281087	2842.021734	1.250	^^	.250	^^
Q14	FET	1.000	142.281087	2842.021734	1.250	^^	.250	^^
Q15	FET	1.000	142.281087	2842.021734	1.250	^^	.250	^^
Q16	FET	1.000	142.281087	2842.021734	1.250	^^	.250	^^
Q17	QSP	1.000	63.727051	636.820508	1.250	^^	.250	^^
A1	IC	1.000	4.985494	37.391206	1.520	^^	1.520	^^
A2	IC	1.000	6.647325	49.854941	1.520	^^	1.520	^^

TABLE G-3. MULTICHANNEL WIRELESS DATA TRANSMITTER MTBF @ 175°C (continued)

MODULE # 3 DYNAMIC STRAIN TRANSMITTER

CIRCUIT REF DESIG	PART CODE	QUANTITY	FAILURES/MILLION HRS UPPER QUAL	LOWER QUAL	DERATING	STRESS
R1	RN50C	1.000	.078304	.326268	.250	.250
R2	RN50C	1.000	.078304	.326268	.250	.250
R3	RC05	1.000	1.075205	2.718013	.250	.250
R4	RN50C	1.000	.078304	.326268	.250	.250
R5	RN50C	1.000	.078304	.326268	.250	.250
R6	RC05	1.000	1.075205	2.718013	.250	.250
R8	RN50C	1.000	.078304	.326268	.250	.250
R9	RC05	1.000	1.075205	2.718013	.250	.250
R10	RC05	1.000	1.075205	2.718013	.250	.250
R11	RN50C	1.000	.078304	.326268	.250	.250
R12	RN50C	1.000	.078304	.326268	.250	.250
R13	RN50C	1.000	.078304	.326268	.250	.250
R14	RN50C	1.000	.078304	.326268	.250	.250
R17	RC05	1.000	1.075205	2.718013	.250	.250
R18	RC05	1.000	1.075205	2.718013	.250	.250
R19	RC05	1.000	1.075205	2.718013	.250	.250
R20	RN50C	1.000	.078304	.326268	.250	.250
R21	RC05	1.000	1.075205	2.718013	.250	.250
R22	RN50C	1.000	.078304	.326268	.250	.250
R23	RN50C	1.000	.078304	.326268	.250	.250
R25	RC05	1.000	1.075205	2.718013	.250	.250
C1	CSR	1.000	19.011041	190.110409	.250	.250
C2	CSR	1.000	19.011041	190.110409	.250	.250
C3	CSR	1.000	19.011041	190.110409	.250	.250
C4	CSR	1.000	19.011041	190.110409	.250	.250
C5	CSR	1.000	19.011041	190.110409	.250	.250
C6	CK	1.000	140.702060	703.530301	.250	.250
C7	CSR	1.000	19.011041	190.110409	.250	.250
C8	CK	1.000	140.702060	703.530301	.250	.250
C9	CSR	1.000	19.011041	190.110409	.250	.250
C10	CSR	1.000	19.011041	190.110409	.250	.250
C11	CK	1.000	140.702060	703.530301	.250	.250
C12	CK	1.000	140.702060	703.530301	.250	.250
C13	CSR	1.000	19.011041	190.110409	.250	.250
C15	CSR	1.000	19.011041	190.110409	.250	.250
C16	CK	1.000	140.702060	703.530301	.250	.250
Q1	QSP	1.000	63.727051	636.820508	1.250 ^^	.250 ^^
D1	CRS	1.000	11.667125	69.852753	1.250 ^^	.250 ^^
D2	CRS	1.000	11.667125	69.852753	1.250 ^^	.250 ^^
D3	ZEN	1.000	17.310698	172.566981	1.250 ^^	.250 ^^
D4	VAR	1.000	351.466681	1752.833403	1.250 ^^	.250 ^^
A1	IC	1.000	99.709882	747.824116	1.520 ^^	1.520 ^^
A2	IC	1.000	149.564823	1121.736175	1.520 ^^	1.520 ^^
A3	IC	1.000	149.564823	1121.736175	1.520 ^^	1.520 ^^
A4	IC	1.000	14.956482	112.173617	1.520 ^^	1.520 ^^
A5	IC	1.000	48.193110	361.448323	1.520 ^^	1.520 ^^

TABLE G-3. MULTICHANNEL WIRELESS DATA TRANSMITTER MTBF @ 175°C (continued)

<<< EQUIPMENT FAILURE TABLE >>>

- EQUIPMENT NAME

MULTICHANNEL WIRELESS DATA TRANSMITTER

- ENVIRONMENTAL SERVICE CONDITION AIRBORNE UNINHABITED

MODULE NAME		QUANTITY	FAILURE/MILLION HRS QUALITY GRADE (UQG)	(LQG)
STATIC STRAIN MODULATOR		1	1989.27795	18243.04451
THERMOCOUPLE SCANNER		1	4191.73609	55369.48845
DYNAMIC STRAIN TRANSMITTER		1	1822.06501	11613.97772
	TOTAL	---	--------	--------
		3	8003.07906	85226.51068

<<< EQUIPMENT MTBF >>>

UQG - 125 HRS LQG - 12 HRS

<<< FAILURE RATE DISTRIBUTION >>>
(RANKED ORDER, UQG)

PART CODE	QUANTITY	FAILURE RATE	PERCENT CONTRIBUTION
CK	25.000	3517.55150	43.952 %
FET	19.000	2703.34065	33.779 %
IC	12.000	829.25385	10.362 %
CSR	21.000	399.23186	4.988 %
VAR	1.000	351.46668	4.392 %
QSP	2.000	127.45410	1.593 %
RC05	30.000	32.25616	.403 %
CRS	2.000	23.33425	.292 %
ZEN	1.000	17.31070	.216 %
RN50C	24.000	1.87930	.023 %
	---	-------	-------
TOTAL	137.000	8003.07906	100.000 %

APPENDIX H

THEORY OF OPERATION OF TRANSMITTER AND RECEIVER SIGNAL CONDITIONING CIRCUITRY

Theory of Operation: Thermocouple Scanner

The thermocouple scanner (see Figure H-1) module provides six channels of temperature measurement. The scanner sequentially selects six thermocouple output voltages, a zero reference, a calibration signal, a module's internal temperature signal and a sync signal for transmission.

The module's internal temperature information is used to derive the cold junction compensation. The output of the scanner is amplified by an AC amplifier and transmitted by the phase-lock transmitter.

Both the positive and negative thermocouple leads are switched by the scanner, thereby providing isolation between the channels. Each channel is scanned once every 2 milliseconds which provides a response bandwidth of 25 Hz, as required.

Theory of Operation: Temperature Demultiplexer

The temperature demultiplexer is shown in Figure H-2. A sync decoder decodes the sync signal and maintains the operation of the demultiplexer in the same sequence as that of the transmitted signal.

The demodulated module temperature is added to the demodulated thermocouple signals for cold junction compensation. Self-calibration is also accomplished by comparing the demodulated calibration signal to a

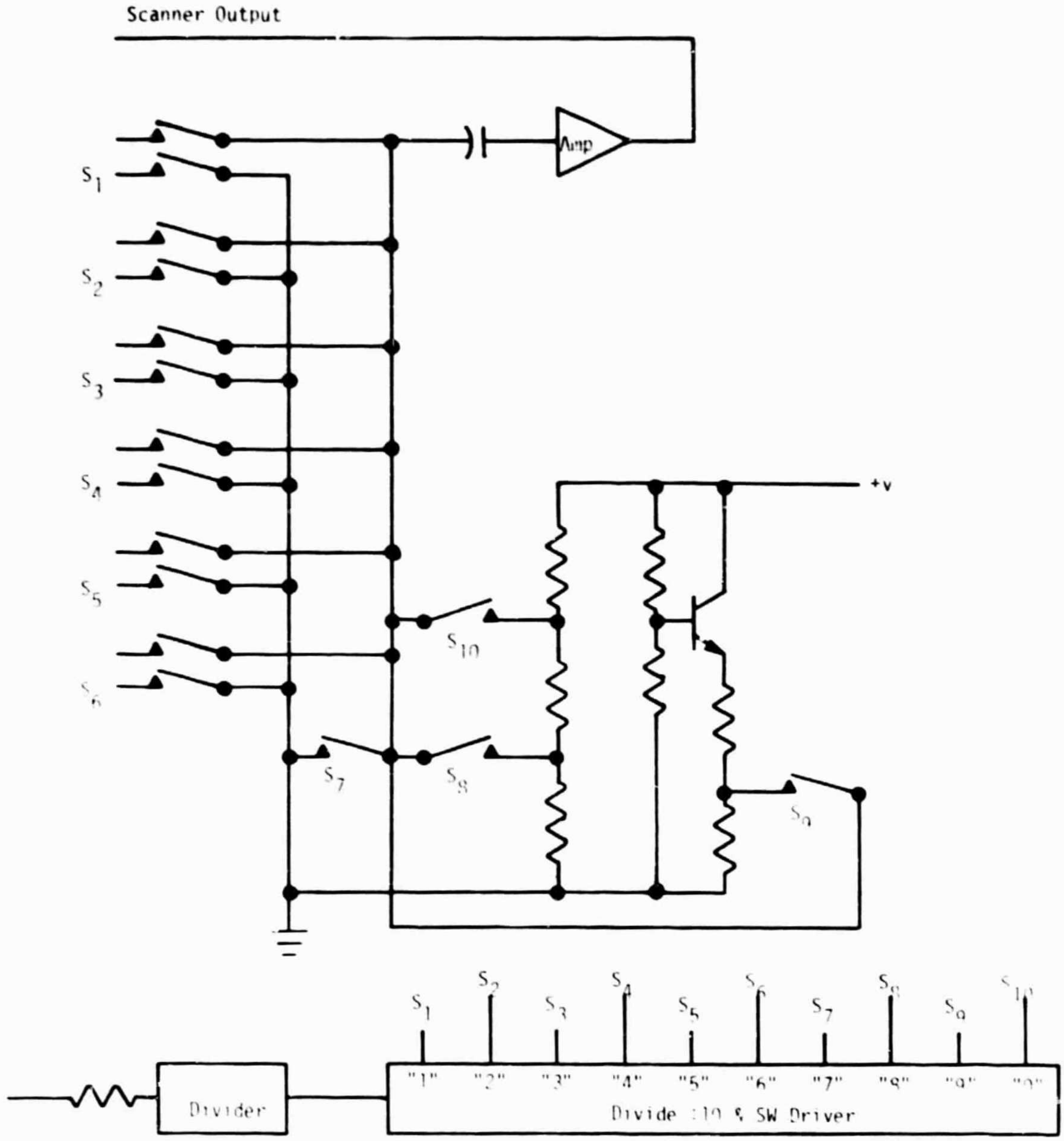

Figure H-1. Thermocouple scanner block diagram.

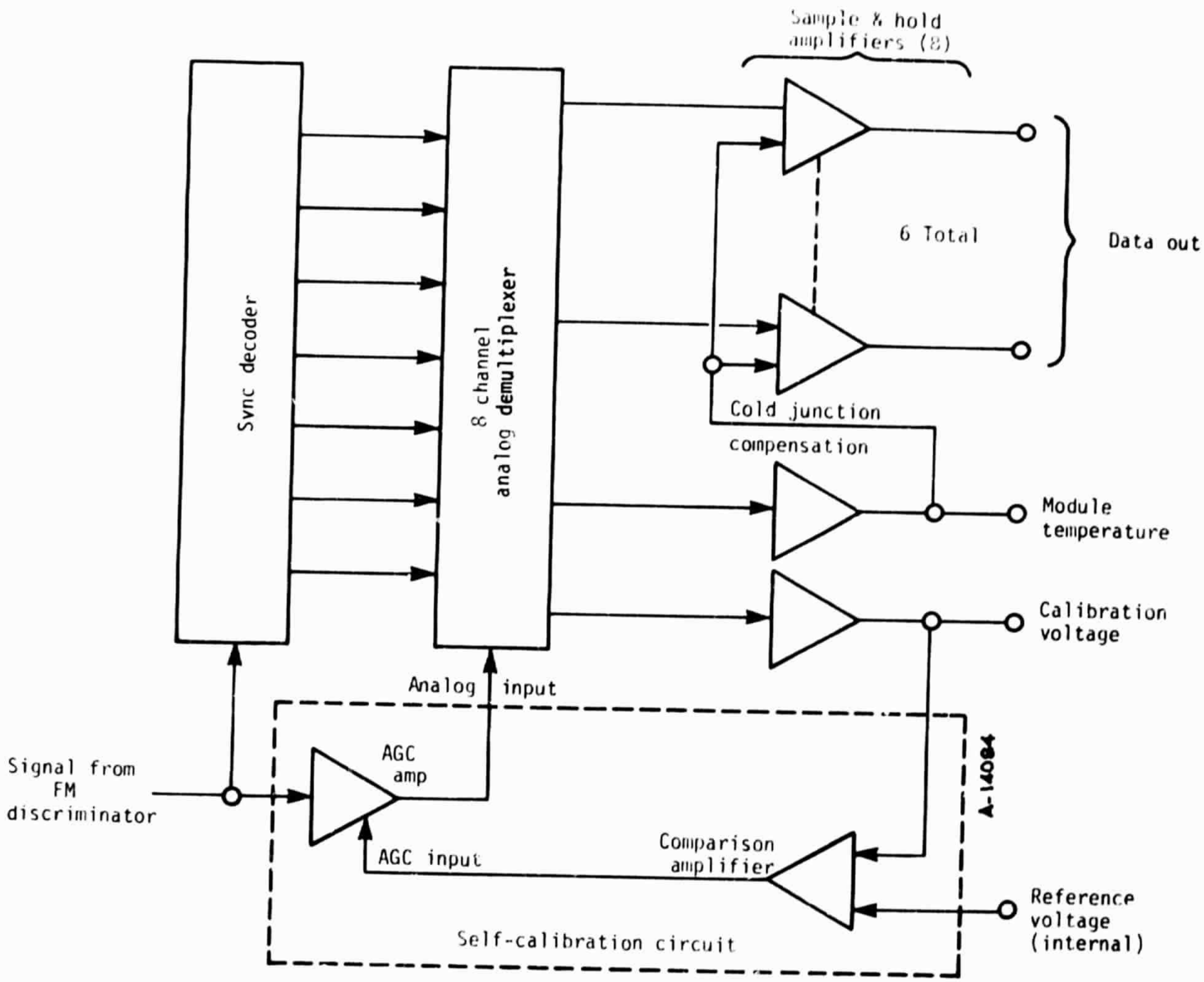

Figure H-2. Block diagram of temperature demultiplexer.

reference voltage and feeding back the error signal to vary the analog gain. This self-calibration feature greatly reduces gain errors over the full range of environmental conditions.

Theory of Operation: Static Strain Modulator

The outputs of the strain gage bridge (see Figure H-3) are sampled alternately by two MOS switches. The differential output signal from the bridge is then converted to 3.125 kHz square waves whose amplitudes correspond to the magnitude of the strain signal. These square waves are amplified and applied to the input of a VCO in a similar manner as in the dynamic strain transmitter.

The sampling switches are driven by signals derived from dividing down the 200 kHz induced power frequency. A test frequency twice that of the sampling frequency was also derived from the same source.

The test signal is injected into the signal processing path and is recovered and utilized in the receiver to calibrate the gain of the system.

Theory of Operation: Static Strain Demodulator

The composite static strain signal from the receiver is further processed by the static strain demodulator module (see Figure H-4). The demodulator module consists of a phase-lock loop, a test signal demodulator and a static strain demodulator.

The phase-lock loop generates two sampling signals whose outputs are in quadrature with each other. When the sampling frequency is equal to the test signal frequency, and exactly 90 degrees out of phase the phase-lock loop is in lock. To speed up locking and increase the capture range of the phase-lock loop. A frequency comparator is used to limit the frequency deviation of the VCO to within 2 Hz of the expected frequency.

A-30268

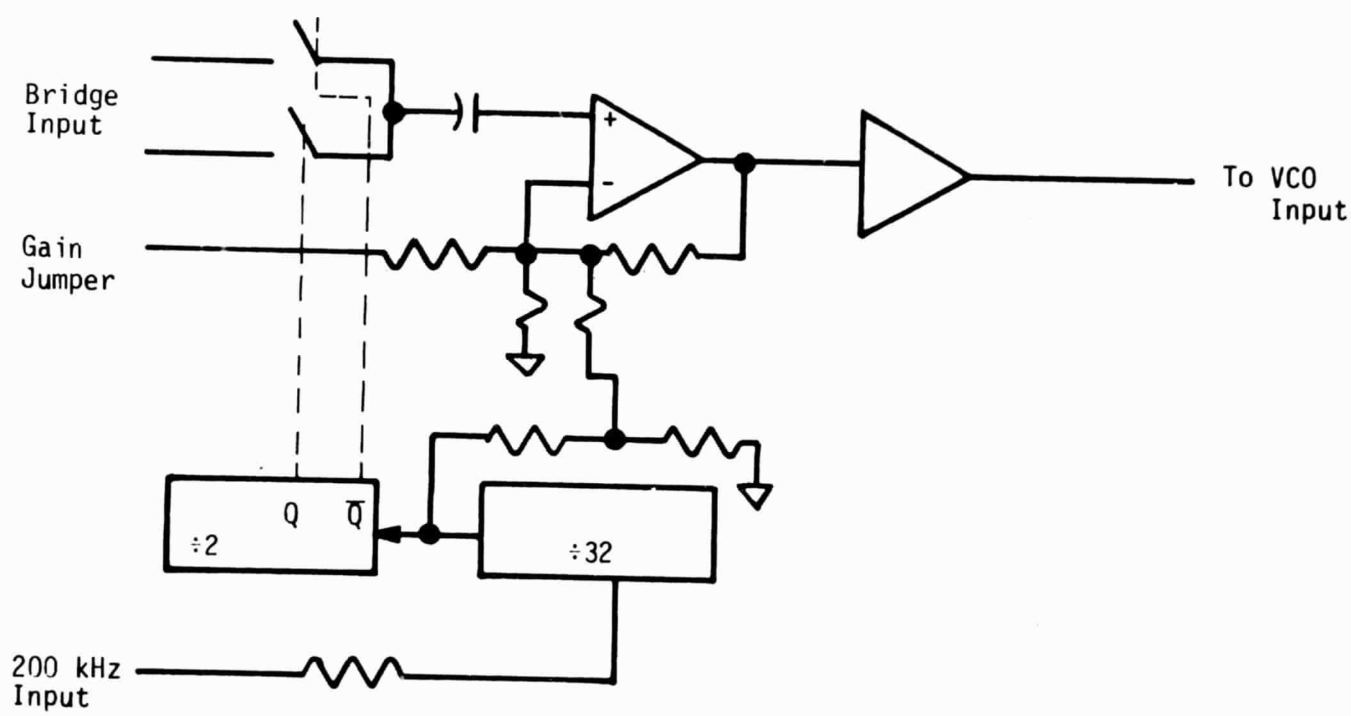

Figure H-3. Static strain modulator block diagram.

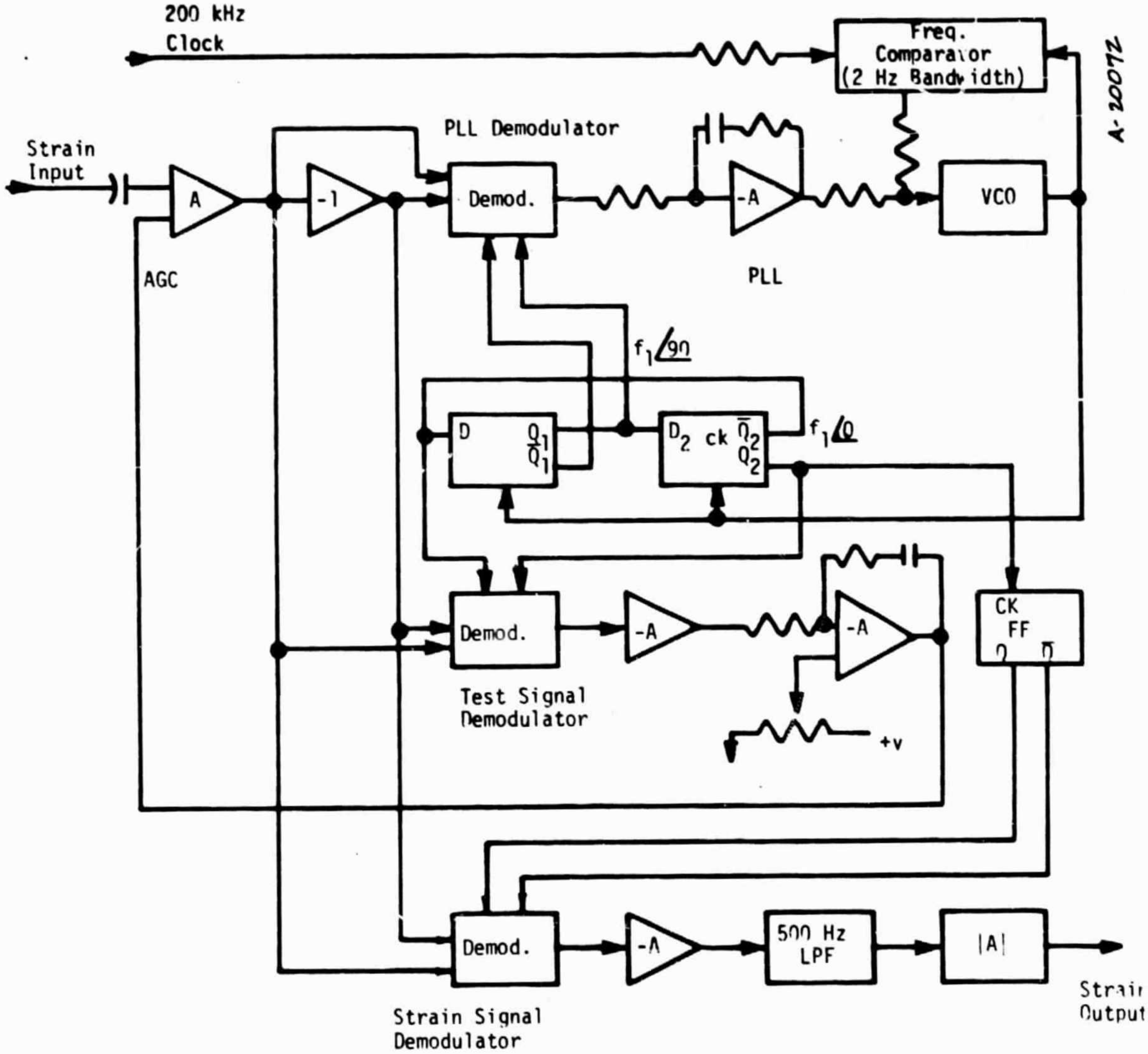

Figure H-4. Static strain demodulator block diagram.

When the PLL is in lock, the 6 kHz test signal is demodulated by the in-phase sampler whose output is amplified and compared with a reference. The comparator produces an output which controls the gain of the input amplifier to maintain a constant system gain.

In this manner the gain of the system is standardized even if the gain of the transmitter varies with temperature. The bridge sensitivity is also automatically corrected should its excitation voltage vary due to temperature. This is because the amplitude of the 6kHz test signal (in the transmitter) is proportional to the bridge excitation voltage.

The test signal sampling frequency is divided again by 2 to drive the static train demodulator. The demodulated strain signal is then amplified and filtered by a 500 Hz bandwidth lowpass filter. Then its absolute value is taken and passed on as the static strain signal is output.

Theory of Operation: Dynamic Strain Module

Referring to the block diagram of Figure H-5, AC power is picked up by the induction coil and applied to the power transformer. Diodes D1, and D2 full-wave rectify the input AC signal, and capacitor C1, filters the AC ripple. The voltage regulator provides a stable +10 volt DC output to power the rest of the circuits. The gage bias is supplied by the regulated DC output through a precision resistor.

A 40 kHz self-test signal is derived from the 200 kHz AC input. The 400 kHz signal from the full-wave rectifier is divided down by a decade counter to 40 kHz. The output of the decade counter feeds the input amplifier. When the input gage is connected this test signal will appear at the output of the transmitter. However, when the gage is open,

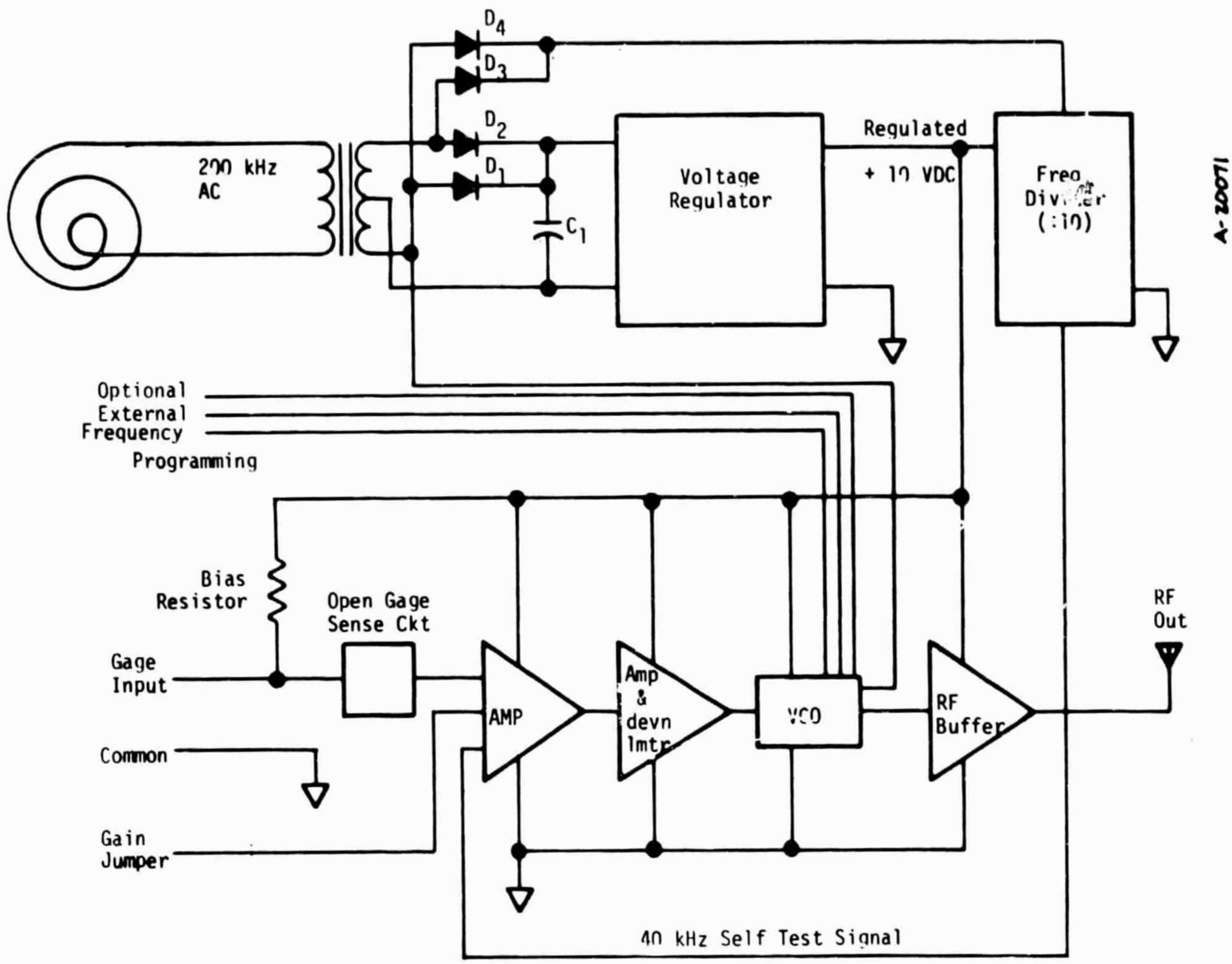

Figure H-5. Dynamic strain transmitter block diagram.

the input amplifier saturates and the test signal disappears.

The gage signal is amplified by a two-stage cascaded amplifier whose gain range can be selected externally by connecting the "gain jumper" terminal to common. The second stage amplifier also acts as a frequency deviation limiter. If the input signal ever exceeds its normal range, usually due to a fault condition, the maximum frequency deviation of the transmitter will be limited by the second amplifier to prevent interference in the adjacent channels.

The VCO is phase-locked to the 200 kHz AC input and since all transmitters operating in the same system are locked onto the same frequency, channel spacing will be maintained throughout the full operating temperature range.

The output of the VCO drives the RF buffer amplifier which in turn drives the antenna.

APPENDIX I

TESTS ON CAPACITIVE ANTENNA

Figure I-1 shows a closeup of two capacitive antennas which were fabricated and tested. The antennas were machined from standard copper-clad glass-epoxy laminated P.C. board stock. Both antennas have a number of conducting tracks. In operation alternate tracks are grounded to serve as guards (or shields) and reduce crosstalks between the adjacent active tracks. Note that in the figure, the configuration at the left has narrow active tracks and wide guard tracks while the configuration on the right has equal widths for all tracks.

The most critical performance parameter for this antenna is crosstalk. Crosstalk increases with spacing between the transmitting and receiving antennas. The following is a summary of measured antenna crosstalk:

Spacing Between Transmitting and Receiving Antennas	Crosstalk	
	Antenna "A" Narrow Active Tracks, Wide Guard Tracks	Antenna "B" All Tracks Equal Width
0.030"	>-40db	-38db
0.060"	-33db	-27db
0.120"	-21db	-13db

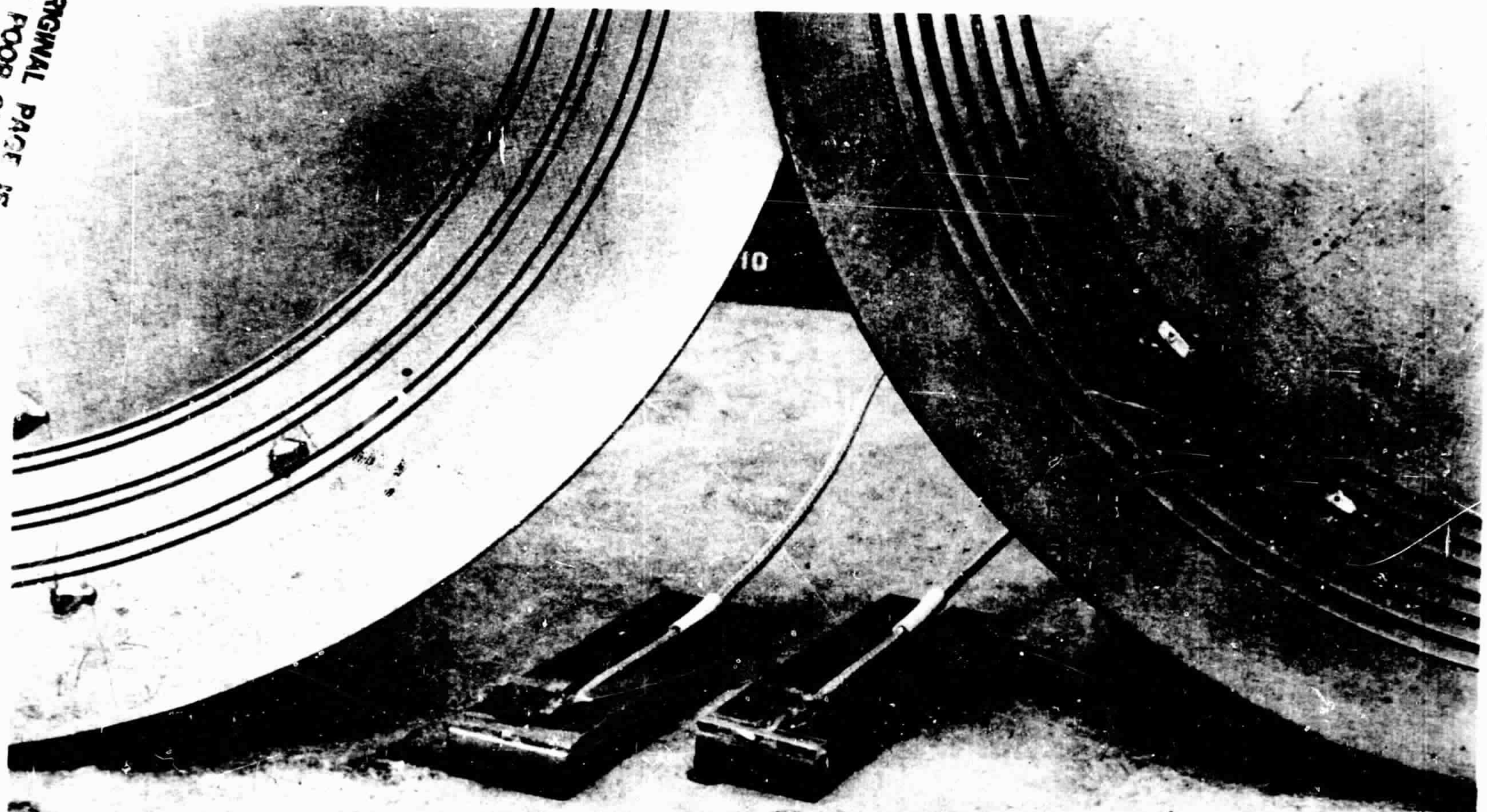

Figure I-1. Closeup of antennas and simulated transmitter modules.

APPENDIX J

ENVIRONMENTAL TEST ON HYBRID TANTALUM CAPACITORS

<u>High Temperature and High G Engineering</u>

Tantalum capacitors were selected for high temperature study. Because of their low strength and large bulk relative to the other components. The initial test comprised eight sample capacitors mounted on four substrates. The electrical properties and mechanical dimensions were recorded at room temperature. Epoxy was used to fill the voids between the capacitor body and the substrate to ensure good mechanical support for the capacitors. The substrates with these capacitors were then installed in a heated centrifuge rotor and spun at 40000 g' and +175^{o}C. Two separate groups were tested. Results of the tests are shown in the following table.

These results are very encouraging. Only one of the sixteen samples would be considered as failing (Unit No. 8 increased its leakage by about 40 times).

It is likely that a high temperature bake or burn-in can be employed to prescreen the capacitors and further reduce the failure rate.

FIRST TEST — 24 HR SPIN @ 175°C/40 Kg's

Sample	Leakage		Capacitance		LX WXH Mechanical Dimension	
	Before	After (%)	Before	After (%)	Before	After
1	9.09×10^{-8} A	+260	4.97 µf	+0.4	0.1540 x 0.1017 x 0.0782	0.1539 x 0.1016 x 0.0785
2	9.55×10^{-8}	+14.3	4.80 µf	-2.3	0.1543 x 0.1042 x 0.0780	0.1542 x 0.1026 x 0.0767
3	9.55×10^{-8}	+14.3	5.01 µf	+0.2	0.1562 x 0.1033 x 0.0747	0.1559 x 0.1032 x 0.0745
4	9.55×10^{-8}	+9.5	5.02 µf	+0.6	0.1532 x 0.1051 x 0.0755	0.1533 x 0.1054 x 0.0755
5	1.00×10^{-7}	+4.6	5.02 µf	+0.6	0.1521 x 0.1012 x 0.0758	0.1528 x 0.1022 x 0.0758
6	9.09×10^{-8}	+315	5.04 µf	+0.79	0.1542 x 0.1039 x 0.0769	0.1549 x 0.1039 x 0.0771
7	6.38×10^{-6}	-0.14	4.8 µf	-39.58	0.1571 x 0.1097 x 0.0737	0.1570 x 0.1070 x 0.0742
8	1.00×10^{-7}	+4354	4.87 µf	+1.64	0.1555 x 0.1025 x 0.0715	0.1553 x 0.1023 x 0.0717

T-358

SECOND TEST — BAKE BEFORE HOT SPIN

Sample	Start		After Bake 24 hrs/175°C		After Spin 24 hrs/175°C/40 kg	
	Leakage	Capacitance	Leakage	Capacitance	Leakage	Capacitance
9	$6.4 \cdot 10^{-6}$ A	--	$6.4 \cdot 10^{-6}$	--	$6.3 \cdot 10^{-6}$ A	--
10	$9.1 \cdot 10^{-8}$	1.015 µf	$8.6 \cdot 10^{-8}$	0.999 µf	$8.6 \cdot 10^{-8}$	0.998 µf
11	$9.5 \cdot 10^{-8}$	0.920 µf	$8.6 \cdot 10^{-8}$	0.972 µf	$8.6 \cdot 10^{-8}$	0.948 µf
12	$9.1 \cdot 10^{-8}$	1.081 µf	$8.6 \cdot 10^{-8}$	1.066 µf	$8.6 \cdot 10^{-8}$	1.066 µf
13	$4.5 \cdot 10^{-6}$	1.010 µf	$5.7 \cdot 10^{-6}$	0.994 µf	$5.5 \cdot 10^{-6}$	0.995 µf
14	$9.5 \cdot 10^{-8}$	1.076 µf	$8.6 \cdot 10^{-8}$	1.065 µf	$8.6 \cdot 10^{-8}$	1.064 µf
15	$9.1 \cdot 10^{-8}$	1.011 µf	$8.6 \cdot 10^{-8}$	0.997 µf	$8.6 \cdot 10^{-8}$	0.997 µf
16	$9.5 \cdot 10^{-8}$	1.011 µf	$8.6 \cdot 10^{-8}$	1.002 µf	$8.6 \cdot 10^{-8}$	1.001 µf

APPENDIX K

ADDITIONAL DRAWINGS

This Appendix contains the following drawings.

Acurex Autodata Number	Title
27271	Block Diagram, 11-22 Frequency Synthesiser
27273	Dynamic Strain Receiver, Block Diagram
28011	Static Strain Demodulator, Schematic
28016	Dynamic Strain Receiver, Schematic
28042	Stationary System Wiring
28045	Dynamic Strain Transmitter, Schematic
28046	Tracking Phase-Locked Loop Receiver, Schematic (Sheet 1)
28046	Tracking Phase-Locked Loop Receiver, Schematic (Sheet 2)
28047	Frequency Comb Spectrum Generator, Schematic
E25508	Dynamic Strain Transmitter Housing NASA
E25518	Dynamic Strain Transmitter Lid

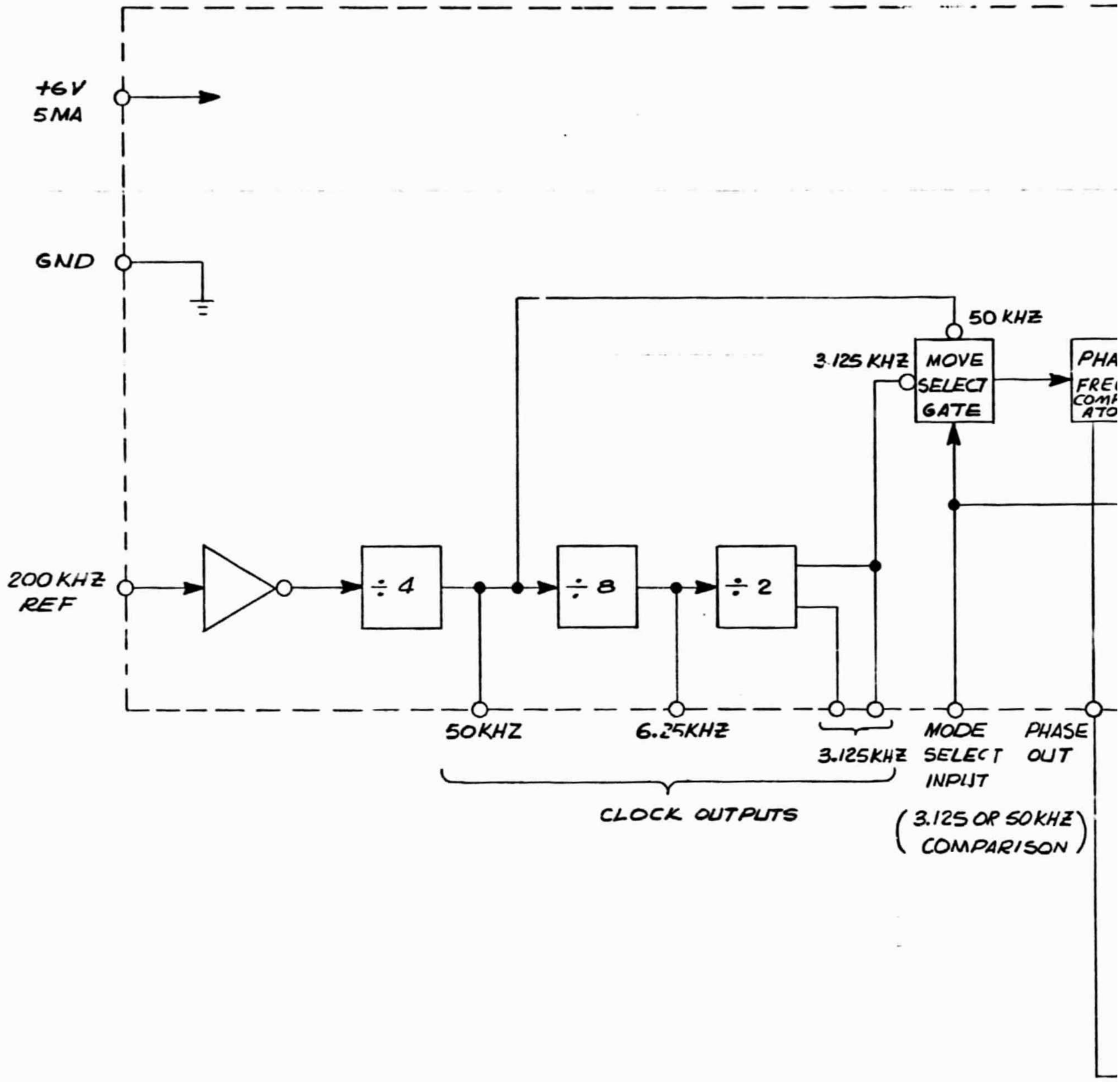

FOLDOUT FRAME

PRECEDING PAGE BLANK NOT FILMED

ZONE	LTR	DESCRIPTION	DATE

REVISIONS

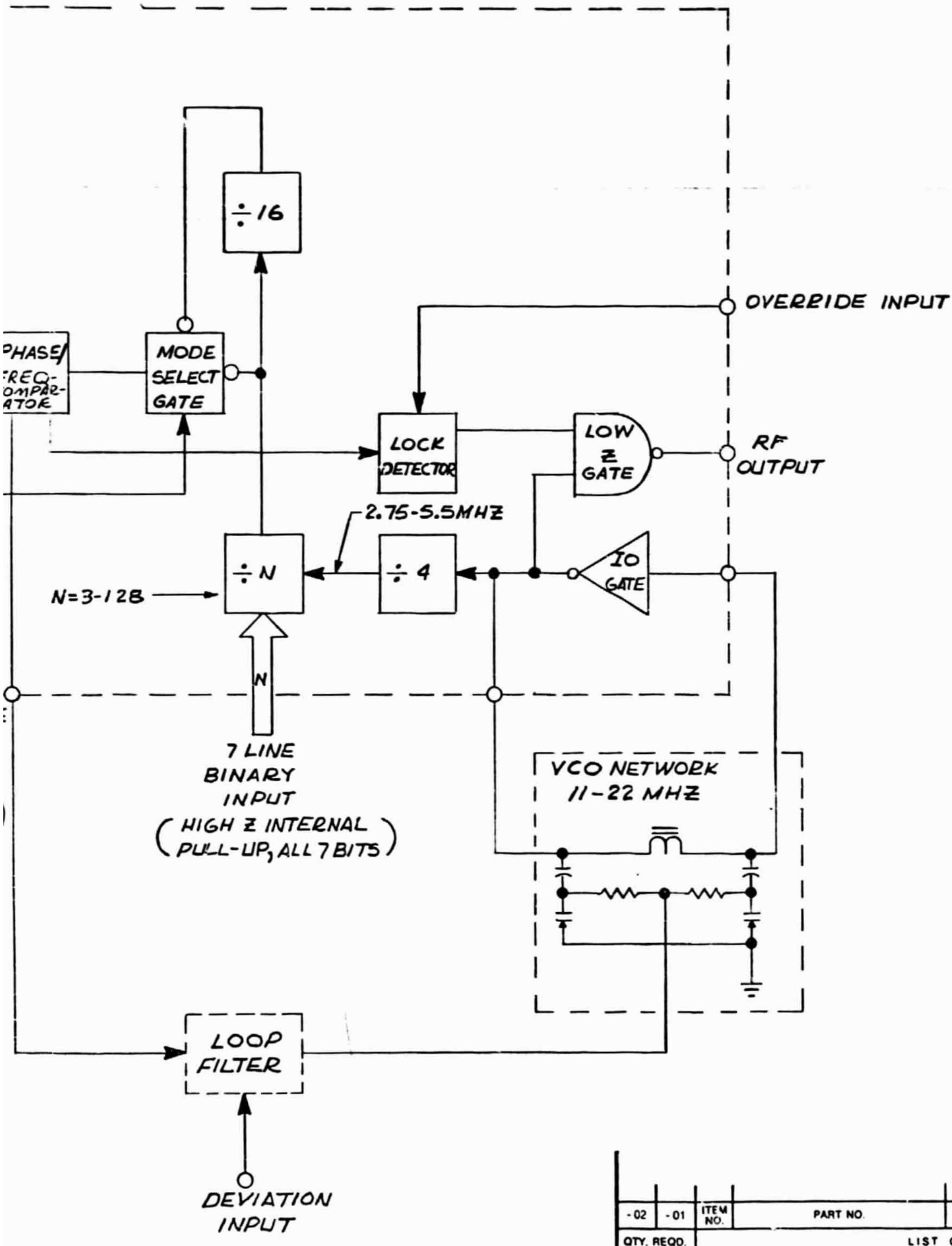

FOLDOUT FRAME 2

-02	-01	ITEM NO.	PART NO.	DESCRIPTION
QTY. REQD.			LIST OF MATERIALS	

UNLESS OTHERWISE SPECIFIED
DIMENSIONS ARE IN INCHES
DECIMALS .XX ±.015 .XXX ±.010 ANGLES ±1°30'
MACH COR—.005 TO .015 R OR CHAM
SH MATL—BREAK EDGES .005 MAX R
ALL ✓ SURFACES TO BE ✓
DIM AND TOL APPLY BEFORE FIN. TREAT
DO NOT SCALE DRAWING
MATERIAL
FINISH

DRAWN Kollege DATE 3-12-75
CHECKED
ENGINEER
APPROVED
RELEASED

ACUREX Corporation
485 CLYDE AVE MOUNTAIN VIEW, CA 94040

BLOCK DIAGRAM,
11-22MHZ FREQUENCY
SYNTHESIZER

SIZE	CODE IDENT NO	DRAWING NO.
D	50726	27271

SCALE — WT — SHEET 1 OF

NEXT ASSY	QTY	USED ON	QTY
APPLICATION			

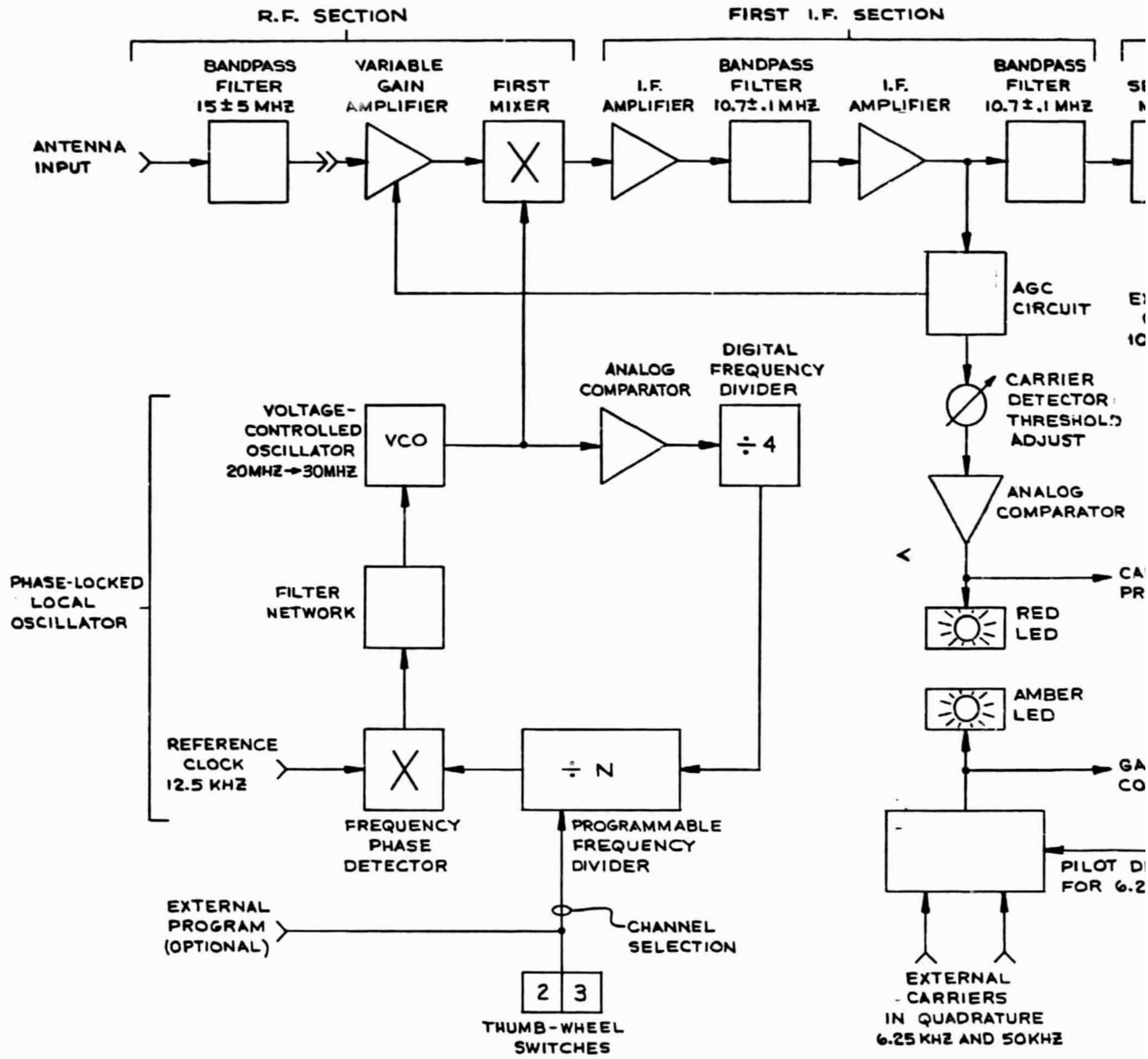

PRECEDING PAGE BLANK NOT FILMED

FOLDOUT FRAME |

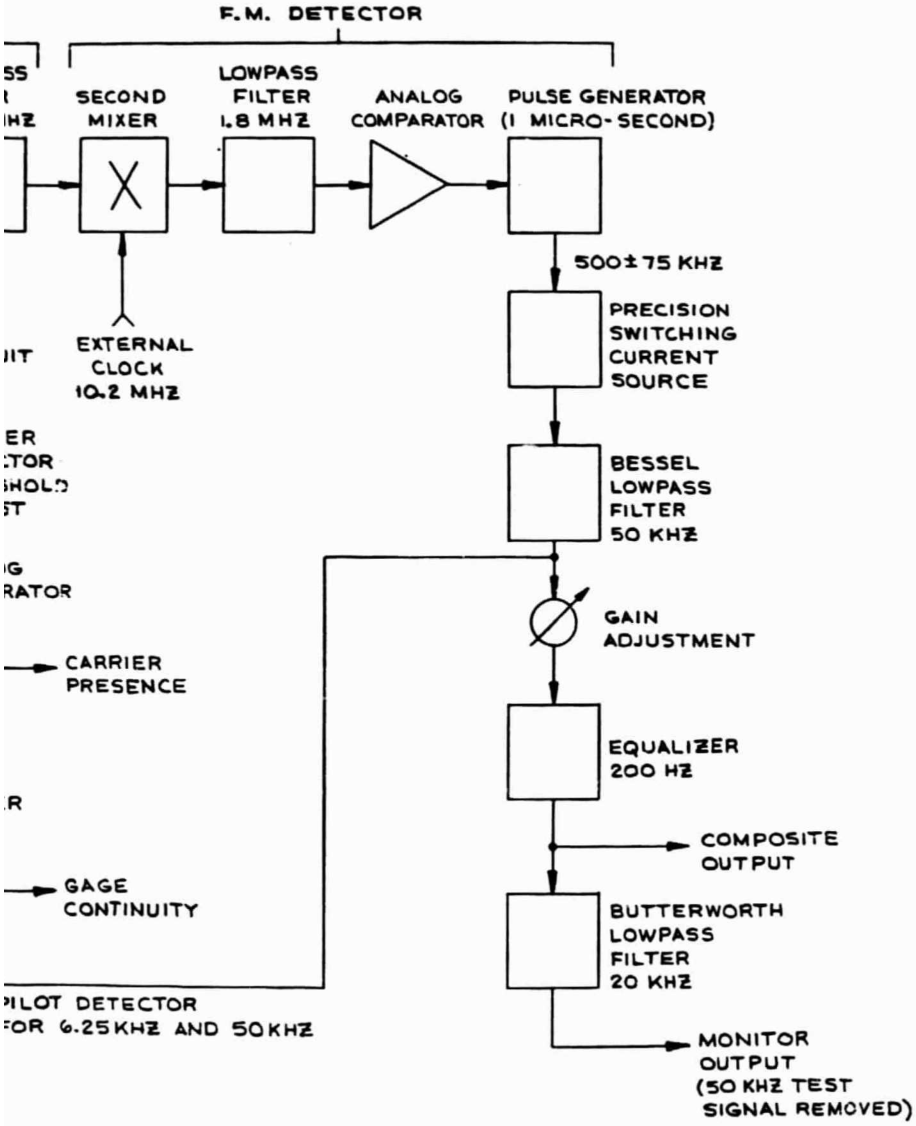

FOLDOUT FRAME 2

ZONE	LTR	DESCRIPTION	DATE

REVISIONS

-02	-01	ITEM NO.	PART NO.	DESCRIPTION
QTY. REQD.			LIST OF MATERIALS	

UNLESS OTHERWISE SPECIFIED DIMENSIONS ARE IN INCHES
DECIMALS .XX ±.015 .XXX ±.010 ANGLES ±0° 30'
MACH COR—.005 TO .015 R OR CHAM
SH MATL—BREAK EDGES .005 MAX R
ALL ✓ SURFACES TO BE ✓
DIM AND TOL APPLY BEFORE FIN TREAT
DO NOT SCALE DRAWING
MATERIAL
FINISH

DRAWN JLG DATE 3-11-78
CHECKED
ENGINEER J. HOEKS
APPROVED
RELEASED

ACUREX Corporation
485 CLYDE AVE., MOUNTAIN VIEW, CA 94040

DYNAMIC STRAIN RECEIVE
BLOCK DIAGRAM

SIZE D | CODE IDENT NO. 50726 | DRAWING NO. 27273
SCALE — | WT | SHEET 1

NEXT ASSY	QTY	USED ON	QTY
APPLICATION			

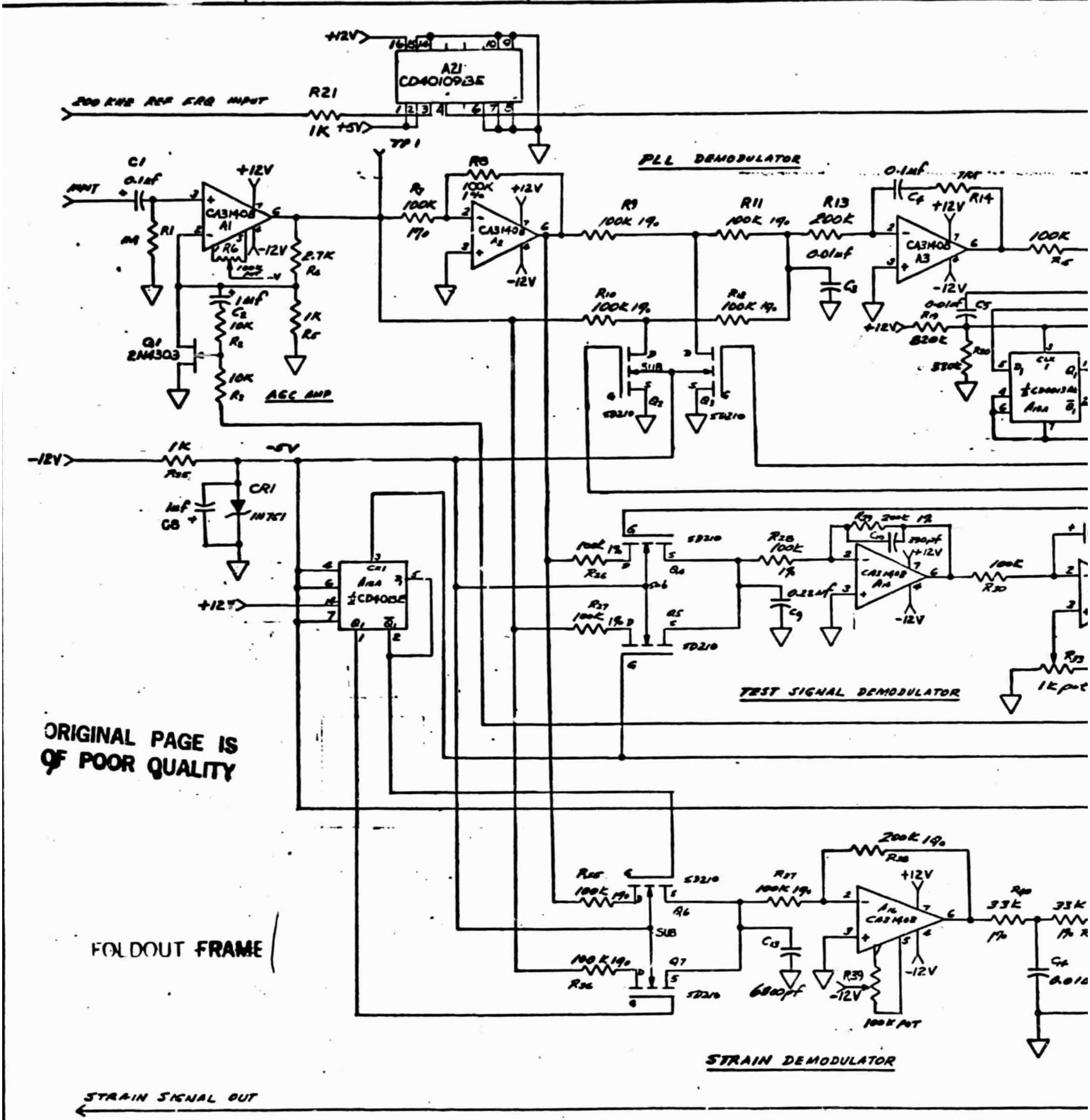

ORIGINAL PAGE IS OF POOR QUALITY

FOLDOUT FRAME

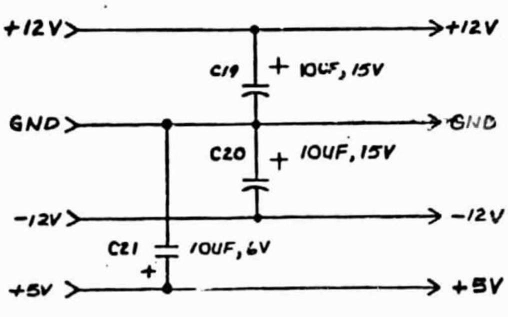

COMPONENTS	
LAST USED	NOT USED
A21	R22
C32	
R49	
CR6	
Q7	

NOTES:

1. ALL R

2. I FILT

3. ALL

FOLDOUT FRAME

PRECEDING PAGE BLANK NOT FILMED

BISHOP GRAPHICS/ACCUPRESS RECORDER NO. A-6903

ZONE	LTR	REVISIONS DESCRIPTION	DATE	APPRO

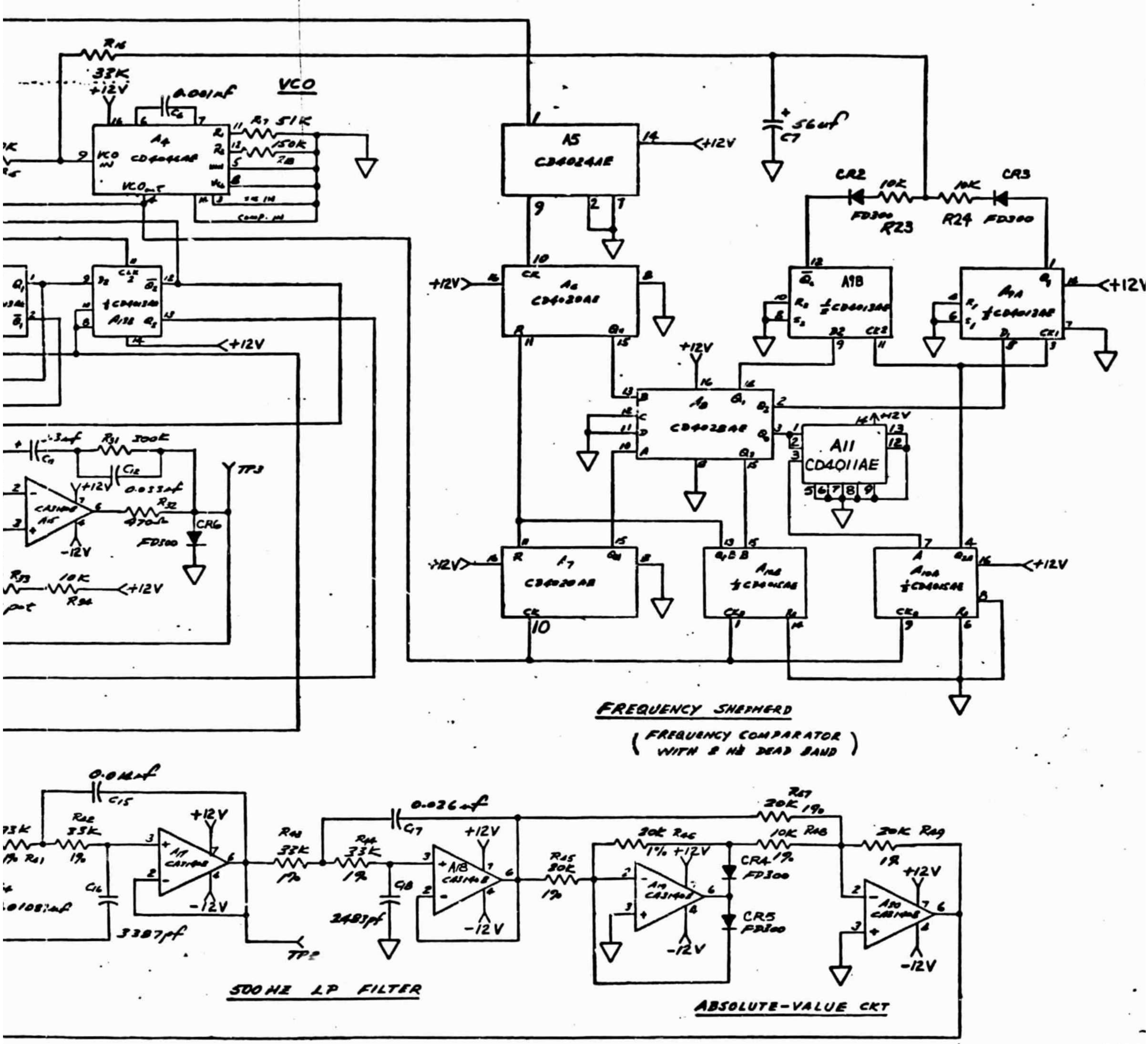

FOLDOUT FRAME

...S: UNLESS OTHERWISE NOTED
...L RESISTORS ARE 1/4 W.
FILTER CAP @ IC, NOT ON OPAMPS. .01UF
...LL OPAMPS ARE TO-5 CASE SIZE

-2	-1	ITEM NO.	CODE IDENT NO.	PART NO.	MANUFACTURER	DESCRIPTION
QTY. REQD.			LIST OF MATERIALS			

NEXT ASSY	QTY	USED ON	QTY
APPLICATION			

UNLESS OTHERWISE SPECIFIED DIMENSIONS ARE IN INCHES
FRACTION ±1/64 DECIMALS .XX ±.01 .XXX ±.005 ANGLES ±0°30'
MACH COR—.005 TO .015 R OR CHAM
SH MATL—BREAK EDGES .005 MAX R
ALL √ SURFACES TO BE √
DIM AND TOL APPLY BEFORE FIN. TREAT.
DO NOT SCALE DRAWING
MATERIAL
FINISH

DRAWN	SAM TOY	DATE 8/?/77
CHECKED		
ENGINEER	SAM TOY	8/25/77
APPROVED		

ACUREX Corporation
485 CLYDE AVE., MOUNTAIN VIEW, CA 94040

STATIC STRAIN DEMODULATOR

SIZE	CODE IDENT NO.	DRAWING NO.	REV
D	50726	28011	

SCALE | WT | SHEET | OF

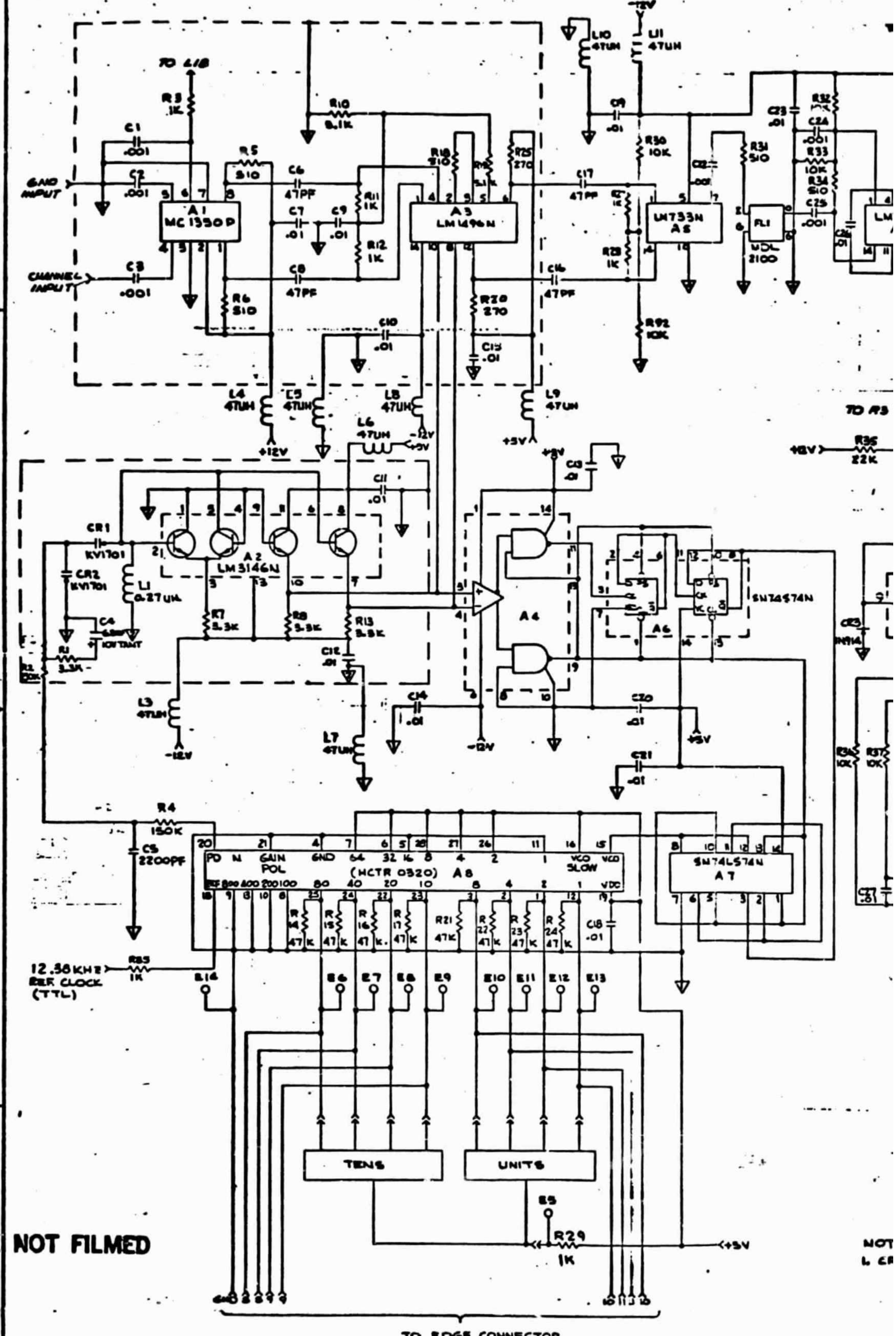

FOLDOUT FRAME

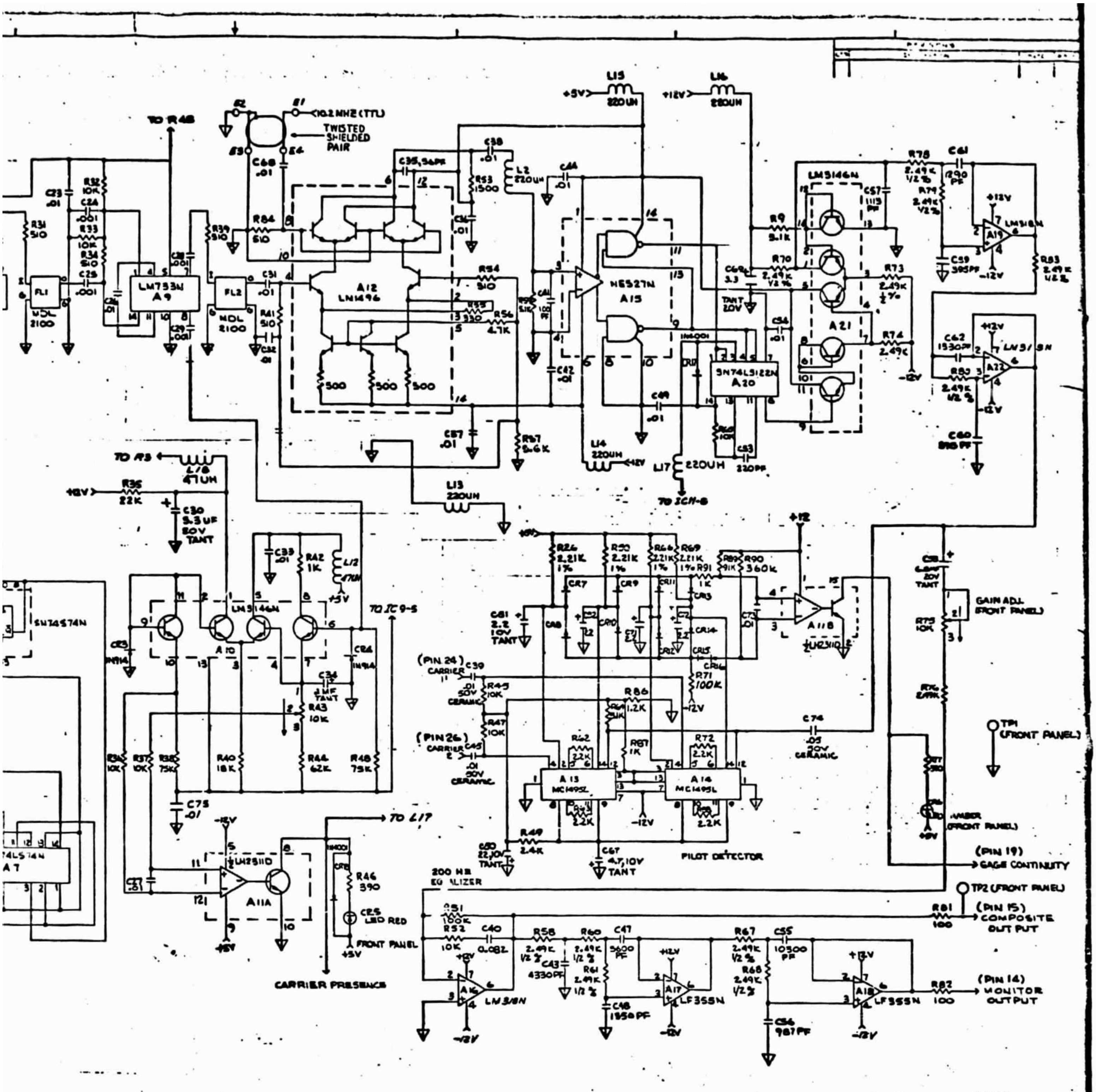

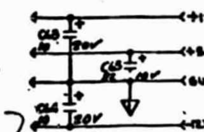

COMPONENTS	
LAST USED	NOT USED
R94	C46, 66, 70
C75	
CR17	
A22	
E14	
TP2	
L18	

NOTES.
1. CR7 THRU CR16 ARE 1N914

FOLDOUT FRAME 2

LIST OF MATERIALS

DYNAMIC STRAIN RECEIVER SCHEMATIC

E 28016

28018	1	28015	1
NEXT ASSY	QTY	USED ON	

APPLICATION

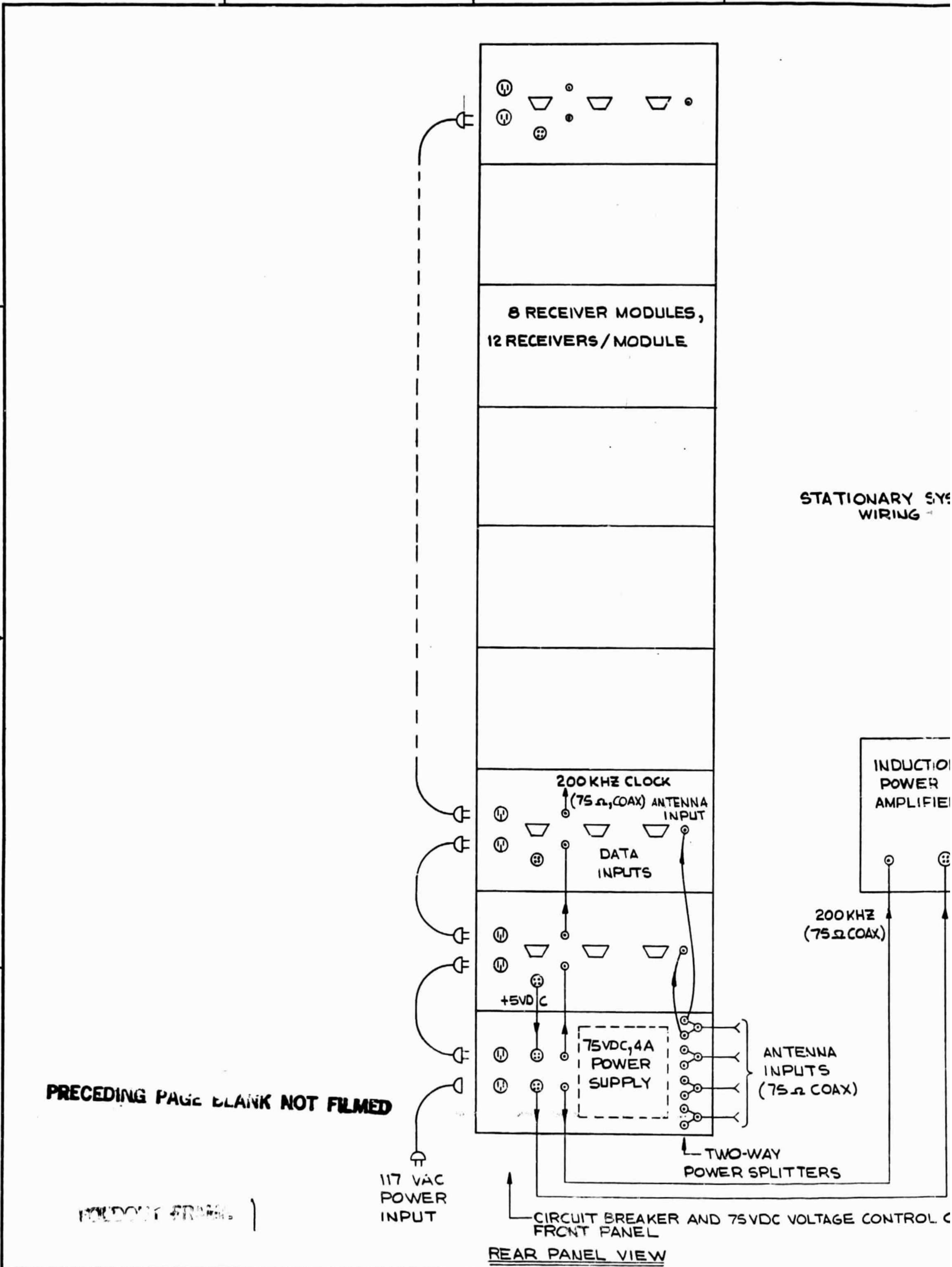

PRECEDING PAGE BLANK NOT FILMED

FOLDOUT FRAME

ZONE	LTR	REVISIONS DESCRIPTION	DATE	APP

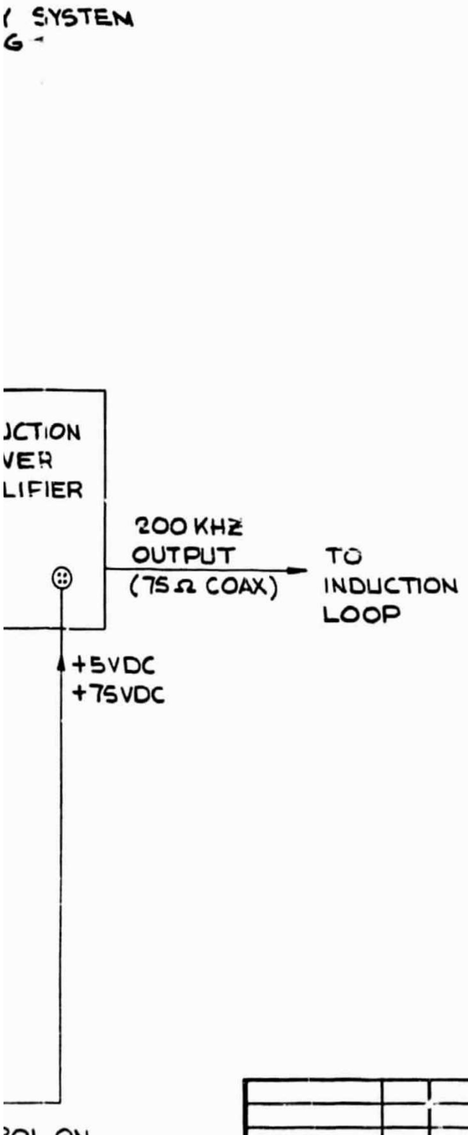

FOLDOUT FRAME 2

-2	-1	ITEM NO.	CODE IDENT NO.	PART NO.	MANUFACTURER	DESCRIPTION
QTY. REQD.			LIST OF MATERIALS			

NEXT ASSY	QTY	USED ON	QTY
APPLICATION			

UNLESS OTHERWISE SPECIFIED DIMENSIONS ARE IN INCHES
FRACTION ±1/64 DECIMALS .XX ±.01 .XXX ±.005 ANGLES ±0°30'
MACH COR—.005 TO .015 R OR CHAM
SH MATL—BREAK EDGES .005 MAX R
ALL ✓ SURFACES TO BE ✓
DIM AND TOL APPLY BEFORE FIN. TREAT.
DO NOT SCALE DRAWING
MATERIAL
FINISH

		DATE
DRAWN	R Galloyd	3-1-78
CHECKED		
ENGINEER	B. HOEKS	
APPROVED		

ACUREX Corporation
485 CLYDE AVE., MOUNTAIN VIEW, CA 94040

STATIONARY SYSTEM WIRING

SIZE	CODE IDENT NO.	DRAWING NO.
D	50726	28042

SCALE | WT | SHEET 1 OF

4 3

D

C

B

A

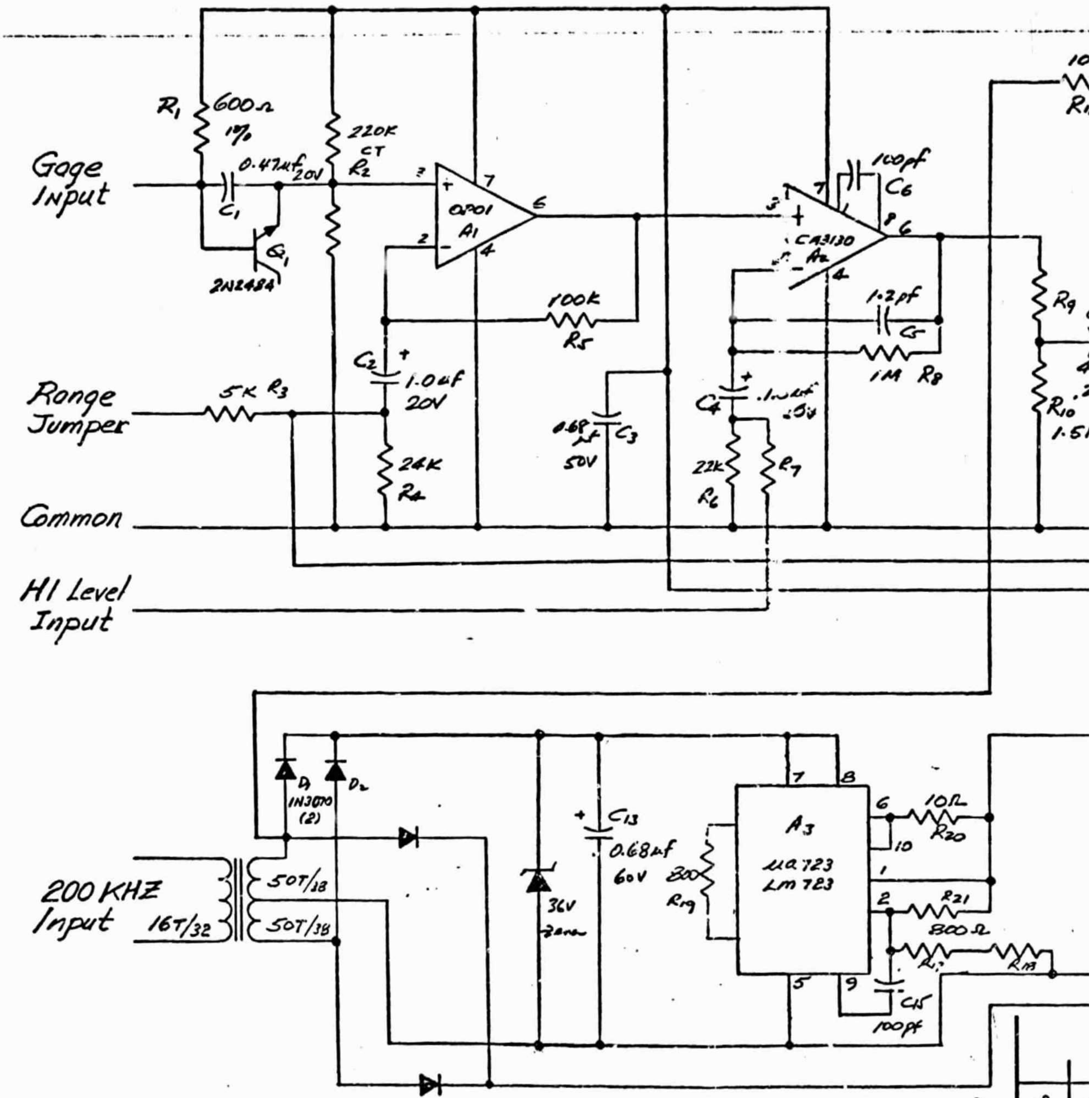

PRECEDING PAGE BLANK NOT FILMED

FOLDOUT FRAME

NEXT ASSY	QTY	USED ON	QTY
APPLICATION			

-2

QTY. REQ

UNLESS OTHERWISE
DIMENSIONS ARE IN
FRACTION DECIMALS
.XX
±1/64 ±.01 ±.00

MACH COR—.005 TO .015
SH MATL—BREAK EDGES

ALL ✓ SURFACES TO BE

DIM AND TOL APPLY BEFO

DO NOT SCALE DR

MATERIAL

FINISH

4 3

REVISIONS				
ZONE	LTR	DESCRIPTION	DATE	APPROVED

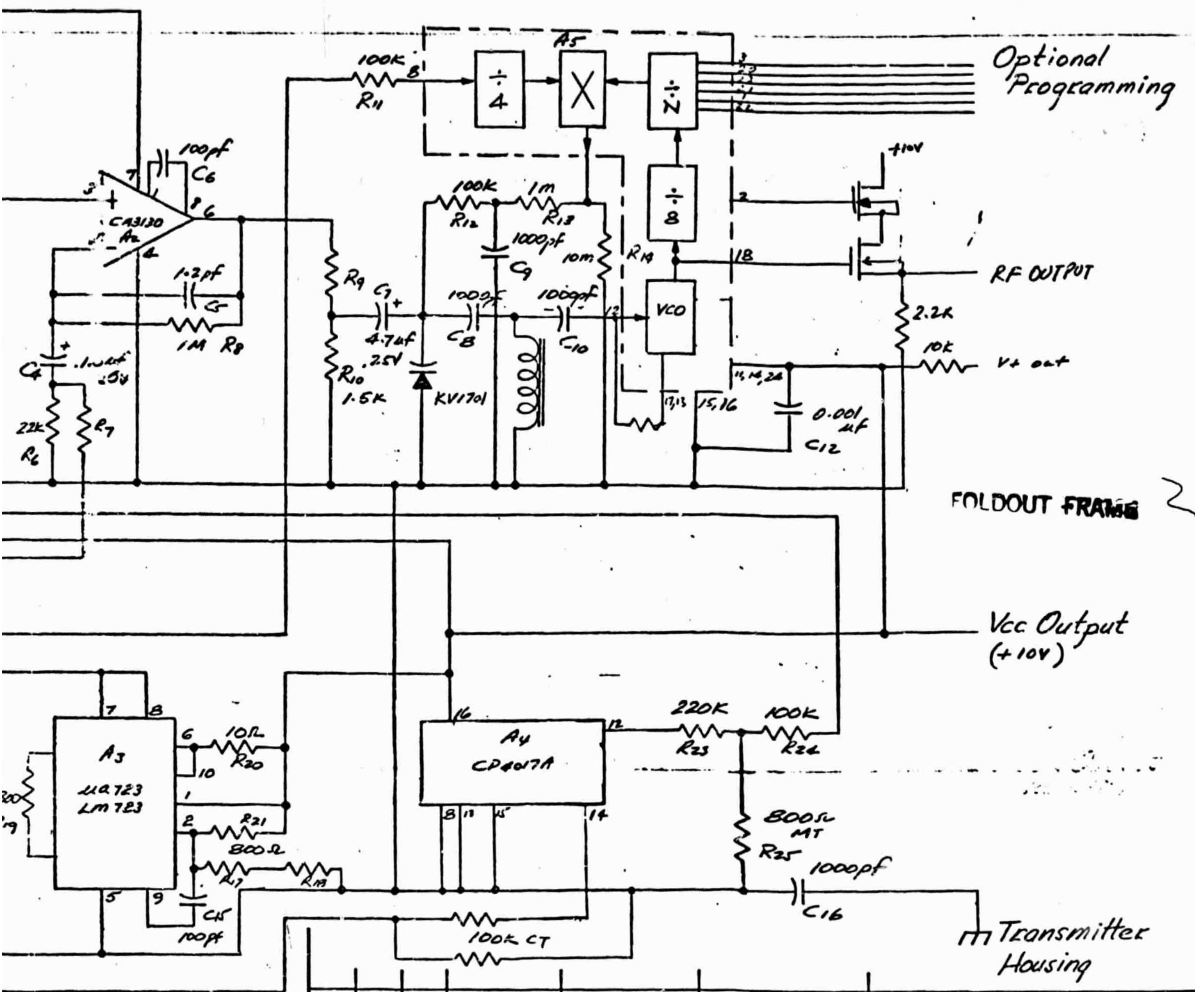

-2	-1	ITEM NO.	CODE IDENT NO.	PART NO.	MANUFACTURER	DESCRIPTION
QTY. REQD.		LIST OF MATERIALS				

UNLESS OTHERWISE SPECIFIED DIMENSIONS ARE IN INCHES
FRACTION ±1/64 DECIMALS .XX ±.01 .XXX ±.005 ANGLES ±0°30'
MACH COR—.005 TO .015 R OR CHAM
SH MATL—BREAK EDGES .005 MAX R
ALL ✓ SURFACES TO BE ✓
DIM AND TOL APPLY BEFORE FIN. TREAT
DO NOT SCALE DRAWING
MATERIAL
FINISH

	DATE
DRAWN	4/11/77
CHECKED	
ENGINEER	4/11/77
APPROVED	

ACUREX Corporation
485 CLYDE AVE., MOUNTAIN VIEW, CA 94040

DYNAMIC STRAIN TRANSMITTER

SIZE	CODE IDENT NO.	DRAWING NO.	REV.
C	50726	28045	

SCALE | WT | SHEET OF

QTY	USED ON	QTY

APPLICATION

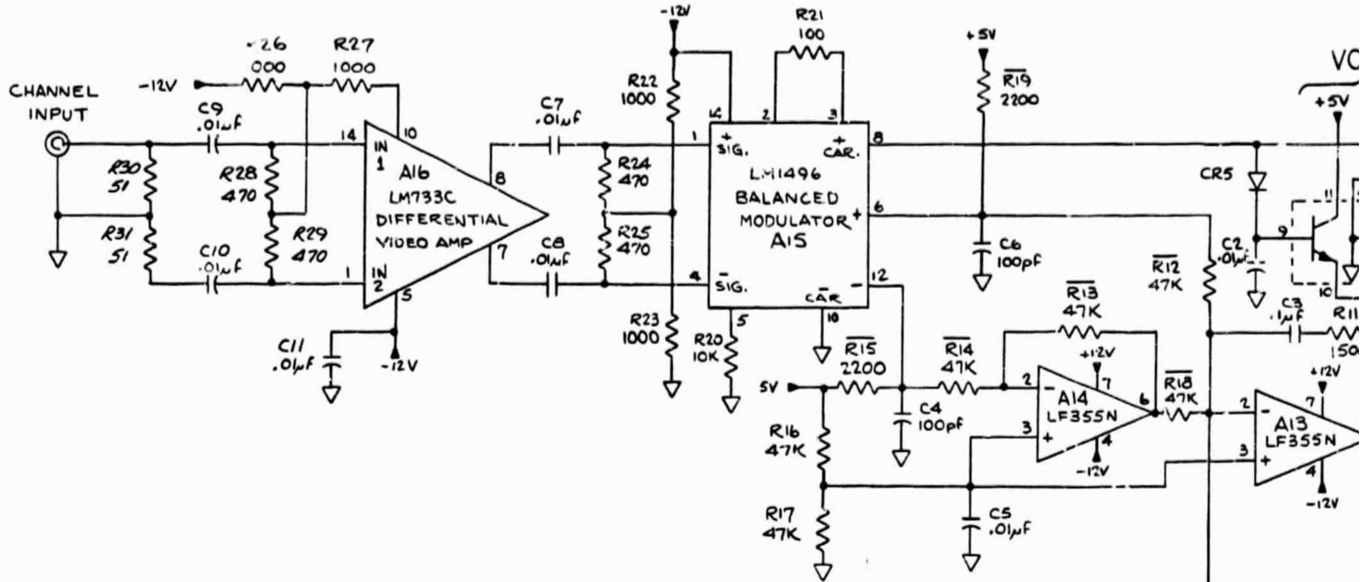

INT. CIRCUIT	TYPE	VCC	GND
A1, A2, A6	SN74S74N	14	7
A3, A7, A9	SN74S161N	16	8
A4, A5	SN74S00N	14	7
A10	SN74S132N	14	7
A8	SN74S160N	16	8

NOTES:
1. POINTS K & L PULLED UP TO +5V VIA 1000 OHMS
2. OVERSCORED RESISTORS ARE 1% OR BETTER
3. RESISTANCE IS IN OHMS
4. CR1-CR2 = FD6666
5. CR3-CR4 = KV1801

PRECEDING PAGE BLANK NOT FILMED

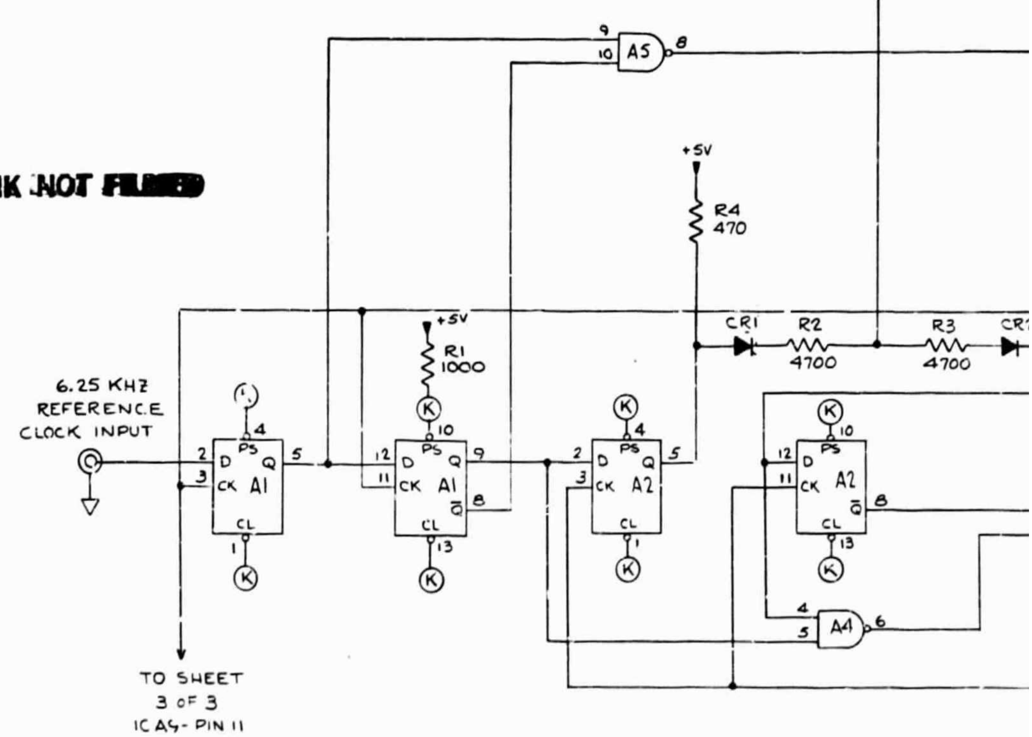

NONLINEAR FREQUENCY DETECTOR (FD)

FOLDOUT FRAME

ORIGINAL PAGE IS OF POOR QUALITY

REVISIONS				
ZONE	LTR	DESCRIPTION	DATE	AP

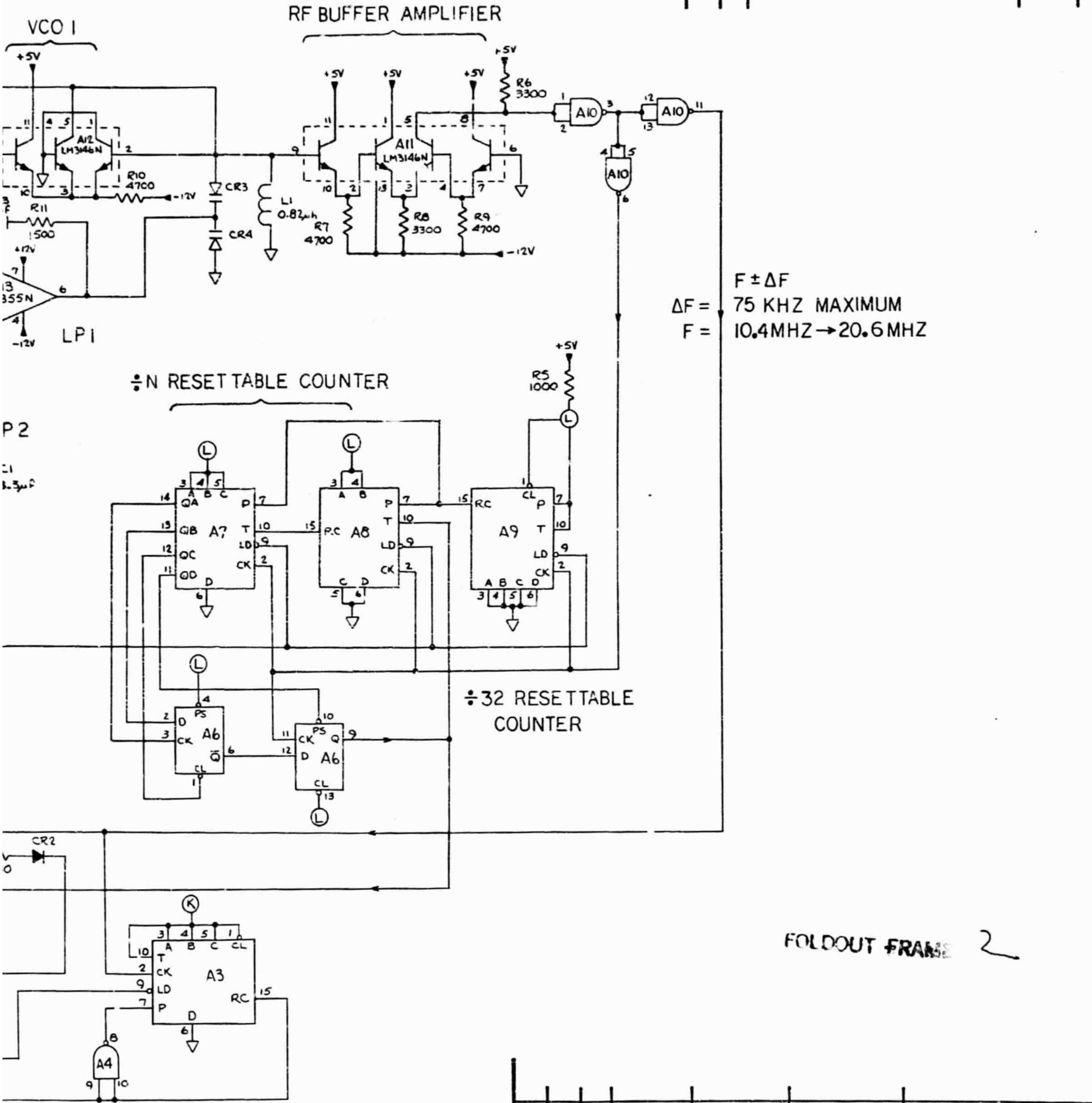

FOLDOUT FRAME 2

-2	-1	ITEM NO.	CODE IDENT NO.	PART NO.	MANUFACTURER	DESCRIPTION
QTY. REQD.		LIST OF MATERIALS				

UNLESS OTHERWISE SPECIFIED DIMENSIONS ARE IN INCHES
FRACTION ±1/64 DECIMALS .XX ±.01 .XXX ±.005 ANGLES ±0°30'
MACH COR—.005 TO .015 R OR CHAM
SH MATL—BREAK EDGES .005 MAX R
ALL ✓ SURFACES TO BE ✓
DIM AND TOL APPLY BEFORE FIN. TREAT.
DO NOT SCALE DRAWING
MATERIAL
FINISH

DRAWN | DATE
CHECKED
ENGINEER
APPROVED

NEXT ASSY	QTY	USED ON	QTY
APPLICATION			

ACUREX Corporation
485 CLYDE AVE., MOUNTAIN VIEW, CA 94040

TRACKING PHASE-LOCKED LOOP RECEIV

SCHEMATIC

SIZE D | CODE IDENT NO. 50726 | DRAWING NO.
SCALE | WT | SHEET 1 OF

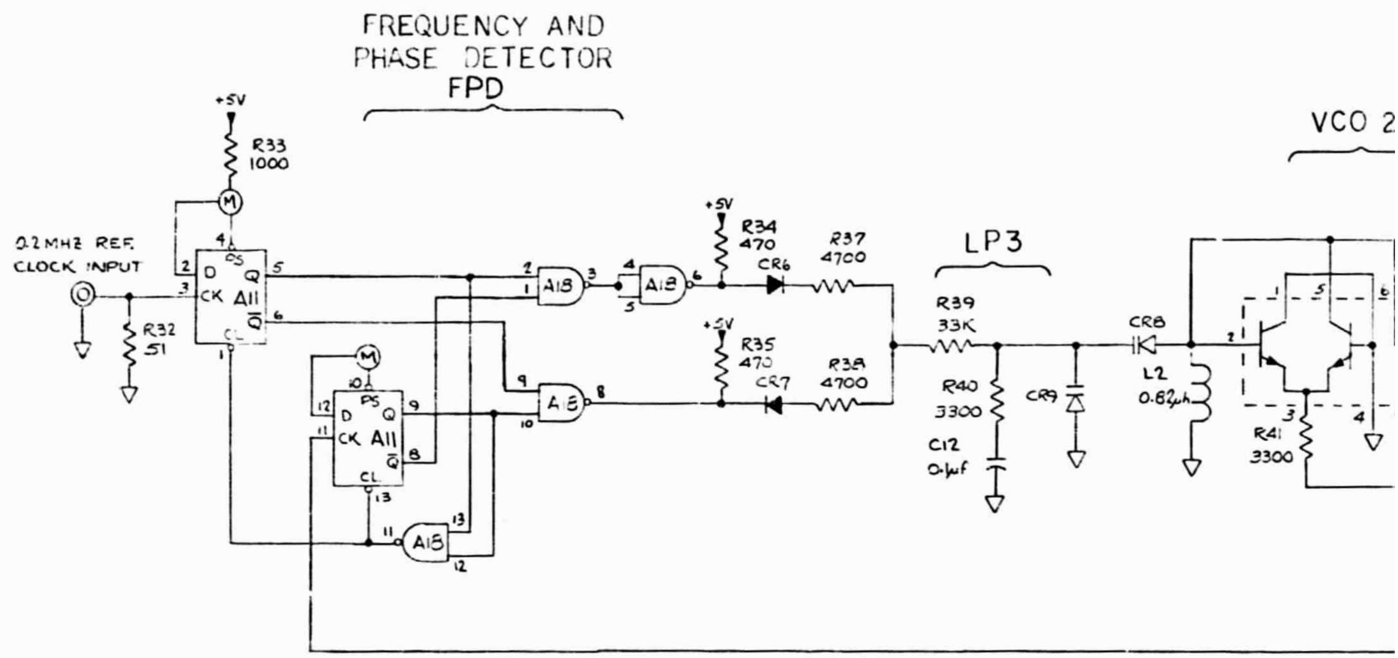

INT. CIRCUIT	TYPE	VCC	GND
A11, A12, A13	SN74S74N	14	7
A14	SN74S160N	16	8
A15	SN74S161N	16	8
A16	SN74121N	14	7
A17	SN74S132N	14	7
A18	SN74S00N	14	7

NOTES:
1. POINT M PULLED UP TO +5V VIA 1000 OHMS
2. RESISTANCE IS IN OHMS
3. CR6 - CR7 = FD6666
4. CR8 - CR9 = KV1801

FOLDOUT FRAM

PRECEDING PAGE BLANK NOT FILMED

ZONE	LTR	DESCRIPTION	DATE

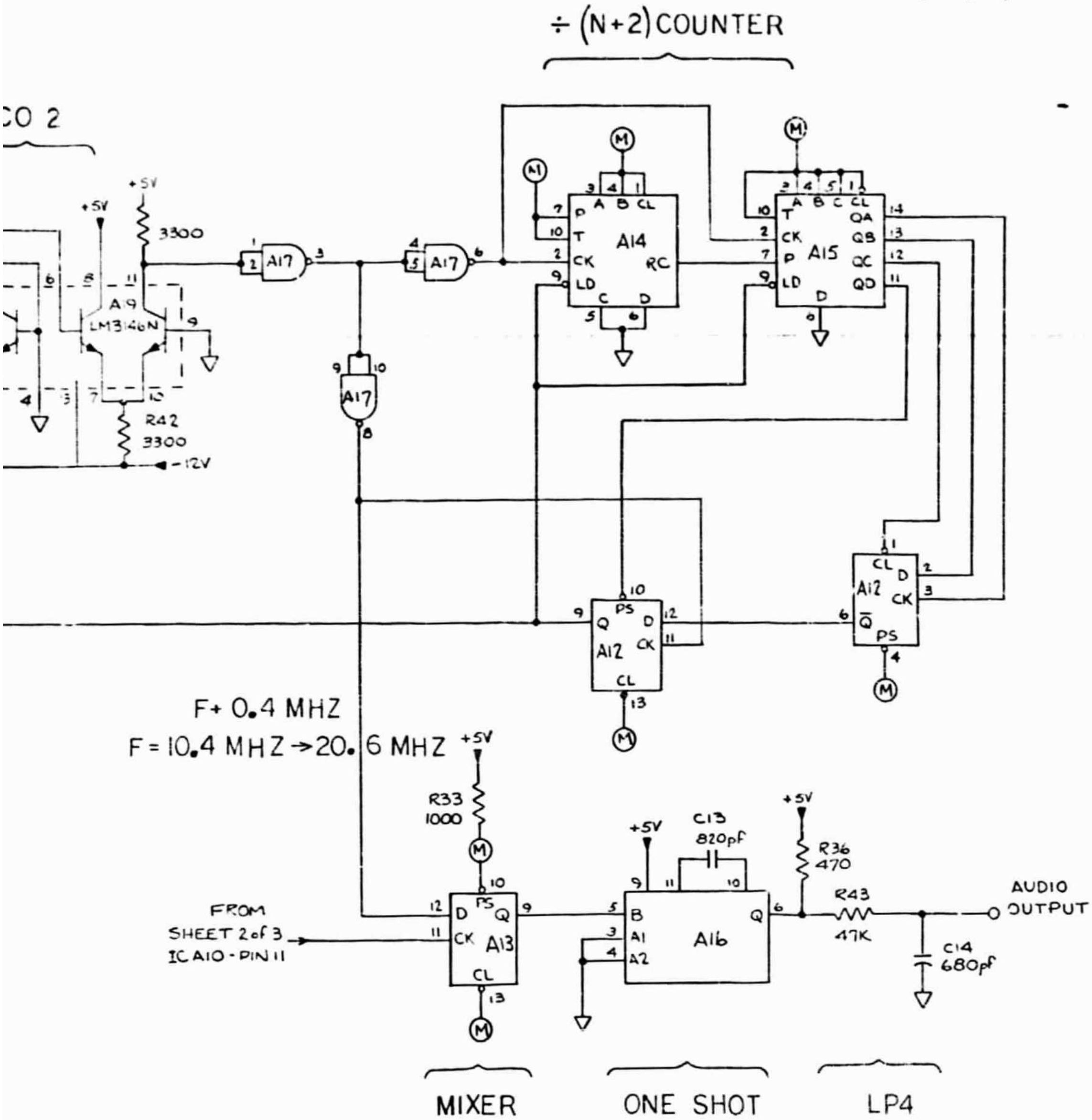

FOLDOUT FRAME 2

-2	-1	ITEM NO.	CODE IDENT NO.	PART NO.	MANUFACTURER	DESCRIPTION
QTY. REQD.			LIST OF MATERIALS			

UNLESS OTHERWISE SPECIFIED DIMENSIONS ARE IN INCHES
FRACTION ±1/64 DECIMALS .XX ±.01 .XXX ±.005 ANGLES ±30'
MACH COR—.005 TO .015 R OR CHAM
BH MATL—BREAK EDGES .005 MAX R
ALL ✓ SURFACES TO BE ✓
DIM AND TOL APPLY BEFORE FIN TREAT.
DO NOT SCALE DRAWING
MATERIAL
FINISH

NEXT ASSY	QTY	USED ON	QTY
APPLICATION			

DRAWN | DATE
CHECKED
ENGINEER
APPROVED

ACUREX Corporation
435 CLYDE AVE., MOUNTAIN VIEW, CA 94040

TRACKING PHASE-LOCKED LOOP RECE

SCHEMATIC

SIZE	CODE IDENT NO.	DRAWING NO.
D	50726	

SCALE | WT | SHEET 2

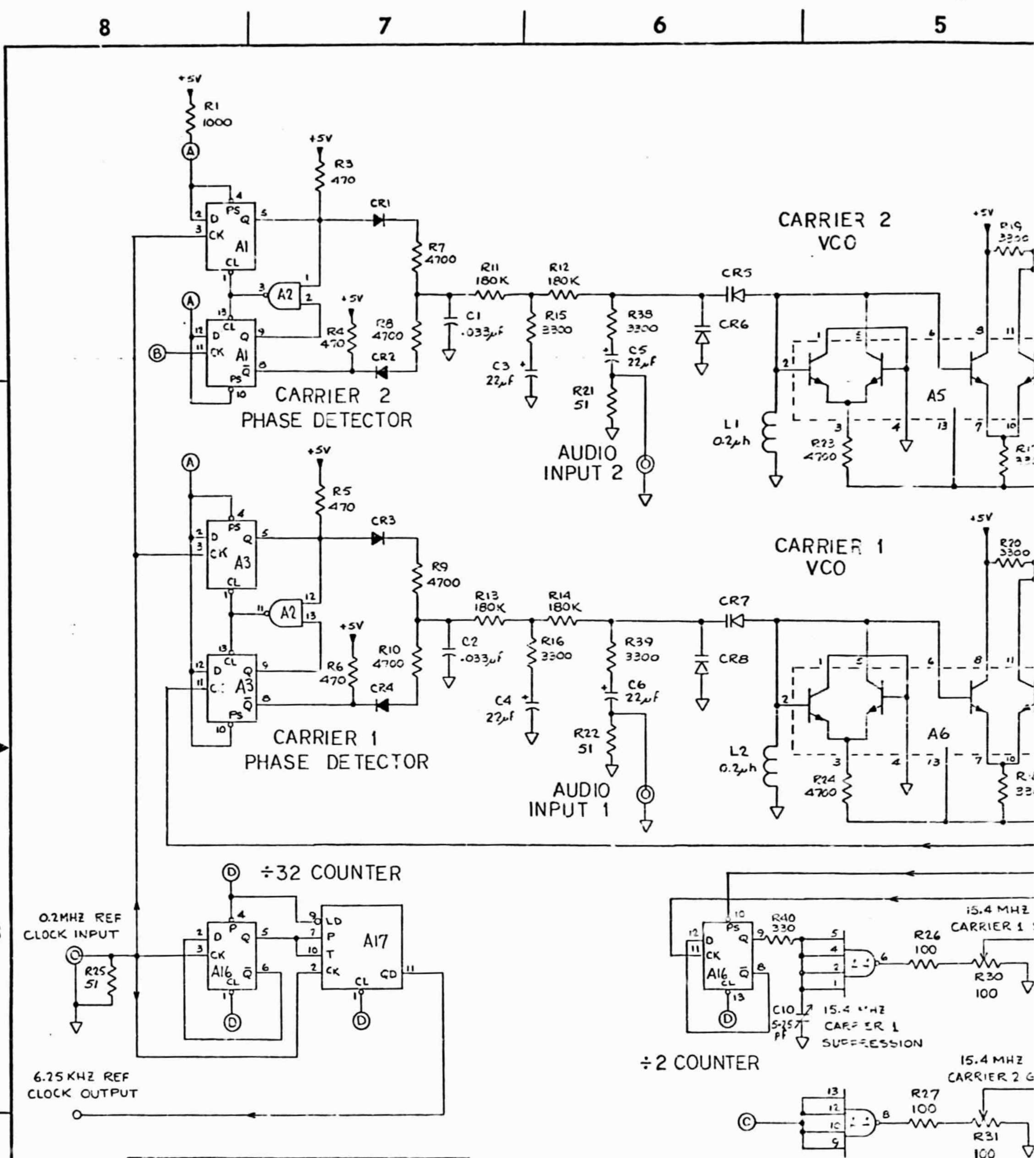

INT CIRCUIT	TYPE	VCC	GND
A1, A3, A7, A13, A16	SN74S74N	14	7
A2	SN74S00N	14	7
A5, A6, A10, A11, A12, A7	SN74S163N	16	8
A4	SN74S132N	14	7
A14, A15	SN74S140N	14	7

NOTES:
1. POINTS A & D PULLED UP TO +5V VIA 1000 OHMS
2. RESISTANCE IS IN OHMS
3. CR1 - CR4 = FD6666
4. CR5 - CR8 = KV1601

FOLDOUT FRAME

PRECEDING PAGE BLANK NOT FILMED

ZONE	LTR	DESCRIPTION	DATE	APP

REVISIONS

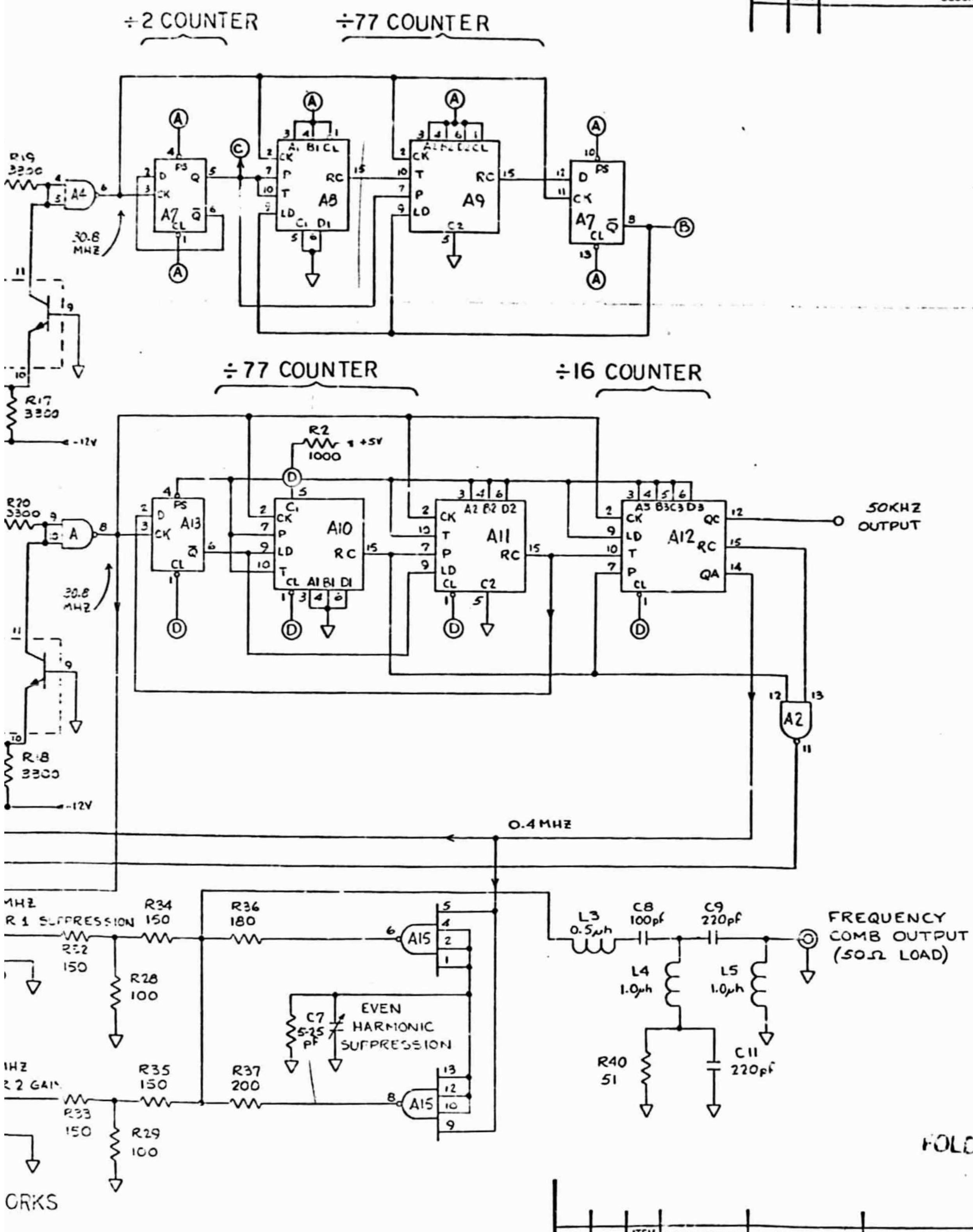

FOLDOUT [redacted] 2

-2	-1	ITEM NO.	CODE IDENT NO.	PART NO.	MANUFACTURER	DESCRIPTION
QTY. REQD.				LIST OF MATERIALS		

NEXT ASSY	QTY	USED ON	QTY
APPLICATION			

UNLESS OTHERWISE SPECIFIED DIMENSIONS ARE IN INCHES
FRACTION ±1/64 DECIMALS .XX ±.01 .XXX ±.005 ANGLES ±0°30'
MACH COR-.005 TO .015 R OR CHAM
SH MATL—BREAK EDGES .005 MAX R
ALL ✓ SURFACES TO RC ✓
DIM AND TOL APPLY BEFORE FIN TREAT
DO NOT SCALE DRAWING
MATERIAL
FINISH

DRAWN | DATE
CHECKED
ENGINEER
APPROVED

ACUREX Corporation
485 CLYDE AVE MOUNTAIN VIEW, CA 94040

SIZE D | CODE IDENT NO. 50726 | DRAWING NO.

SCALE | WT | SHEET 1 OF

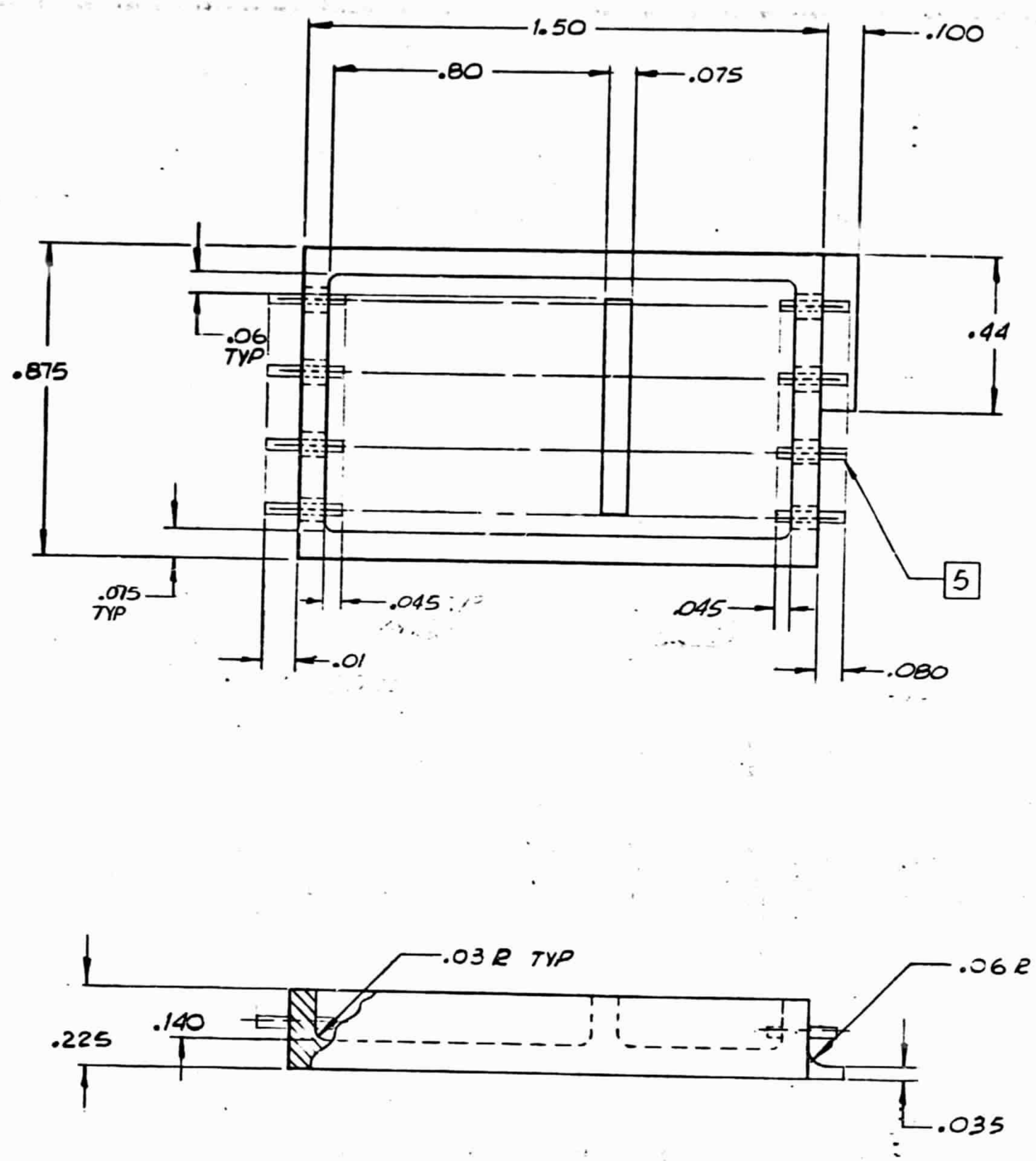

PRECEDING PAGE BLANK NOT FILMED

ORIGINAL PAGE IS
OF POOR QUALITY

FOLDOUT FRAME

ZONE	LTR	DESCRIPTION	DATE	APPRO

REVISIONS

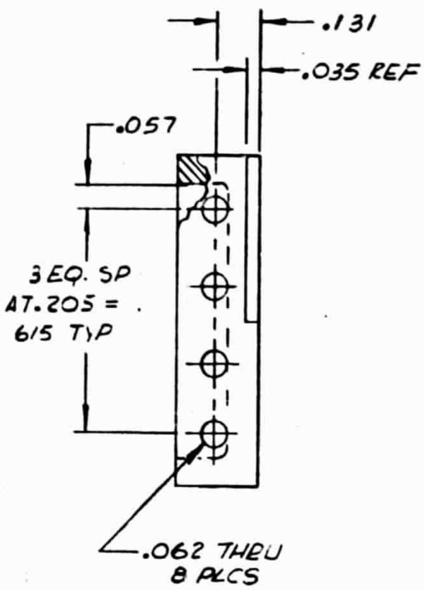

NOTES:

1. INTERPRET DRAWING PER MIL-STD-10C
2. BREAK ALL SHARP EDGES .010 MAX & REMOVE ALL BURRS
3. MATERIAL: 17-4 PH CRES, H900 COND
4. MACHINED SURFACES TO BE $\sqrt[32]{}$.
5. PINS TO BE 1/2 HARD BERYLIUM, GOLD PLATED

FOLDOUT FRAME 2

-2	-1	ITEM NO.	CODE IDENT NO.	PART NO.	MANUFACTURER	DESCRIPTION
QTY. REQD.				LIST OF MATERIALS		

UNLESS OTHERWISE SPECIFIED DIMENSIONS ARE IN INCHES
FRACTION ±1/64 DECIMALS .XX ±.01 .XXX ±.005 ANGLES ±0°30'
MACH COR—.005 TO .015 R OR CHAM
SH MATL—BREAK EDGES .005 MAX R
ALL ✓ SURFACES TO BE ✓
DIM AND TOL APPLY BEFORE FIN TREAT.
DO NOT SCALE DRAWING

MATERIAL 3

FINISH 4

DRAWN	DATE 4-2
CHECKED	
ENGINEER	
APPROVED	

ACUREX Corporation
485 CLYDE AVE., MOUNTAIN VIEW, CA 94040

DYNAMIC STRAIN TRANSMITTER HOUSING NASA

SIZE	CODE IDENT NO.	DRAWING NO.	RE
D	50726	E25506	

SCALE 4/1 | WT — | SHEET 1 OF 1

NEXT ASSY	USED ON	QTY
APPLICATION		

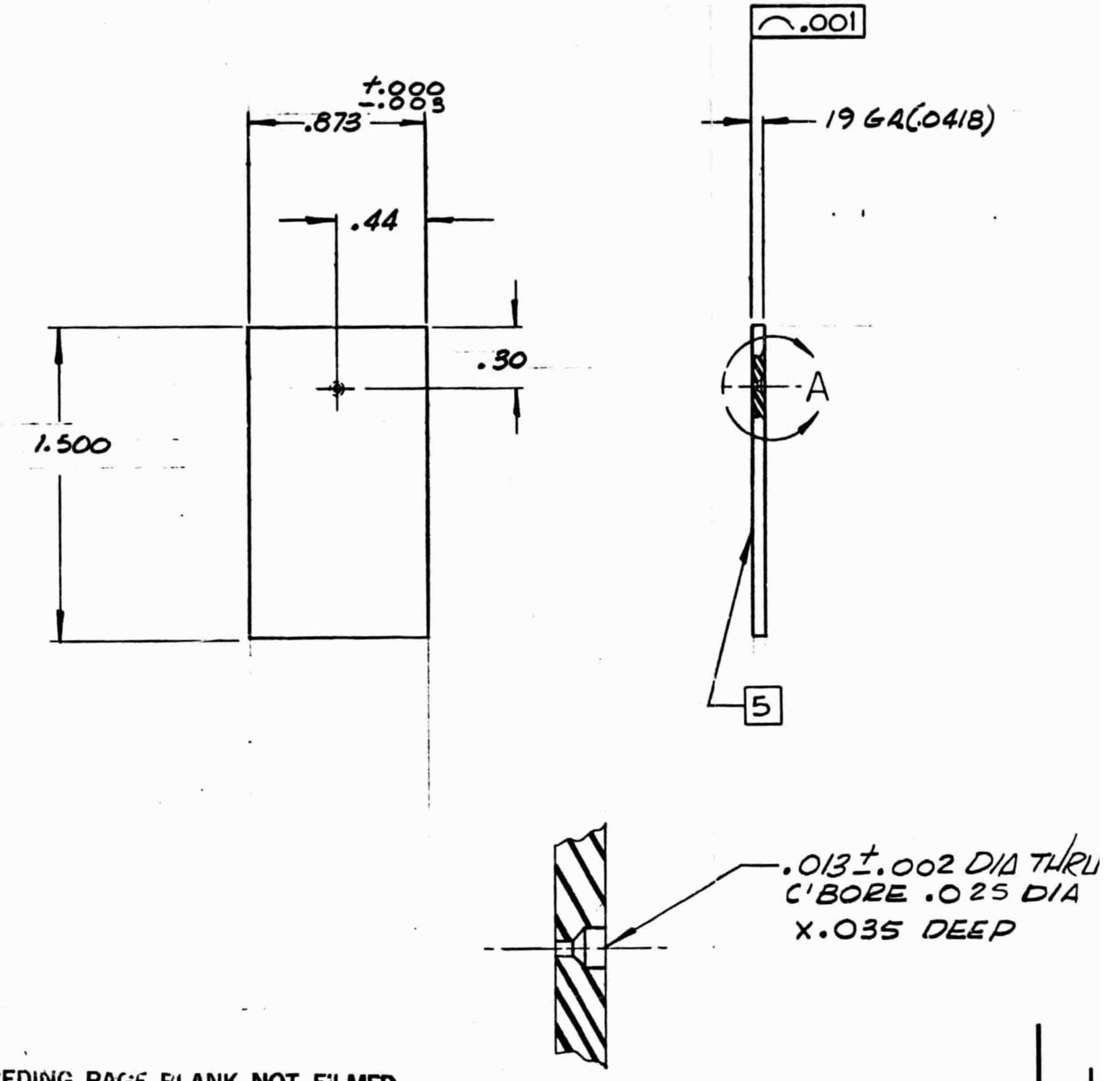

DETAIL-A-
SCALE: 10/1

PRECEDING PAGE BLANK NOT FILMED

ORIGINAL PAGE IS
OF POOR QUALITY

FOLDOUT FRAME

-2	
QTY. RI	

UNLESS OTHERWISI
DIMENSIONS ARE
FRACTION DECIMAI
.XX
±1/64 ±.01 ±.
MACH COR—.005 TO .0
SH MATL—BREAK EDG
ALL ✓ SURFACES TO I
DIM AND TOL APPLY BEI
DO NOT SCALE I
MATERIAL
3 19 GA.(.0
FINISH
4

NEXT ASSY	QTY	USED ON	QTY
APPLICATION			

ZONE	LTR	DESCRIPTION	DATE	APPROVED
REVISIONS				

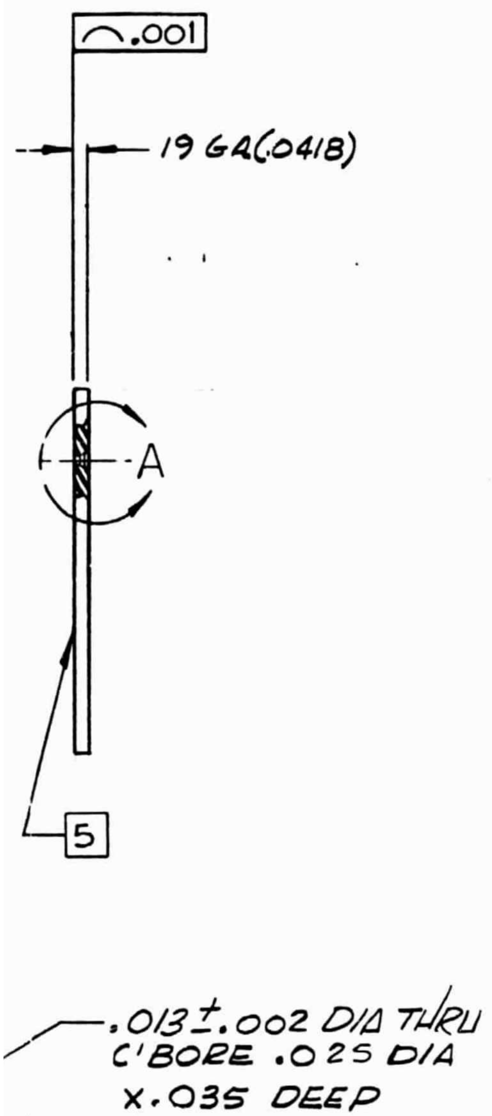

NOTES:

1. INTERPRET DRAWING PER MIL-STD-100B
2. BREAK ALL SHARP EDGES .010 MAX & REMOVE ALL BURRS
3. MATERIAL: 17-4 PH CRES, H900 COND
4. MACHINED SURFACES TO BE 32√.
5. FINE GRIT BLAST THIS SURFACE

FOLDOUT FRAME 2

-2	-1	ITEM NO.	CODE IDENT NO.	PART NO.	MANUFACTURER	DESCRIPTION
QTY. REQD.		LIST OF MATERIALS				

UNLESS OTHERWISE SPECIFIED DIMENSIONS ARE IN INCHES
FRACTION ±1/64 DECIMALS .XX ±.01 .XXX ±.005 ANGLES ±0°30'
MACH COR—.005 TO .015 R OR CHAM
SH MATL—BREAK EDGES .005 MAX R
ALL √ SURFACES TO BE √
DIM AND TOL APPLY BEFORE FIN. TREAT.
DO NOT SCALE DRAWING
MATERIAL 3 19GA.(.0418)
FINISH 4

	DATE
DRAWN	6-3-71
CHECKED	
ENGINEER A. ADLER	
APPROVED	

ACUREX Corporation
485 CLYDE AVE., MOUNTAIN VIEW, CA 94040

DYNAMIC STRAIN TRANSMITTER LID

SIZE	CODE IDENT NO.	DRAWING NO.	REV.
C	50726	E25518	

SCALE 2/1 NOTED WT SHEET OF

QTY	USED ON	QTY
APPLICATION		

REFERENCES

1. Panter, P. F.: Modulation, Noise and Spectral Analysis. McGraw-Hill, New York, 1965.

2. Corrington, M. S.: Frequency Modulation Distortion Caused by Common -- and Adjacent -- Channel Interference. RCA Review, Vol. 7, pp. 522 - 560, December, 1946.

3. Carlson, A. B.: Communication Systems, McGraw-Hill, New York, 1975.

PRECEDING PAGE BLANK NOT FILMED